Dependency of shoulder muscle activation on simulated labral conditions during isometric and functional tasks

by

Fergus Lam

A thesis

presented to the University of Waterloo

in fulfillment of the

thesis requirement for the degree of

Master of Science

in

Kinesiology and Health Sciences

Waterloo, Ontario, Canada, 2023

AUTHOR'S DECLARATION

I hereby declare that I am the sole author of this thesis. This is a true copy of the thesis, including any required final revisions, as accepted by my examiners.

I understand that my thesis may be made electronically available to the public.

ABSTRACT

Glenohumeral (GH) joint stability depends on a combination of shoulder muscular action and the glenoid labrum. Labral injuries and degenerations can affect glenohumeral joint reaction forces and potentially modify shoulder muscular efforts. However, the relationship between shoulder labral condition and muscle demands lacked clarity as compensatory muscle strategies accompanying labral compromise were unidentified. Targeted analysis was required to determine each muscle's activation, as traditional non-invasive biomechanical physical measurements could not readily assess the influence of labral damage. This study aimed to determine how simulated labral statuses influenced shoulder muscle activations using a customized mathematical biomechanical shoulder model. Secondarily, this study investigated potential links between observed variations in muscle recruitment and potential muscle overuse.

Six isometric and six functional movement tasks kinematic data were collected using a passive 3D motion capture system to generate necessary geometric inputs for the musculoskeletal model from a single male participant. A total of 13 labral conditions were simulated for each isometric and functional movement task by altering the glenoid stability constraints within an existing computational shoulder model. The percentage of maximal predicted muscle group capability (%MMGC) of the rotator cuff (RC) muscles and glenohumeral articulating (GA) muscles and glenohumeral joint contact forces were predicted by the shoulder model to illustrate the potential responses from the shoulder (i.e., changes in muscle demand and the relationship of joint contact-shear force) to changes in the stability of the GH joint between simulated conditions. Task performance and potential for muscle fatigue were ranked and evaluated by comparing the changes in muscle group recruitment, the percentage changes in

%MMGC and glenohumeral shear forces, and the directional changes in glenohumeral shear forces among simulated labral conditions.

RC muscles showed a substantial increase in muscular activation level of 5%–41% in activities when engaging in more physically demanding tasks, such as isometric external rotation, isometric abduction and weight relief lifting, compared to the intact condition. These large increases particularly occurred in simulated conditions with no labrum and a degenerated labrum in older age groups (ages over 60). This illustrated the aging impacts on GH joint stability and muscle recruitment strategies. Further, the high RC muscle activity contributed to a decrease in joint shear forces by further stabilizing the GH joint through the compression mechanism which is consistent with reduced humeral translation. Simulated surgical repairs effectively lowered the activation level of muscle groups, and the level of muscle activation was further decreased by surgical bone augmentations, such as posterior bone blocks, which further stabilized the GH joint.

This study provided insight into the muscle strategies that may arise to compensate for directional shoulder instabilities. This information can be used as a guideline for secondary injury prevention by identifying connections between tissue overload during certain tasks and previously reported potential shoulder pathologies. In conclusion, this study can help raise awareness and inform considerations relative to compromised labral management and mechanistic bases for functional capacity.

ACKNOWLEDGEMENTS

First and foremost, I would like to thank my academic advisor Dr. Clark Dickerson for his patient support throughout my time as his student. You provided me with the opportunity to discover my interest and passion for biomechanics research. Thanks to your encouragement and support, I am always able to remain enthusiastic and positive throughout my study. I am grateful for having you as a mentor and value the time I spent learning from you.

Thank you for being a part of my committee, Dr. Nikolas Knowles and Dr. Tyson Beach. I am thankful for your advice and valuable feedback, as well as your encouragement to evaluate all aspects of this study. I am sincerely grateful for your time and efforts in helping me improve the quality of my work and grow as a researcher.

In addition, I would like to thank my DIESEL lab mates, Cristina, Jacklyn, Kat, and Kayla and all the co-op and undergraduate helpers whom I had worked and interacted with. I treasure every moment we spent together in the lab and events, as well as our time in OBC 2023. I truly appreciate the support and advice on this project and the impact you all had on me.

Last but not least, I would like to thank my family. Mom and Dad, thank you for your unconditional love throughout my journey. You have always been supportive and confident in my decisions. Thank you to my sister for all of her support. I am truly grateful to have such a tight and loving family. Thank you for giving me the strength and courage to keep going.

TABLE OF CONTENTS

LIST OF FIGURES

LIST OF TABLES

LIST OF ABBREVIATIONS

%MMC	=	Percentage of Maximal Predicted Muscle Capability
%MMGC	=	Percentage of Maximal Predicted Muscle Group Capability
%Change	=	Percentage Change
ADLs	=	Activities of Daily Living
ASF	=	Anterior Joint Shear Force
BKT	=	Bankart Lesion
EMG	=	Electromyography
GA	=	Glenohumeral Articulating
GH	=	Glenohumeral
ISF	=	Inferior Joint Shear Force
JCF	=	Joint Compression Force
JSF	=	Joint Shear Force
L-O-A	=	Lines-of-Action
LTJ	=	Latarjet
PBB	=	Posterior Bone Block
PCSA	=	Physiological Cross-Sectional Area
PSF	=	Posterior Joint Shear Force
RBKT	=	Reverse Bankart Lesion
RC	=	Rotator Cuff
ReBKT	=	Repaired Bankart Lesion
ReRBKT	=	Repaired Reverse Bankart Lesion
ReSLAP	=	Repaired Superior Labrum Anterior and Posterior Lesion
ROM	=	Range of Motion
RSF	=	Resultant Shear Force
SLAM	=	Shoulder Loading Analysis Modulus
SLAP	=	Superior Labrum Anterior and Posterior Lesion
SSF	=	Superior Joint Shear Force

I. Introduction

The glenohumeral (GH) joint has the greatest range of motion (ROM) of any joint in the human body due to its joint structure, resulting in inherent instability (Dumont et al., 2011; Ladd et al., 2021; Mutlu et al., 2013). Between 1989 and 2004, shoulder instability accounted for 23% of all shoulder injuries in the National Collegiate Athletic Association (NCAA) (Owens et al., 2009), and occurred in approximately 2% of the general population (Dumont et al., 2011). The stability of the joint is dependent on the synergies of bones, ligaments, muscles and cartilage. In particular, the labrum is an integral part of preventing shoulder dislocation by enhancing the concavity of the glenoid to limit humeral translation on the glenoid (Lippitt & Matsen, 1993).

Glenoid labral tears are a common cause of shoulder subluxation and dislocation in overhead athletes and the general population. Sports involving overhead throwing motions are more likely to cause repetitive microtrauma to the glenoid labrum and increase the risk of labral tears (Bigliani et al., 1997; Fleisig et al., 1995; Gulotta et al., 2014; Mihata et al., 2004). Between 2012 and 2016, 581 shoulder procedures were performed on Major League Baseball (MLB) players with more than 60% of the procedures involving the glenoid labrum, of which 67% involved a labral repair (Chalmers et al., 2019). Superior tear is the most common labral lesion that occurs in overhead athletes and the general population, followed by anterior-inferior tear (Bankart lesion) and posterior-inferior tear ("reverse Bankart lesion") (Clavert, 2015; DeFroda et al., 2018). Likewise, an aging-related degenerative labrum is more prone to structural destruction than young healthy shoulders. According to Pfahler et al. (2003), age-dependent physiologic changes have a significant adverse impact on the structural integrity of the labrum and increase the tendency and severity of labrum tears with age. Therefore, older individuals and overhead athletes often experience glenoid labrum damage.

The management of pathologic labrum is complex, and the ideal treatment remains controversial. Most patients with labrum tears are initially treated nonoperatively, such as through physiotherapy with a strengthening program, activity modification and pain control medications. Although successful conservatively managed labra result in significant functional improvement and pain relief with improved quality of life, 51% of the patients underwent arthroscopic fixation after initial nonoperative treatment failure (Edwards et al., 2010). Nonoperatively managed labra have a higher risk of recurrence than surgically managed labra, especially in young and overhead athletes (Dumont et al., 2011; Jakobsen et al., 2007; Robinson et al., 2006; Wheeler et al., 1989). Furthermore, a cost-effective analysis conducted by Crall et al. (2012) demonstrated the clinical and cost-effectiveness of primary arthroscopic stabilization for first-time shoulder dislocation. Hence, surgical management is preferred in high-risk groups to reduce recurrence and maximize functional outcomes.

The labrum can be stabilized and repaired surgically, both openly and arthroscopically. Though arthroscopies are highly favourable due to superior cosmetic results, they significantly increase the surgical time. According to DeFroda et al. (2021), arthroscopic fixation, the current "gold standard" for managing Bankart lesions, and arthroscopic coracoid graft (Latarjet) have been widely performed since 2003. After years of continuous modification and refinement of the arthroscopic techniques, the approximate operative time has been cut from 4 hours to 45 minutes and numerous demonstrated advantages over open procedures exist (Lafosse & Boyle, 2010). Although both open and arthroscopic procedures produce similar clinical outcomes with low rates of postsurgical complications and re-operation (Horner et al., 2018; Owens et al., 2015), arthroscopy not only provides a lower risk of adhesions and clinical stiffness but also improves

early pain control and a high rate of return to sports (Lafosse & Boyle, 2010). So, arthroscopy is preferred if the surgeon has extensive knowledge and experience with the instruments.

The rotator cuff muscles have long been recognized as important GH joint stabilizers and diminished muscle strength may have an impact on the GH joint stability (Lippitt & Matsen, 1993; Mulla et al., 2020). Postoperative stiffness, associated with limited external rotation ROM, is a common complication following shoulder arthroscopies. This is caused by the disruption of the transverse sliding movement of the subscapularis tendon (Ando et al., 2012). Subscapularis stiffness is frequently observed following rotator cuff tear repair, resulting in scapulohumeral imbalance and the possibility of shoulder dislocation (Linderman et al., 2021; Péan et al., 2022). In addition, potential compensatory muscle activation strategies and associated risk of muscle fatigue due to reduced muscle capabilities have been identified in vulnerable populations (Brookham et al., 2018; Brookham & Dickerson, 2016; Chopp-Hurley et al., 2016). However, the relationship between compensatory muscle recruitment strategies and the stability of the shoulder joint remains unknown.

The glenoid labrum is an integral component that provides stability to the GH joint where damages may alter the strategies of muscle activation. The potential relationship between compensatory muscle strategies and compromised labral conditions needed to be understood to improve the effectiveness of shoulder injury prevention (Högfors et al., 1987). Further, it may help define the efficacy of the biomechanical and clinical outcomes of arthroscopic procedures. However, due to ethical issues in soft tissue modification and challenges in patient recruitment, a musculoskeletal model (Dickerson et al., 2007) can be applied which the system can be formalized and systematically modified to simulate different labrum conditions to study the effect of the labrum quality on muscle activations.

1.1 Research Purpose

The primary purpose of this study was to determine how simulated labral statuses (age-related labral degeneration, athletic labral damage, and types of labral reconstructions) influenced the shoulder muscle activation strategies during isometric and functional activities of daily living (ADLs). Secondarily, investigated potential links between observed variations in muscle recruitment strategies and the risk of overload of shoulder tissues.

1.2 Research Questions

1) How do the simulated labral conditions vary the muscle activation strategies of the upper limb and torso while performing both ADLs and postural-specific exercise tasks?

2) How do simulated arthroscopic torn labrum repairs change the likelihood of muscle fatigue while performing physical and functional tasks?

3) Do degenerative labrum and torn labrum present comparable risks of muscle fatigue due to the use of similar compensatory muscle strategies?

1.3 Hypotheses

1) Muscle activations within a task will differ with changes in total muscle demand depending on the locations and severity of the simulated labrum instability, which is sensitive to the direction of translational force while performing both functional and physical tasks (Lippitt & Matsen, 1993).

2) The muscle activation level will decrease after the labrum is surgically managed in which arthroscopic bone augmentations will result in a more pronounced reduction of activation of defined muscle groups as they further stabilize the GH joint.

3) Both degenerated labra and torn labra will result in changed muscle recruitments with increased magnitude in defined muscle groups, but these increases will be higher in torn labra due to the severity of the lesion (Pfahler et al., 2003).

II. Literature Review

2.1 Anatomical and Mechanical Functions of the Glenoid Labrum

The glenoid labrum is a multi-functional vascularized fibrocartilaginous ring attached to the rim of glenoid articular cartilage. The labrum deepens the GH joint socket by 50% (Howell & Galinat, 1987) and increases the area of the articulate surface between the humeral head and the glenoid cavity, thereby increasing the concavity of the joint socket and allowing for a wide ROM in the shoulder. The labrum increases glenoid concavity, and the enhanced effectiveness of concavity compression varies with the applied shear force direction (Lippitt & Matsen, 1993). Based on the pear shape of the glenoid, the increased stability of concavity compression in the superior-inferior direction (Figure 1-A) is due to the increased width and depth compared to the anterior-posterior direction. Further, removing the labrum significantly reduced joint resistance to shear force by an average of approximately 20% (Figure 1-B).

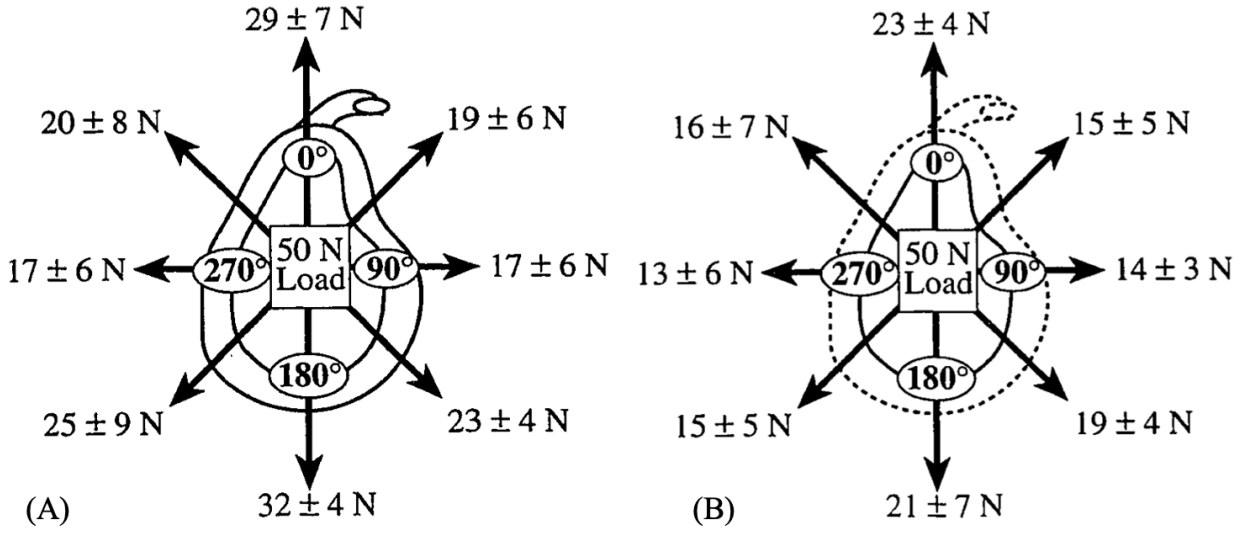

Figure 1. The average maximum shear force resisted with labrum (A) and without labrum (B) in 8 directions with a 50N compression load applied into the glenoid (Lippitt & Matsen, 1993).

2.2 Age-dependent Labral Changes

The physiological structure of the labrum changes with age and potentially leads to higher shoulder instability in older age. Labra are composed of mesenchymal tissue with small but distinct chondrocytes in fetal and age 1 year (Prodromos et al., 1990). Mesenchymal tissues are replaced by well-defined fibrocartilage tissues from aged 2 to 7. Eventually, all mesenchymal cells will be replaced. From the age of 30, signs of aging, such as changes in structures and tissue compositions, are likely to exhibit in superior and anterosuperior direction (Pfahler et al., 2003).

The aged labrum is composed of dense bundles of fibrous connective tissue with poor vascularity which limits the potential healing capability of an injured labrum. Concurrently, the dense connective tissue is less organized, with more cartilage cells between the labral tissue and the hyaline cartilage of the glenoid fossa (Kreitner et al., 1998). Likewise, degenerative labra demonstrated intralabral alterations, such as chondroid metaplasia, formations of scar tissue and intralabral hemorrhage; along with the decreased number of blood vessels with increasing age, thereby reducing the potential capability of healing at the labrum (Prodromos et al., 1990). Moreover, the thickness and glenoid depth of the labra are significantly reduced by an average of approximately 6% in all eight directions (Alashkham et al., 2020). These morphometric changes potentially correlate with the high prevalence of labrum pathology in older age.

2.3 Injury Mechanisms

2.3.1 Acute Excessive Translational Forces

Overhead athletes are particularly vulnerable to traumatic acute labral tears (Bigliani et al., 1997; DeFroda et al., 2018; Fleisig et al., 1995; Gulotta et al., 2014). Excessive shoulder external rotation and abduction during the corking phase of throwing (Figure 2-A) causes extreme translation of the humeral head (Mihata et al., 2004); thereby, forcefully entrapping the labrum between the humeral head and the glenoid rim and leading to labral tears (Fleisig et al., 1995). After the corking phase and followed by the deceleration phase (Figure 2-B), the contraction of the biceps brachii provides elbow flexion torque and resists humeral distraction when extending the elbow. If the athlete is throwing with improper mechanics, i.e., an inefficient arm path (Fortenbaugh et al., 2009), a potential increase in shoulder compression force can significantly increase the muscle activity of the biceps (Gowan et al., 1984). This dynamic muscle imbalance may cause a large tensile load to the attachment site of the long head of the biceps tendon, resulting in labral avulsion via the "peel-back" mechanism (Burkhart & Morgan, 1998).

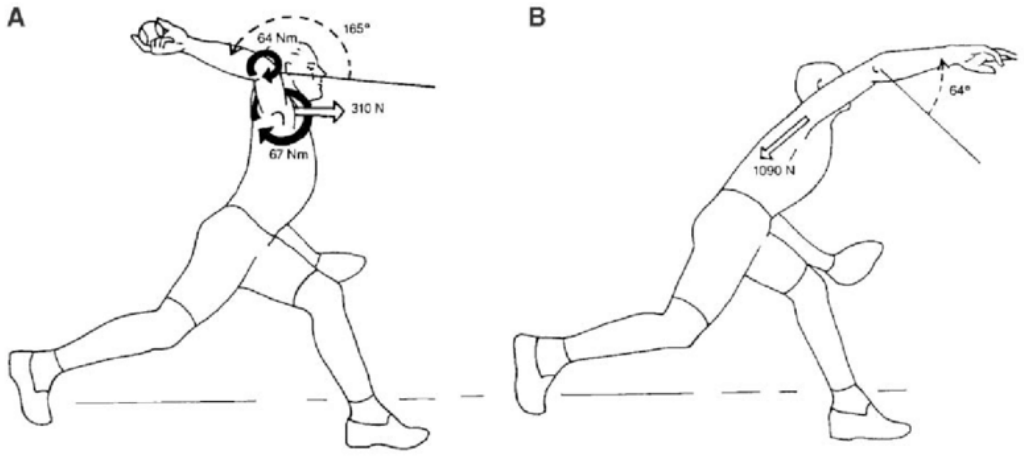

Figure 2. The critical instances of potential labral injuries during (A) the corking phase and (B) the arm deceleration phase (Fleisig et al., 1995).

2.3.2 Repetitive Microtrauma

Long-term constant stress exposure from repeated movements is a well-known cause of labrum pathology in athletes (Burkhart & Morgan, 1998). Repetitive movements in overhead throwing sports are constantly placing high local shear stress and tensile load on the labrum via translation and biceps contraction, respectively (Fleisig et al., 1995). These repetitive stresses and strains on the tissue result in repetitive microtrauma, which may gradually lead to early degenerative changes (Miniaci et al., 2002; Pfahler et al., 2003). Conceptually, this may lead to long-term pathology if adequate resting periods were not provided between micro-traumatic events.

2.4 Classifications of Labrum Lesions

The classifications of labrum lesions are based on the location of the lesions (Figure 3) (Clavert, 2015). Superior labral tears in sector 1 are known as Superior Labrum Antero-to-Posterior lesions (SLAP) which are the most common labral pathology in the shoulder. SLAP was separated into different types based on the severity of the tear of which types I to IV SLAPs are the more common types of superior lesions (Clavert, 2015; Snyder et al., 1990):

- Type I is considered a degenerative lesion where no labral detachment is involved.
- Type II is the most reported type of SLAP (Li et al., 2010) which involved the avulsion of the superior labrum and the long head of the biceps tendon from the glenoid.
- Type III is rare which involves the avulsion of the superior labrum via the “bucket-handle” mechanism.
- Type IV is a bucket-handle tear of the superior labrum, involving the long head of the biceps brachii, and is often associated with anterior labrum lesions in sectors 2.

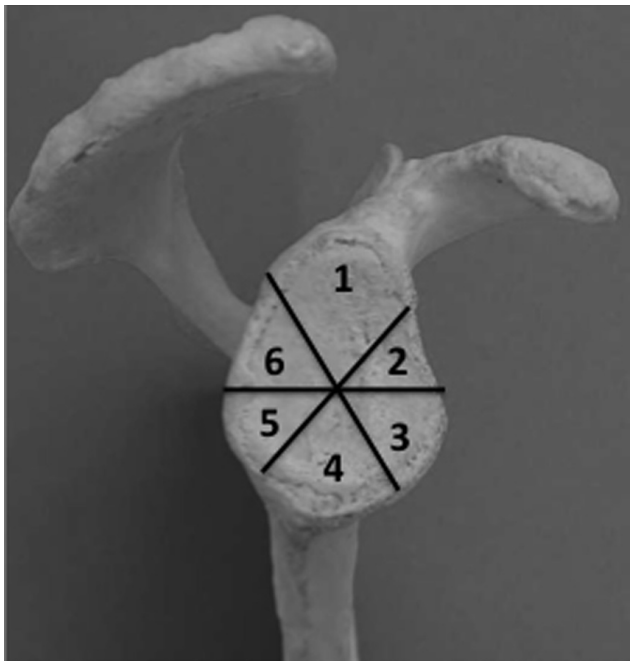

Figure 3. The subdivisions of the glenoid cavity in 6 sectors (Clavert, 2015).

The detachments of the anteroinferior labrum, which potentially extend to the anterior periosteum of the scapular neck, within sectors 3 and 4 are classified as Bankart lesions (Clavert, 2015). This type of lesion is caused by the avulsion of the middle and inferior glenohumeral ligaments, mostly associated with first-time anterior shoulder subluxation which potentially leads to recurrent dislocation due to the failure of healing (Owens et al., 2010; Robinson et al., 2006). 8% of the cases may extend to the posteroinferior direction in sectors 4 and 5 and refer to as reverse Bankart lesions (Clavert, 2015). Reverse Bankart lesions are rarely isolated as most are associated with posteroinferior cartilage damage. Labral-induced instability may trigger high activation of the scapulohumeral muscular stabilizers to keep the humeral head within its contact area with the glenoid to prevent dislocations.

2.5 Glenohumeral Joint Stabilizers

The roles of scapulohumeral muscles, which are the rotator cuff muscles and other shoulder girdle muscles, are to move the humerus at the shoulder joint and balance the shoulder joint reaction force and keep the humeral head within the stable arc provided by the glenoid concavity (Fig. 4) (Lippitt & Matsen, 1993). The rotator cuff muscles and teres major are the primary GH stabilizers by enforcing joint compression and contribute to maintaining the superior stability of the GH joint, except for the supraspinatus (Mulla et al., 2020). On the other hand, the deltoids and coracobrachialis act as the inferior stabilizers during early arm elevation where contributions decreased with increasing humeral elevation angle. Further, the subscapularis, teres major, middle, and posterior deltoid behaved as anterior stabilizers. Whereas the infraspinatus, supraspinatus, teres minor, coracobrachialis, and anterior deltoid were the posterior humeral stabilizers. The role of these stabilizers is to allow a wide ROM at the glenohumeral joint, and simultaneously keep the net joint reaction force vector within the glenoid arc (Figure 4). Unfortunately, unbalanced joint reaction forces are likely to exhibit in certain populations due to muscle weakness and stiffness.

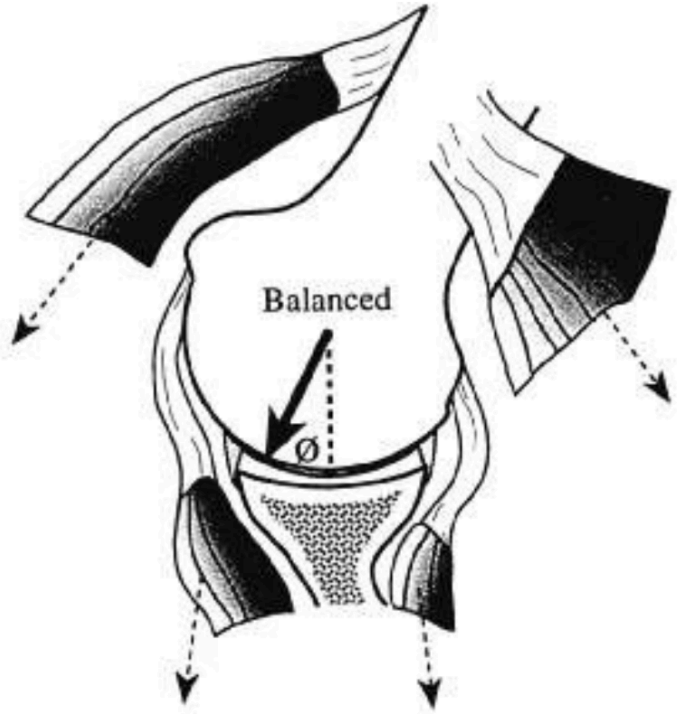

Figure 4. Scapulohumeral muscles stabilized the glenohumeral joint (GH) by balancing the net joint reaction force within the glenoid cavity (Lippitt & Matsen, 1993).

Certain vulnerable groups, such as breast cancer survivors, exhibited signs of muscle weakness and impingement pain with restricted arm elevation and external rotation (Brookham et al., 2018; Brookham & Dickerson, 2016). To compensate for the compromised ability of GH instability, compensatory muscle strategies are applied (Chopp-Hurley et al., 2016; Lang et al., 2019), which result in greater rotator cuff muscle activation during their respective rotation-type exertions (Brookham & Dickerson, 2016). The significantly increased rotator cuff muscle activation may plausibly gradually cause severe degrees of muscle overuse and related rotator cuff disease, and potential secondary damage to the glenoid labrum under prolonged exposures (Brookham & Dickerson, 2016; Ebaugh et al., 2011; Gallagher & Schall, 2017).

2.6 Arthroscopic Labral Repair Procedures

When compared to open surgeries, arthroscopies are the preferred type of labral repair procedure due to better cosmetic results and a low risk of postoperative complications and reoperation (Horner et al., 2018). Arthroscopic procedures allow for the treatment of concomitant labral pathologies while also resulting in less postoperative pain, faster recovery, and a higher rate of return to sport and work (Lafosse & Boyle, 2010). To treat shoulder labral instability, arthroscopic suture anchor fixations and bone augmentations are frequently employed (DeFroda et al., 2021).

2.6.1 Suture Anchor Fixations

Suture anchor fixations are commonly used to surgically treat labrum lesions and can be performed with either knotted or knotless suture anchors (Figure 5) with comparable biomechanical outcomes (Wu et al., 2021). Knotless suture anchors result in a shorter operation time as knot tying is not required (Bents et al., 2017; Matache et al., 2021). Additionally, there were fewer reported cases of postoperative stiffness, pain in overhead activities, suture anchor failure, and osteolysis after the knotless procedures (Knapik et al., 2020). This functional equivalence technique eliminated the risk of postoperative complications that were caused by poor knot-tying techniques with weak knot strength (Bents et al., 2017). Eventually, failure to repair labrum lesions will cause recurrent shoulder instability. Thus, a more robust approach needs to be applied to further stabilize the system and avoid further tissue damage to the labrum.

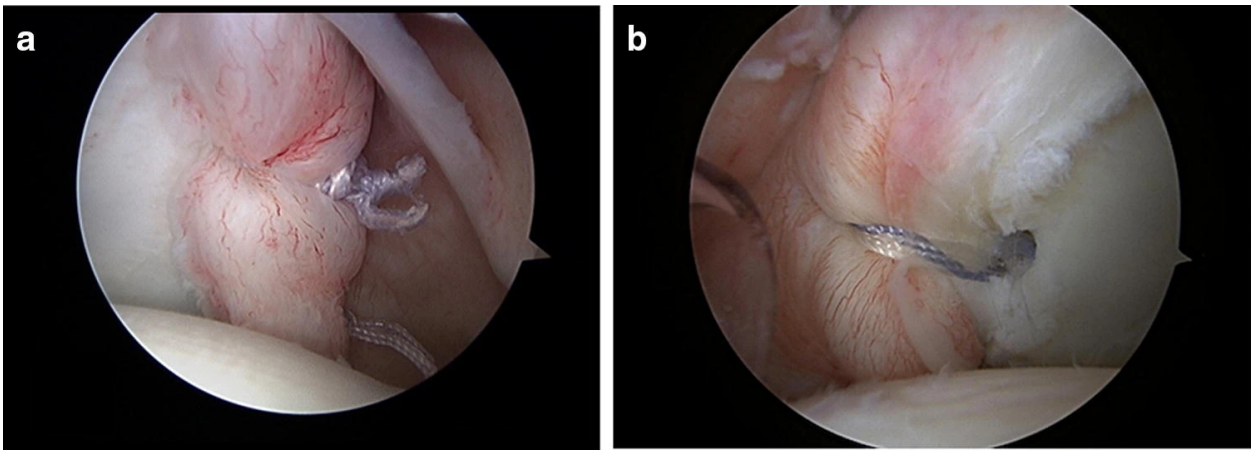

Figure 5. Labral fixation using (a) knotted and (b) knotless suture anchors (Wu et al., 2021).

2.6.2 Bone Augmentations

Bone augmentations are a more robust approach to avoid further labral damage and potential recurrent dislocation by further stabilizing the GH joint in the event of failed labrum repairs. Failures in labrum repair are caused by the poor quality of fixations in areas where further labral tissue damage exists. Several detailed clinical and radiologic evaluations will be performed following repair failures to identify postoperative glenoid bone loss, humeral bone loss, and additional soft tissue damage, as well as the need for glenoid augmentation procedures (Lafosse & Boyle, 2010).

Coracoid transfer procedure, also known as Latarjet procedure, is commonly performed on patients who are associated with postoperative instability following Bankart repair or who are at high risk of recurrence due to the intensity and type of activity that they are likely to engage in. The Latarjet procedure involves translating the coracoid bone onto the labral attachment site, with the lateral surface of the coracoid congruent with the glenoid articular surface (Figure 6) (DeFroda et al., 2021). Theoretically, this procedure improves shoulder stability in three ways (DeFroda et al., 2021; Lafosse & Boyle, 2010), maximizes the glenoid contact area, creates a sling by repositioning the conjoint tendon around the subscapularis, and reconstructs the capsule

using the remnant of the coracoacromial ligament. Latarjet procedures demonstrated a superior long-term stabilizing effect with a low rate of recurrent instability compared to Bankart repairs (Imam et al., 2020), as well as a shorter rehabilitation time to return to sports activity at a comparable level (Lafosse & Boyle, 2010).

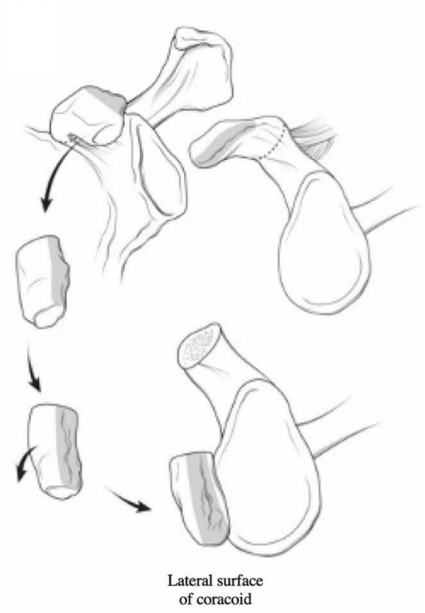

Figure 6. The Latarjet technique which the lateral surface of the coracoid is congruent to the glenoid (DeFroda et al., 2021).

Another bone augmentation technique, known as the posterior bone block, was previously mentioned by Levigne et al. (2005) as a treatment for recurrent posterior shoulder instability. In this approach, the graft was harvested from the ipsilateral iliac crest at the level of the gluteus medius tubercle and placed the graft with the lateral surface on the posterior aspect of the glenoid with the cancellous bone graft faced anteriorly. This bone block technique significantly improved posterior and posteroinferior stability by limiting the translation of the humeral head in those directions (Wellmann et al., 2011). Bone augmentations on SLAP tears, on the other hand, had never been reported, possibly due to the pear shape of the glenoid and the limited attachment space between the acromial arch and the superior glenoid.

2.7 Mathematical Biomechanical Models

In biomechanical research, mathematical models are used to non-invasively study the system responses to various experimental conditions when experimental approaches are impractical or unfeasible. In experimental research, electromyography (EMG) and 3-dimensional motion capture systems are instruments that are commonly used to study muscle activities and human kinematics, respectively. However, there are limitations in EMG to determine the activation of an individual muscle due to the difficulties in isolating individual muscle activity. Moreover, these experimental instruments can only indirectly measure muscle and tissue mechanical properties (e.g., muscle force, joint reaction force, and tissue mechanical responses) which is important information to outline the relationship between tasks and the mechanical cost of the system. Even though tissue mechanics can be studied through cadaveric studies, the quality of the tissue is not simply the same as in a living human body. In addition, certain tasks and modified conditions are difficult to introduce to certain groups in an experimental setting and may face challenges in the recruitment of certain clinical populations, like those comprised of individuals with an injured labrum. Yet using a biomechanical model can overcome these restrictions and allow us to gain insight into the properties and changes within the system.

Computational musculoskeletal models are one common type of biomechanical model used to study human limb movement and dynamics (Chaffin, 1997). These models can be customized through Matlab® (MathWorks, Massachusetts, USA) using different assumptions that are based on literature and empirical data sets (Dickerson et al., 2007), and reused to evaluate the responses of the system when alterations to the model are introduced (Hu et al., 2020). These models formulated the muscle configurations, which include the defined bone length and muscle lines-of-action (L-O-A). Then, the calculation of internal forces, such as

muscle and bone-on-bone forces, can be used to predict muscle contributions by combining the experimental kinematics data with the weight of the applied loads. To decompose joint moments into individual muscle forces, model optimizations are an effective method.

2.7.1 Use of Optimization in Muscle Force Predictions

Optimization is a mathematical technique that is frequently performed to estimate the strategy of muscular activation, including muscle co-activation, and force of individual muscles. It introduces objective functions and constraints to solve the mechanical redundancy in the system and predict model outputs. A common approach is to minimize muscle stress (Dul et al., 1984) so that the ratio of muscle force to maximal force is proportional to both the moment arm and the physiological cross-sectional area (PCSA) of the muscle (Collins, 1995; Prilutsky & Zatsiorsky, 2002) to maintain physiological realism. Further, these constraints are employed to non-linearly formulate the minimum fatigue criterion (Dul, Johnson, et al., 1984) to represent the synergistic muscle action which first activates large muscles and slow-twitch fatigue-resistant fibres to maximize the muscle endurance time (Crowninshield & Brand, 1981). Musculoskeletal models can predict muscle activity patterns that account for muscles' PCSA when performing functional and physical tasks (Prilutsky & Zatsiorsky, 2002) and allow modification with additional programming efforts if desired.

2.7.2 SLAM Model

The Shoulder Loading Analysis Modulus (SLAM) model (Dickerson et al., 2007) is a computational shoulder musculoskeletal model created in Matlab® (MathWorks, Massachusetts, USA) to evaluate exposures when performing exertions. This model includes three linked modules: 1) a geometric musculoskeletal module; 2) an external dynamic shoulder torque module; and 3) a muscle force prediction module. The required inputs for the overall model are experimental motion data; subject data including height, weight, and sex; and task data such as applied forces (Figure 7). The SLAM model outputs the orientation and positions of the defined segments, the torques and forces on the shoulder joint, and muscle data including L-O-A, length, and forces (Figure 7).

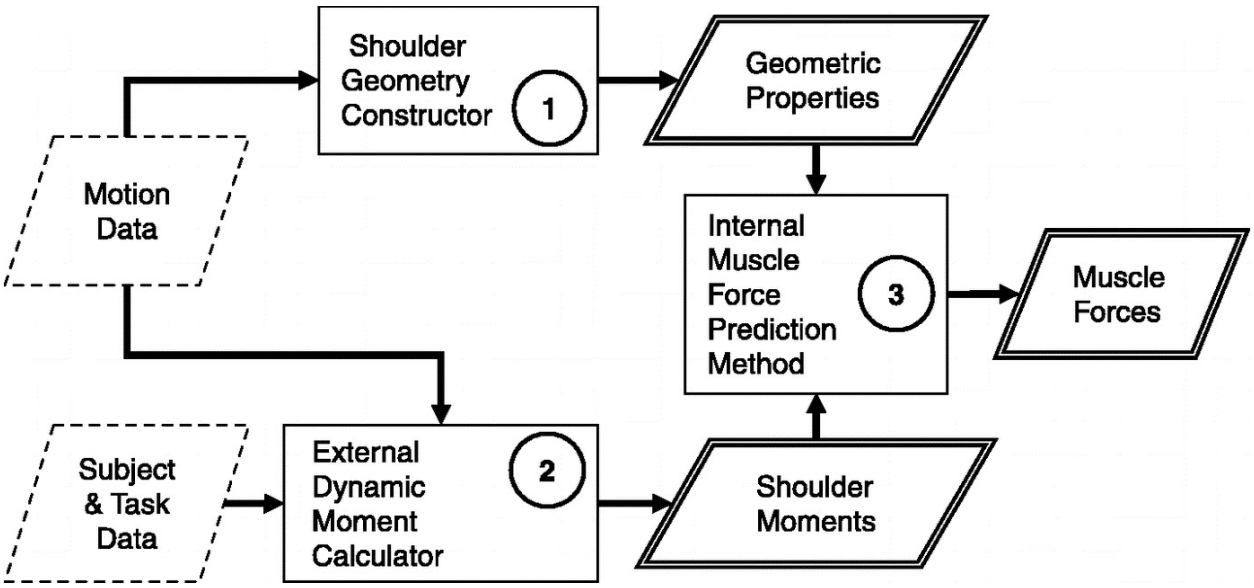

Figure 7. The data flow chart of the SLAM model (Dickerson et al., 2007).

2.7.2.1 Geometry Module

The shoulder geometry module uses kinematic data to calculate the instantaneous orientation and relative positions of the shoulder segments (Figure 7). Bone segments and segmental coordinate systems, including the sternum, scapular, clavicle, humerus, forearm, and torso, were defined and modelled based on the experimental motion data (Dickerson et al., 2007; Högfors et al., 1987). A functional constraint was employed to keep the inferior and superior angles of the scapula outside of the ribcage to retain physiological realism. The bone-centric parameters were scaled to the height and segment orientations of the participant (Figure 8) from the collected motion data and were expressed as proportions of bone length (Högfors et al., 1987; Makhsous et al., 1999). The relationship between the positions of defined segments was implemented using the previously described coordinate systems (Högfors et al., 1991; Makhsous et al., 1999), and represented in Euler angle sequences.

Two different wrapping techniques were employed to represent the L-O-A of the 23 muscles (38 muscle elements) in the SLAM model. Spherical (van der Helm, 1994) and cylindrical (Charlton & Johnson, 2001) muscle wrapping techniques were applied to modify the muscle L-O-As to improve the physiological realism of the model. Before the muscle wrapping techniques were employed, collision detection procedures were performed on each specified muscle in a given posture to minimize the alteration of muscle moment arms (Dickerson et al., 2007).

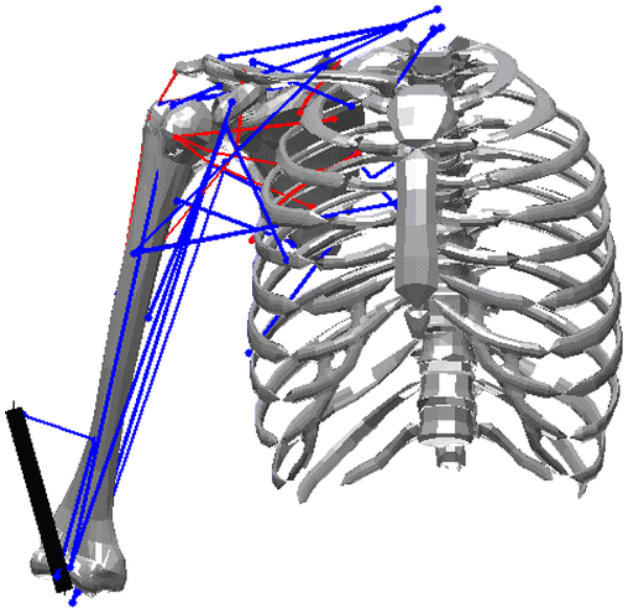

Figure 8. The geometric parameters of bone and muscle using the model (Dickerson et al., 2007). Red lines indicate wrapped muscles and blue lines indicate unwrapped muscles (Charlton & Johnson, 2001).

2.7.2.2 External Dynamic Moment Module

The second module is the shoulder torque estimation module. Its required inputs are kinematic data and participant data (stature, weight and sex) and the applied hand forces (Figure 7). Three connected rigid segments (hand, forearm, and upper arm) were modelled, and parameters (mass and moments of inertia) were calculated using sex- and stature-based regression equations (Zatsiorsky & Seluyanov, 1985). The joint centre locations of the glenohumeral, elbow, and wrist were estimated using reported motion data (Nussbaum & Zhang, 2000) where the locations of the centre of mass of each segment were expressed relative to the segment length (Clauser et al., 1969). The Joint Coordinate System technique (Nigg & Herzog, 1994), an Euler angle-based technique, was used to determine the angular kinematics. The orientations of the upper arm and forearm (Eq. 1) and hand (Eq. 2) were defined using two different rotation sequences. Angular velocity and acceleration were calculated by taking the first

and second derivatives of the Euler angles (Vaughan et al., 1992), respectively. The external joint load was calculated at the proximal end of each segment using the force equilibrium equation (Eq. 3) and determined by the movement and mass of the segment and the applied hand load. Lastly, the sum of the external joint torque (Eq. 4) was calculated as the rate of change of segmental angular momentum. It was considered the cross-product of the sum of forces and their corresponding moment arm at the proximal end of each segment.

$$\begin{Bmatrix} x \\ y \\ z \end{Bmatrix} = \begin{bmatrix} \cos\psi\cos\theta & \sin\psi\cos\theta & -\sin\theta \\ (\sin\psi\sin\phi - \cos\psi\sin\theta\cos\phi) & (\cos\psi\cos\phi + \sin\psi\sin\theta\sin\phi) & \cos\theta\sin\phi \\ (\sin\psi\sin\phi + \cos\psi\sin\theta\cos\phi) & (-\cos\psi\sin\phi + \sin\psi\sin\theta\cos\phi) & \cos\theta\cos\phi \end{bmatrix} \begin{Bmatrix} X \\ Y \\ Z \end{Bmatrix} \quad \text{(Eq. 1)}$$

$$\begin{Bmatrix} x \\ y \\ z \end{Bmatrix} = \begin{bmatrix} \cos\psi\cos\theta & \sin\theta & -\sin\psi\cos\theta \\ (\sin\psi\sin\phi - \cos\psi\sin\theta\cos\phi) & \cos\theta\cos\phi & (\cos\psi\sin\phi + \sin\psi\sin\theta\cos\phi) \\ (\sin\psi\sin\phi + \cos\psi\sin\theta\cos\phi) & -\cos\theta\sin\phi & (\cos\psi\cos\phi + \sin\psi\sin\theta\sin\phi) \end{bmatrix} \begin{Bmatrix} X \\ Y \\ Z \end{Bmatrix} \quad \text{(Eq. 2)}$$

$$\sum F = m_{segment} \times a_{COM_{segment}} \quad \text{(Eq. 3)}$$

$$\sum M = \dot{H} \quad \text{(Eq. 4)}$$

2.7.2.3 Muscle Force Prediction Module

The last module of SLAM is the muscle force prediction module which uses the outputs of the previous modules (geometric properties and shoulder moment) to predict the temporal individual muscle forces throughout a task (Figure 7). Optimization was implemented to solve the statically indeterminate problem of external load distribution amongst the muscles. The objective (cost) function of SLAM was to minimize the sum of the cubed muscle stresses (Eq. 5) (Crowninshield & Brand, 1981); and to promote external load sharing between muscles when performing different loading tasks. Joint forces and torques are bound along with 22 mechanical equilibrium constraints in the model. Muscle forces were bounded to remain positive with zero as the minimum. Shoulder ligaments between segments were modeled as no force contribution to the system (Crowninshield & Brand, 1981; Jinha et al., 2006). The maximum allowable individual muscle forces were proportional to the PCSA of the corresponding muscle. The PCSA of each muscle was obtained from a cadaveric study (Högfors et al., 1987) with a specific tension of 88 N/cm^2 (Wood et al., 1989). Eighteen equilibrium equations, both in the angular and linear domains, were used to constrain the glenohumeral, acromioclavicular, and sternoclavicular joints. Simultaneously, one equilibrium equation was introduced to constrain the elbow joint moment. At last, three additional constraints (one in each global direction) were added, based on the directional shoulder stability ratio (Eq. 6) derived from prior empirical cadaveric data (Lippitt & Matsen, 1993). The threshold values of glenohumeral dislocation were defined in eight equally spaced compass directions on the glenoid (Figure 9) to ensure the GH joint was intact and vented in all successful simulations.

$$\Theta = \sum_{i=1}^{38} \left(\frac{f_i}{PCSA_i} \right)^3 \quad \text{(Eq. 5)}$$

$$S_i = \frac{F_s}{F_c} \quad \text{(Eq. 6)}$$

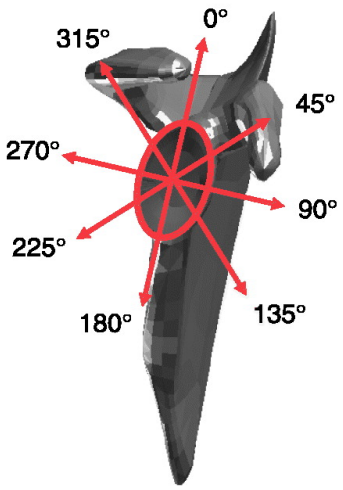

Direction	Dislocation Force Ratio Threshold (Shear/Compression) (%)
0	51
45	33
90	29
135	40
180	56
225	43
270	30
315	35

Figure 9. The shoulder stability ratios indicate the tolerance of the directional shear force to the compression force in 8 equally spaced compass directions of the glenoid (Dickerson et al., 2007).

2.7.2.4 Clinical Applications of the Mathematical Shoulder Model

Mathematical shoulder models have been widely used to study compensatory muscle strategies among populations with different pathologies. Shoulder models identified compensatory muscle activation patterns in breast cancer survivor populations who were associated with muscle weaknesses and decreased ROM, leading to enhanced muscle effort with a higher risk of fatigue (Brookham et al., 2011, 2018; Brookham & Dickerson, 2016; Chopp-Hurley et al., 2016). Further, models were applied to simulate rotator cuff pathologies, specifically rotator cuff impingements, to determine the movement adaptations and the performance (risk of fatigue) of ADLs (Chopp & Dickerson, 2012; Dickerson et al., 2011; Hall et al., 2011). Model simulations demonstrated stabilizer muscular imbalances associated with various compensatory strategies, agreeing with the relationships from both clinical and cadaveric studies (Mihata et al., 2007; Wood et al., 2011). Although the indeterminacy of muscle load distribution in subluxed shoulders, as a consequence of stabilizer muscle weaknesses, was identified, the relationship between an unstable shoulder joint and muscle activity was not well understood.

The linkage between directional shoulder instability and muscle efforts is essential to develop strategies to further prevent shoulder pathologies. The relationship between the quality of the shoulder labrum and the risk of muscle overuse remains unclear as the compensatory muscle strategy among labral conditions has not been identified. The patterns of muscle activation need to be first determined to understand the muscle compensatory strategies. However, each muscle has a specific, posturally-sensitive stabilizing role and requires targeted analysis to determine its activation strategies, which traditional non-invasive physical biomechanical measurements cannot easily achieve. Using the SLAM model with alterations can

simulate different scenarios and predict the activity level for each involved muscle. With further interpretation, these predicted values can help indicate potential tissue overload that may precede fatigue in various movements under certain conditions. Therefore, the relationship between muscle activation strategies and labral status is crucial and requires a better understanding to prevent recurrent instability and potential injuries.

III. Methodology

3.1 Participant

One participant was recruited to provide subject and kinematic data for the shoulder biomechanical mathematical model. Participant's information was indicated in Table 1. The participant was not experiencing any shoulder pain, had no shoulder injury within the last six months, or had not undergone shoulder surgery.

Table 1. Participant information.

Sex	Age (years)	Mass (kg)	Height (m)
Male	21	93.6	1.9

3.2 Instrumentations

3.2.1 Motion Capture

Three-dimensional kinematic data of the right upper limb and torso was collected using a VICON MX20 passive motion capture system (VICON, Oxford, UK) at a sampling rate of 50 Hz. Before the participant's arrival, the collection space was calibrated. The global coordinate system was set based on the coordinate system described in the SLAM model where +Z represents up, +Y represents forward and +X represents to the left of the origin (Dickerson et al., 2007; Nigg & Herzog, 1994). Thirteen individual reflective markers were placed over bony landmarks of the right upper limb and torso, and 2 additional rigid marker clusters were placed on the right forearm and right upper arm (Table 2, Figure 10) (Dickerson et al., 2007). These marker placements help to generate necessary task-specific kinematic inputs for the SLAM model.

Table 2. VICON marker and cluster placements on defined segments (Dickerson et al., 2007).

Segments	Anatomical Landmarks
Thorax	Xiphoid Process (XP)
	Suprasternal Notch (SS)
	Spinous Process of the 7th Cervical Vertebra (C7)
	Spinous Process of the 5th Lumbar Vertebra (L5)
	Right Acromion Process (AP)
	Left Posterior Superior Iliac Spine (LPIS)
	Right Posterior Superior Iliac Spine (RPIS)
Right Humerus	Lateral Epicondyle (LE)
	Medial Epicondyle (ME)
	Upper Arm Cluster (UA_1, UA_2, UA_3)
Right Forearm	Ulnar Styloid Process (US)
	Radial Styloid Process (RS)
	Forearm Cluster (FA_1, FA_2, FA_3)
Right Hand	2nd Metacarpal Joint (MCP2)
	5th Metacarpal Joint (MCP5)

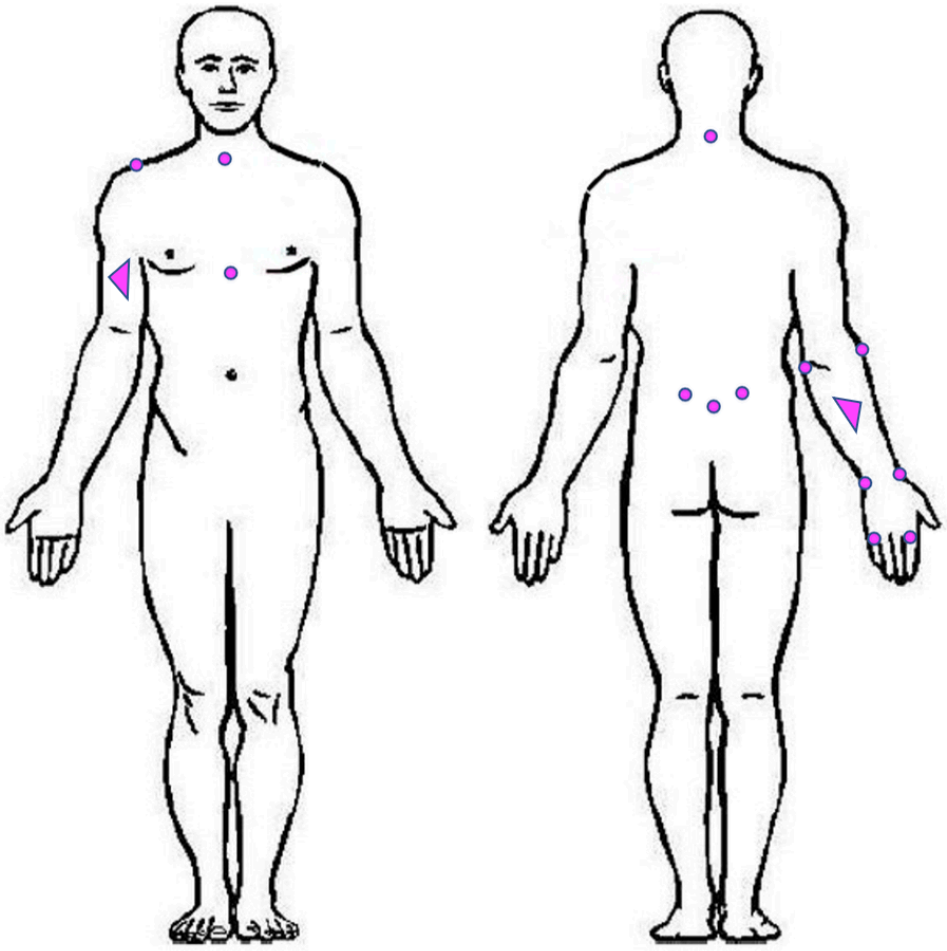

Figure 10. VICON marker placements on the anterior (left) and posterior (right) upper limb and torso (Dickerson et al., 2007; Högfors et al., 1987). Dots indicate individual markers and triangles represent rigid marker clusters.

3.2.2 Force Transducer

A force transducer was used to monitor the force exertion level of the participant when performing the 6 10-second standing isometric exercises (listed in Table 3). Isometric hand force was measured at a sampling frequency of 1500 Hz by a 6-degree-of-freedom AMTI MC3A force transducer (AMTI, Massachusetts, USA). Visual cues were provided to ensure the participant was producing 40N force when performing isometric tasks. A handle was attached to the force transducer to enable force application (Figure 11). The force transducer coordinate system was set to match the global coordinate system in the SLAM model where the +z-axis force was set to point into the transducer, the +y-axis force was set as the upward force, and the +x-axis force was set as the horizontal force pointing toward the left of the transducer (Figure 12).

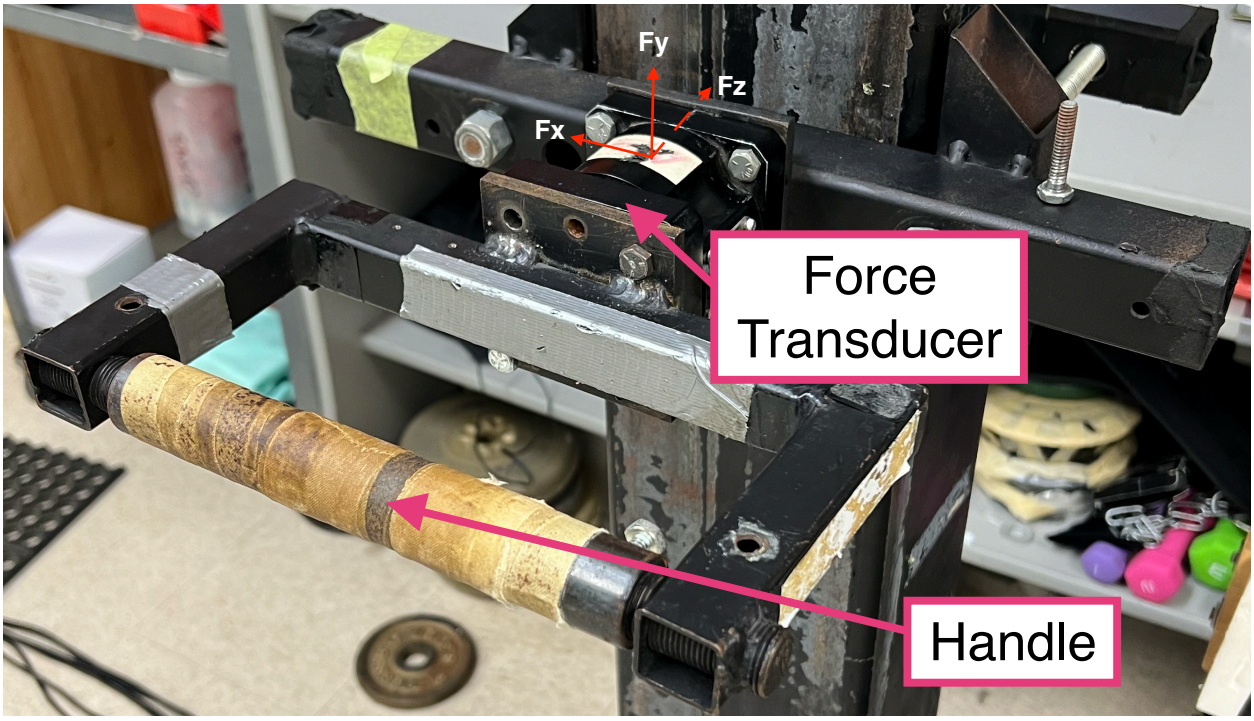

Figure 11. The set-up of the force transducer with the handle in each standing isometric task. F_x, F_y and F_z represent the +x-, +y- and +z-axis force of the transducer, respectively.

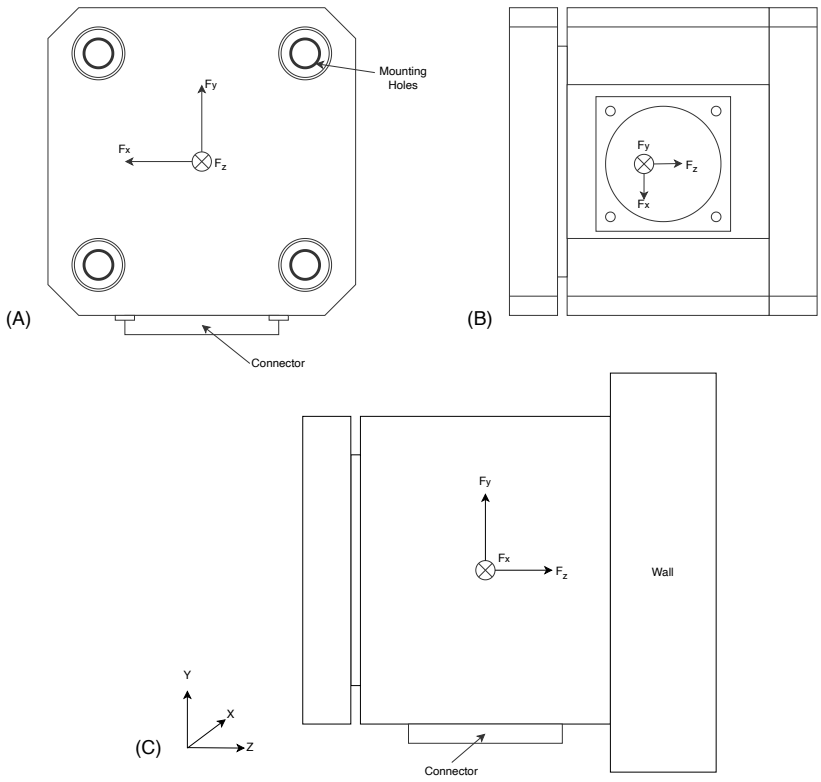

Figure 12. Three perpendicular force axes (F_x, F_y, F_z) of the AMTI MC3A force transducer (AMTI, Massachusetts, USA). (A) Front surface view. (B) Bottom view. (C) The side view indicates how the force transducer was mounted on the wall in the global coordinate system.

3.2.3 Home Exercise Machine

Three dynamic tasks (i.e., one-arm row, one-arm chest press and one-arm face pull) were performed using the Tonal Smart Home Gym Machine (Tonal, California, USA) (Figure 13). When performing these three tasks, the resistance of the cables was set at 44.5 N (10 lbs) based on the setting of the Tonal machine. The handle was connected to the adjustable arm of the exercise machine. The height and the elevation angle of the arm were adjusted according to the height and arm length of the participant. The direction of the applied force was aligned and parallel with the direction of the resistance of the cable.

Figure 13. The Tonal home gym machine and equipment (Tonal, California, USA).

3.3 Collection Protocol

The participant attended two collection sessions of approximately one to one and a half hours. The age, sex, height, and weight of the participant were taken. Then, reflective markers and marker clusters were placed on the right upper limb and torso. Before kinematic collection, a 5-second static calibration trial was taken with the participant standing in an anatomical position.

The participant performed six isometric exercises, modified from the reported rehabilitation programs for baseball players (Table 3) (Townsend et al., 1991), in a standing position. The participant produced a 40 N force toward the force transducer and stayed at the same force level in position for 10 seconds. The participant rested for 1 minute between each exercise to alleviate the risk of fatigue. In another collection session, the participant performed six dynamic functional ADL tasks (Table 4). A 44.5 N force from the Tonal home gym machine (Tonal, California, USA) or a tool was applied to the right side. Three sets of both isometric exercises and functional tasks were performed in each corresponding session. The trial with the greatest data quality, which was the trial with the lowest number of missing frames, out of all three trials was used as the input for the SLAM model.

Table 3. Six isometric physical tasks and their corresponding postures (Townsend et al., 1991).

Posture	Position
Internal Rotation	Humerus 0° abducted and elbow flexed 90° with palm faces medially
External Rotation	Humerus 0° abducted and elbow flexed 90° with palm faces medially
Abduction	Humerus abducted 30° and elbow fully extended with palm facing down
Adduction	Humerus abducted 60° and elbow fully extended with palm facing down
Flexion	Humerus flexed 30° and elbow fully extended with palm faces medially
Extension	Humerus flexed 90° and elbow fully extended with palm faces medially

Table 4. The description of the dynamic tasks.

Task	Description
Grooming	Arm on the side of the body at rest. Raised the arm and moved the hand toward the forehead with the palm facing the forehead. Moved the hand from the forehead toward the top of the head. Then, toward the back of the head. Returned to the resting position.
Box lifting	At rest, lift a 44.5 N (10 lbs) weight with both extended arms from waist level to chest level. Held the weight for 3 seconds at chest level. Then, lowered the weight back to the waist level.
One-Arm Chest Press	The weight was set at 44.5 N (10 lbs) with the machine arm set at 90° and at chest level (Figure 14-A). At rest, held the handle at chest level with the back facing the Tonal machine. Pushed the handle towards the front slowly and extended the arm fully (Figure 14-B). Held for 3 seconds, and returned to the starting position.
One-Arm Row	The weight was set at 44.5 N (10 lbs) with the machine arm set at 90° and at chest level (Figure 15-A). At rest, held the handle with the humerus flexed at 90° and the elbow fully extended (Figure 15-B). Slowly pulled the cable and brought the handle toward the side of the chest. Held for 3 seconds. Then, returned to the starting position.
One-Arm Face Pull	The weight was set at 44.5 N (10 lbs) with the machine arm set at 150° and at head level (Figure 16-A). In a standing position, held the handle with the humerus flexed at 150° and the elbow fully extended (Figure 16-B). Slowly pulled the cable and brought the handle toward the side of the forehead. Held for 3 seconds. Then, returned to the starting position.
Weight Relief Lifting	In a seated and resting position, put both hands on the table (Figure 17-A). Pushed down and lift the weight of their body with their hands (Figure 17-B). Stood up and rested for 3 seconds (Figure 17-C). Then, returned to the resting position.

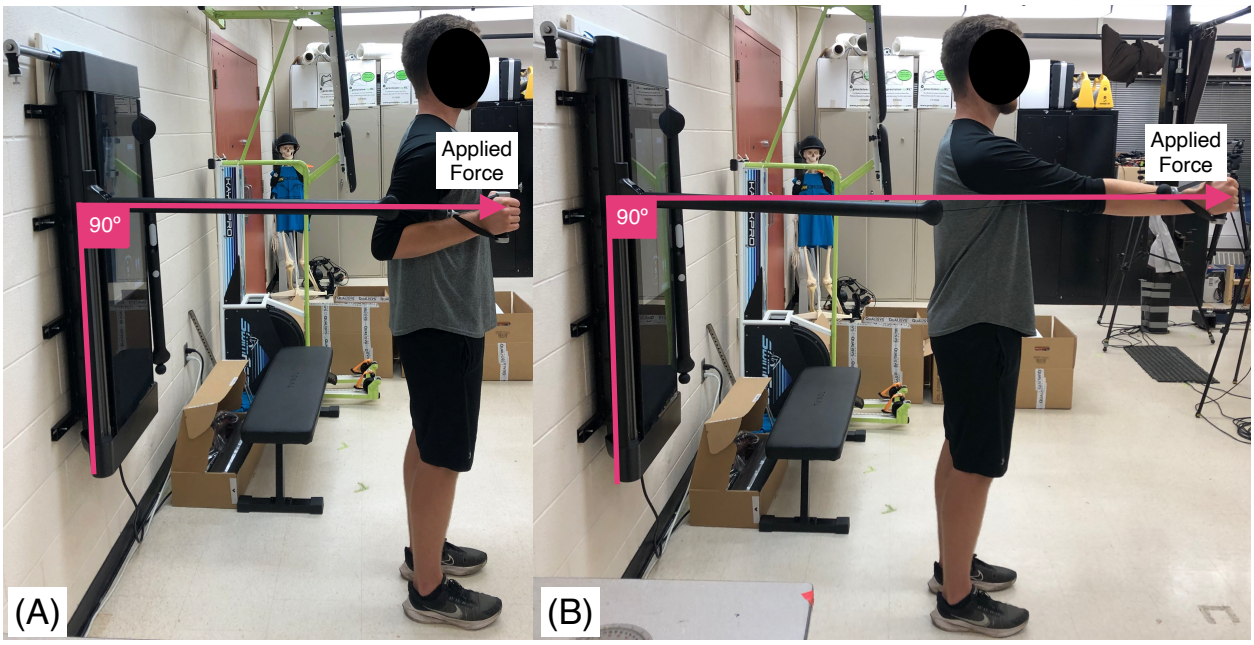

Figure 14. The one-arm chest press task with the Tonal machine arm set at 90º in (A) starting position and (B) ending position.

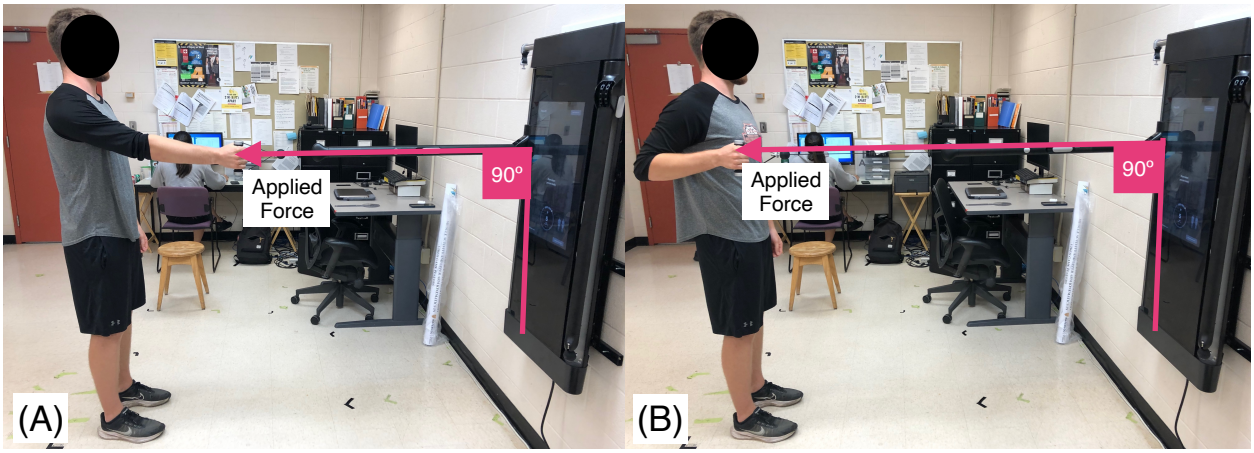

Figure 15. The one-arm row task with the Tonal machine arm set at 90º in (A) starting position and (B) ending position.

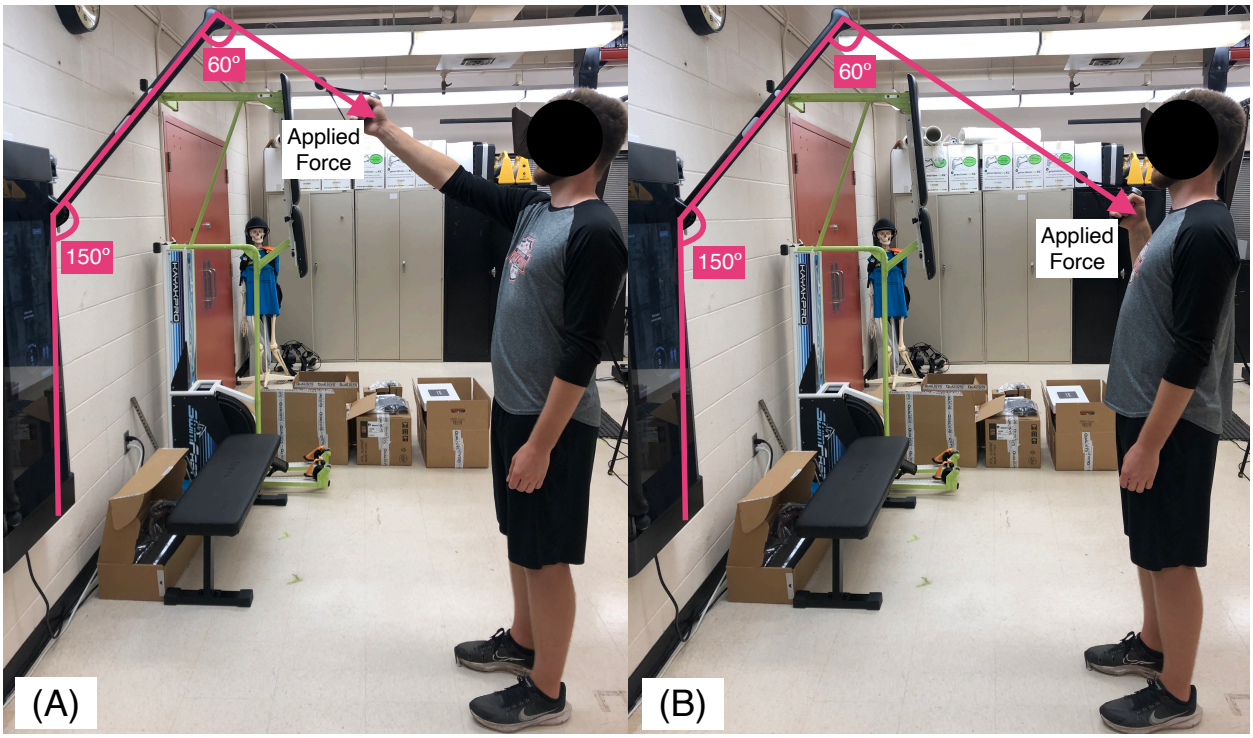

Figure 16. The one-arm face pull task with the Tonal machine arm set at 150º in (A) starting position and (B) ending position.

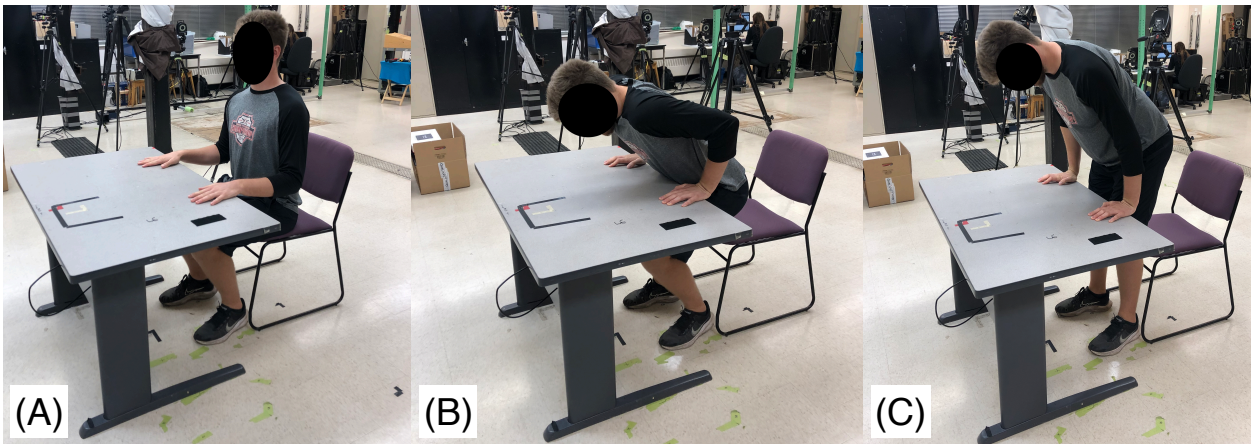

Figure 17. The weight relief task in (A) starting position, (B) lifting position, and (C) standing position.

3.4 Data Processing

3.4.1 Motion Capture Processing

Raw kinematic data was digitized with marker landmarks labelled using VICON Nexus software (VICON, Oxford, UK). If any individual marker was blocked or dropped out and the missing window was 50 frames or less (Howarth & Callaghan, 2010), the local coordinate of the marker was reconstructed based on the calibrated anatomical landmarks of the marker cluster. Digitized kinematic data was converted from CSV files to LOC files (Figure 18), then filtered using a low-pass, 2nd order, dual-pass Butterworth filter with an effective cut-off frequency of 6 Hz (per Dickerson et al., 2007).

The filtered data were used to calculate the local coordinate systems and the unit vectors of the right hand, right forearm, and right upper arm (Dickerson et al., 2007; Nigg & Herzog, 1994). The joint centre of the glenohumeral, elbow and wrist joints was defined (Nussbaum & Zhang, 2000). The centre of the glenohumeral joint was defined as 60 mm from the acromial process caudally along the z-axis of the torso segment. Both the elbow joint centre and wrist joint were defined as the mid-point of the medial and lateral epicondyles, and the ulnar and radial styloid processes, respectively. Rotation matrices and rotation axes were formulated based on the LCS of the defined segments, then Euler rotational sequence was generated for each segment (Eq. 1 & 2). Global glenohumeral joint forces and torques were calculated based on the LCS of the defined segments through inverse dynamic equilibriums (Eq. 3 & 4). Then, transformed into the glenoid coordinate system. All these calculations were done through the SLAM model using Matlab 2022b (MathWorks, Massachusetts, USA). Then, each experiment task was evaluated based on the SLAM model predicted muscle forces.

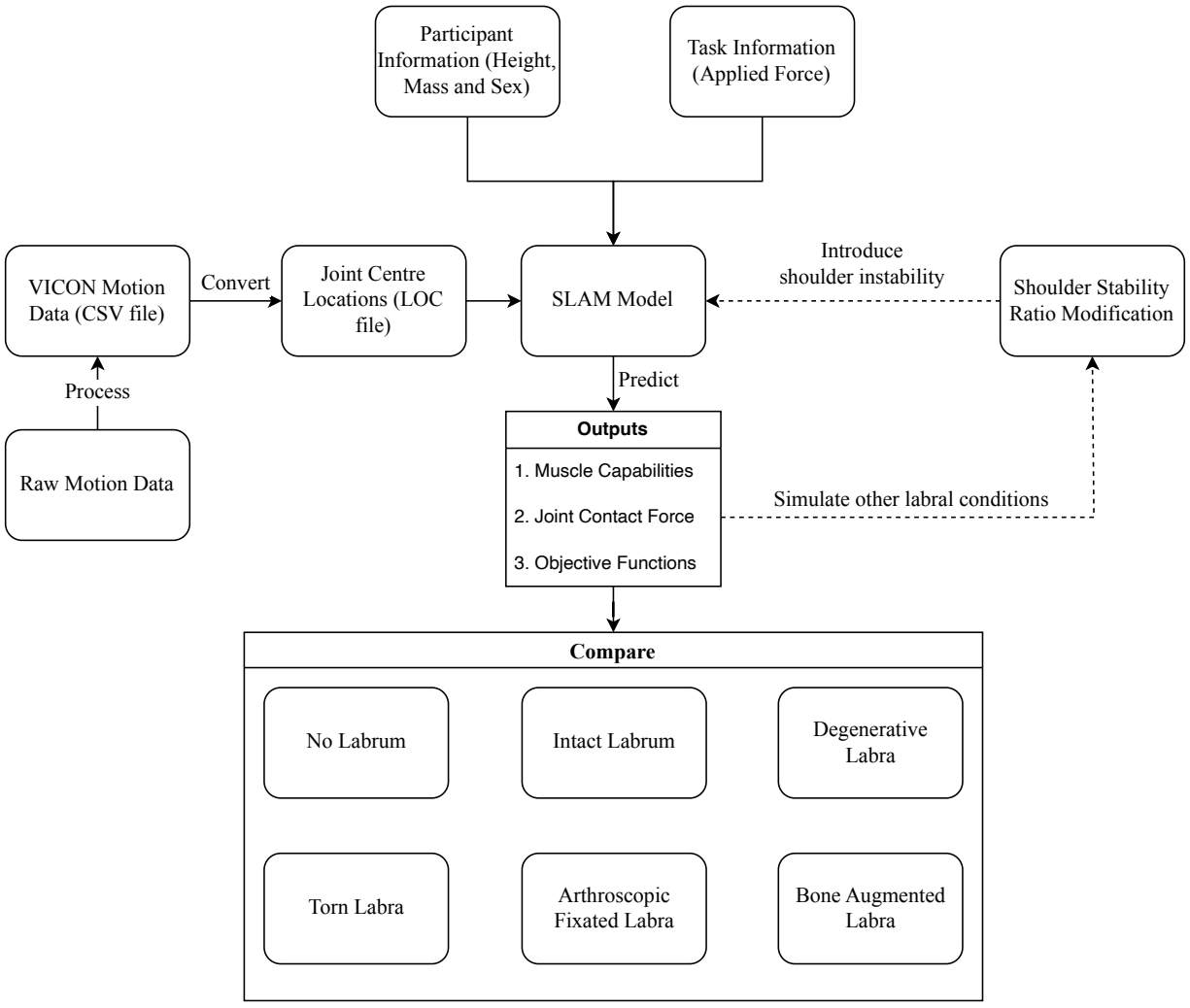

Figure 18. The data flow to simulate and predict task performance in different labral conditions. The dotted lines indicate the alteration of the shoulder stability ratio to simulate another labral condition after task simulation.

3.4.2 Modifications of the SLAM model

Since the goal of this study was to evaluate the variations in muscle activation with different labral conditions, alterations to the glenoid stability ratio (Figure 9) were applied within the muscle force prediction module, specifically changing some combination of the directional shoulder stability vectors (S'_i) by introducing instability ratios (I) to equation 5 (Eq. 7) to modify the glenohumeral contact force constraints in the model (Figure 18). A total of 13 labral conditions, including the intact labrum, no labrum, age-degenerative labra (3), torn labra (3), and arthroscopically managed labra (5), were simulated via the SLAM model (Table 5). The magnitudes of modification were based on previously reported biomechanical and histological changes (Alashkham et al., 2020; Black et al., 1999; Clavert, 2015; Kleiner et al., 2016; Lippitt & Matsen, 1993; Panossian et al., 2005; Patzer et al., 2012; Pfahler et al., 2003; Wellmann et al., 2011).

$$S_i' = \frac{F_s}{F_c} * I \qquad \text{(Eq. 7)}$$

Table 5. Descriptions of simulated labrum conditions.

Condition	Scenario	Stability Ratio Modification (*I*)
1	Intact Labrum (Ages 18–40)	No modification (Pfahler et al., 2003).
2	No Labrum	An average of 24% decreased in all 8 directions (Lippitt & Matsen, 1993).
3	Ages 41–60 (Type I SLAP)	An average of 7% decreased at 0° and 45° (Alashkham et al., 2020; Pfahler et al., 2003).
4	Ages 61–80	An average of 7% decreased in all 8 directions (Alashkham et al., 2020; Pfahler et al., 2003).
5	Ages >80	An average of 13% decreased in all 8 directions (Alashkham et al., 2020; Pfahler et al., 2003).
6	Type II SLAP	An average of 16% decreased at 0°, 45° and 315° (Clavert, 2015; Panossian et al., 2005; Patzer et al., 2012).
7	Bankart Lesion	An average of 25% decreased at 90°, 135° and 180° (Black et al., 1999; Clavert, 2015).
8	Reverse Bankart Lesion	An average of 38% decreased at 180°, 225° and 270° (Clavert, 2015; Wellmann et al., 2011).
9	Repaired SLAP	An average of 42% improved from condition 7 at 0°, 45° and 315° (Panossian et al., 2005; Patzer et al., 2012).
10	Repaired Bankart	An average of 71% improved from condition 8 at 90°, 135° and 180° (Black et al., 1999; Clavert, 2015).
11	Repaired Reverse Bankart	An average of 120% improved from condition 9 at 180°, 225° and 270° (Wellmann et al., 2011).
12	Latarjet	An average of 128% improved from condition 8 at 45°, 90° and 135° (Kleiner et al., 2016).
13	Posterior Bone Block	An average of 135% improved from condition 9 at 180°, 225° and 270° (Wellmann et al., 2011).

Note: SLAP = Superior Labrum Antero-to-Posterior Lesion.

3.5 Data Analysis

Descriptive outputs from all labrum conditions were generated by the SLAM model. A total of 13 conditions were simulated for each task (12 tasks) which entailed 156 simulations that generated outputs including peak and sum of muscle forces, glenohumeral joint contact forces, and cost function magnitudes. %MMC (percentages of maximal predicted muscle capacity) of each muscle element based on their PCSA (including latissimus dorsi (2), pectoralis major (2), deltoids (3), coracobrachialis, infraspinatus (2), subscapularis (3), supraspinatus, teres major and minor, biceps (2), triceps (1)) were used to highlight changes in muscle recruitment strategies when performing each movement task under each condition where 0%MMC represents no recruitment for the corresponding muscle. In addition, task cost and demand of each task were represented using the magnitude of the cost function (sum of the cubed muscle stresses) (Eq. 5).

Since there were more than 5000 variables to report, rankings of changes in %MMC between the two major shoulder muscle groups (Table 6) which are the rotator cuff muscles and the glenohumeral articulating muscles were used instead to consolidate and streamline the bulky dataset. The percentage of maximal predicted muscle group capability (%MMGC) was calculated as the sum of scaled muscle forces and scaled based on the proportional PCSA of the corresponding muscles within the muscle group (Table 6) (Karlsson & Peterson, 1992). Next, these groups were evaluated for the potential changes in the recruitment of muscle groups, absolute changes in %MMGCs and percentage changes in %MMGCs. Specifically, this entailed descriptive comparisons of %MMGC levels between:

1) Age groups
2) Degenerative labra and torn labra
3) Repaired labra and the intact labrum

Table 6. List of muscles with proportional PCSA within the two shoulder muscle groups (Karlsson & Peterson, 1992).

Rotator Cuff (RC) Muscles	Normalized PCSA	Glenohumeral Articulating (GA) Muscles	Normalized PCSA
Supraspinatus	0.16	Anterior Deltoid	0.09
Infraspinatus (Superior)	0.16	Middle Deltoid	0.12
Infraspinatus (Inferior)	0.17	Posterior Deltoid	0.11
Subscapularis (Superior)	0.13	Teres Major	0.09
Subscapularis (Middle)	0.12	Coracobrachialis	0.04
Subscapularis (Inferior)	0.16	Pectoralis Major (Sternum Part)	0.09
Teres Minor	0.08	Pectoralis Major (Clavicle Part)	0.06
		Latissimus Dorsi (Superior)	0.06
		Latissimus Dorsi (Inferior)	0.07
		Biceps Brachii (Long Head)	0.05
		Biceps Brachii (Short Head)	0.04
		Triceps Brachii (Long Head)	0.19

Note: PCSA = Physiological Cross-Sectional Area.

Additionally, the changes in GH joint shear forces were compared among conditions, to highlight the relationship between the changes in joint contact forces and potential compensatory muscle strategies. The percentage changes in magnitude and directional changes in GH joint shear forces were reported in the horizontal (anterior(+)/posterior(-)) and vertical (superior(+)/inferior(-)) directions, along with changes in joint compression forces. Further, directional changes of resultant joint shear forces were reported in all 8 equally-spaced directions (Figure 9) and related to potential muscle group fatigue. In addition, mean and maximum values of %MMGCs and contact forces for dynamic tasks were calculated from the 7^{th} repetition of the corresponding dynamic activity where the model was able to simulate all conditions successfully. Task performance rankings and changes in joint contact forces were used to reflect potential shoulder challenges associated with the simulated conditions and activities.

IV. Results

The results are presented by task and focused on the apparent changes across all 6 isometric exercises and functional ADLs. Cost function magnitudes are presented as task costs. The results for each task first compare the percentage changes in mean and maximum %MMGCs of each activity among all simulated labral conditions. Then, the results of the percentage changes in mean directional shear forces and compression forces of each task under simulated labral conditions are contrasted. Finally, the directional changes in mean resultant shear forces were compared for each task. Results for each task's mean, maximum and percentage changes in %MMGCs; mean and percentage changes in costs under all simulated labral conditions by tasks are reported in Appendix A. Also, mean and percentage changes in directional shear forces; mean and percentage changes in resultant shear forces; and mean directions of the resultant shear forces under all simulated labral conditions by task are reported in Appendix B.

4.1 Isometric Internal Rotation

During isometric internal rotation, minor increases in mean and maximum %MMGCs occurred under certain simulated labral conditions. When compared to the intact scenario, the %MMGCs of RC muscles increased by 1%–3% when the labrum was removed and at ages over 60 (Figure 19) where task demands increased by 2%–7% (Table 7). Similarly, the activation level of GA muscles was elevated by 7% under the above-simulated conditions and in reverse Bankart lesion (RBKT). %MMGCs in both muscle groups returned to a similar level as in intact condition after surgical repairs. For context, the activation levels of GA muscles were about half the levels of RC muscles under all simulated conditions.

Noticeable changes in GH joint contact forces occurred as posterior joint shear forces (PSFs) decreased by 5%–25% under no labrum, at ages over 60 and RBKT (Table 7). Also, inferior joint shear forces (ISFs) increased by 17% and 75% in no labrum and RBKT, respectively. Moreover, ISFs decreased by 14%–36% at ages over 60, with a SLAP lesion (SLAP), and a posterior bone block (PBB). In addition, resultant shear force directions (RSFs) were between 223.8°–248.5° (Figure 15) with 4%–15% decreases in no labrum, ages over 60 and SLAP; a 17% increase in RBKT (Table 7). In no labrum and RBKT, joint compression forces (JCFs) increased by about 1% (Table 7).

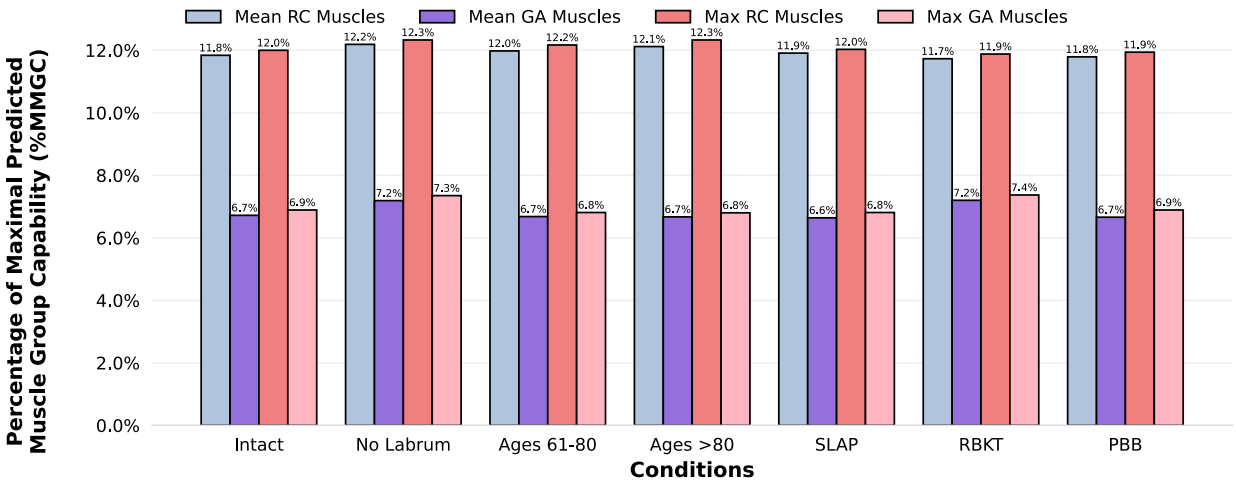

Figure 19. Mean and maximum percentages of maximal predicted muscle group capability (%MMGC) of rotator cuff (RC) muscles and glenohumeral articulating (GA) muscles during isometric internal rotation under certain simulated conditions.

Table 7. Mean glenohumeral joint contact forces and task costs during isometric internal rotation under certain simulated conditions.

Condition	ASF(+)/PSF(-) (N)	SSF(+)/ISF(-) (N)	RSF (N)	JCF (N)	Cost (N^3cm^6)
Intact	-181.91	-100.38	207.8	928.36	566733
No Labrum	-137.38	-117.8	180.99	941.37	605959
Ages 61–80	-172.22	-81.34	190.49	927.73	576228
Ages >80	-163.77	-64.71	176.19	927.89	587393
SLAP	-180.68	-84.25	199.42	926.49	569526
RBKT	-167.92	-175.17	242.7	940.07	573644
PBB	-197.62	-86.34	215.76	926.67	561932

Note: ASF = Anterior Joint Shear Force; PSF = Posterior Joint Shear Force; SSF = Superior Joint Shear Force; ISF = Inferior Joint Shear Force; JCF = Joint Compression Force; SLAP = Superior Labrum Antero-to-Posterior Lesion; RBKT = Reverse Bankart Lesion; PBB = Posterior Bone Block. Cost represents the magnitude of the cost function.

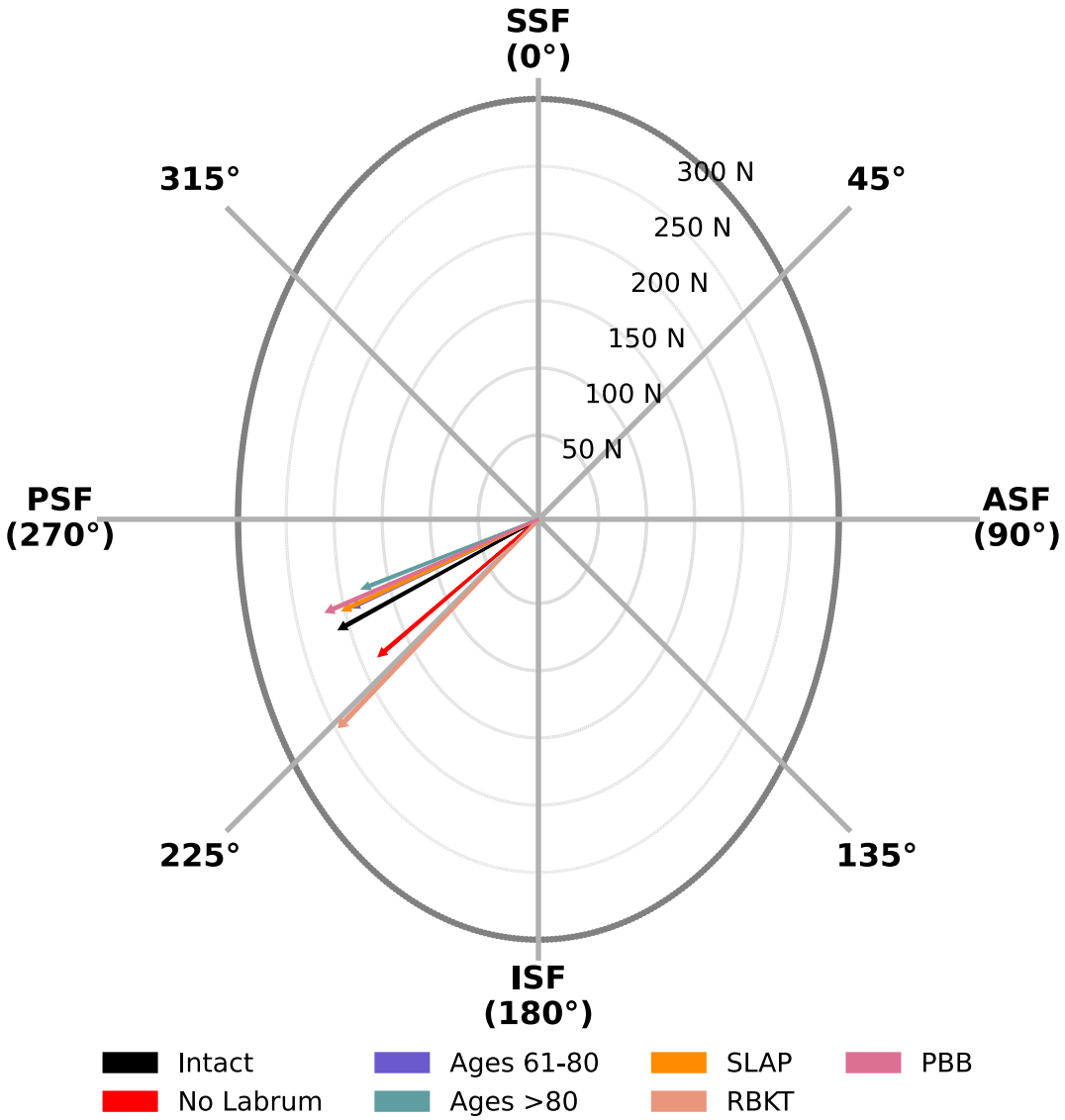

Figure 20. Mean glenohumeral joint resultant shear forces in 8 equally spaced compass directions of the glenoid during isometric internal rotation under certain simulated conditions. The length of each arrow represents the magnitude of resultant shear forces under corresponding simulated conditions.

4.2 Isometric External Rotation

Throughout the isometric external rotation, substantial increases in %MMGCs existed for several simulated conditions. In RC muscles, %MMGCs increased by 13%–40% in no labrum and ages over 60 (Figure 21) along with 33%–141% increases in task costs (Table 8). A minor 7% raise in RC muscle activation level with a 16% increase in task cost occurred in SLAP. Similarly, the %MMGCs of GA muscles increased by 5%–30% in no labrum and ages over 60. However, %MMGCs of both muscle groups appeared not noticeably change to intact after repairs. Additionally, %MMGCs in RC muscles were about 4 times higher than in GA muscles under all conditions.

Among some simulated conditions, minor changes in joint contact forces arose compared with an intact labrum. PSFs increased by 2%–6% with ISFs increased by 1%–7% in no labrum, ages over 60 and SLAP (Table 8). Further, the directions of RSF were not notably changed among all simulated conditions. However, minor (1%–7%) increases in RSF magnitudes existed for some conditions (Figure 22). In addition, JCFs increased by 6%–33% in no labrum, ages over 60 and SLAP (Table 8).

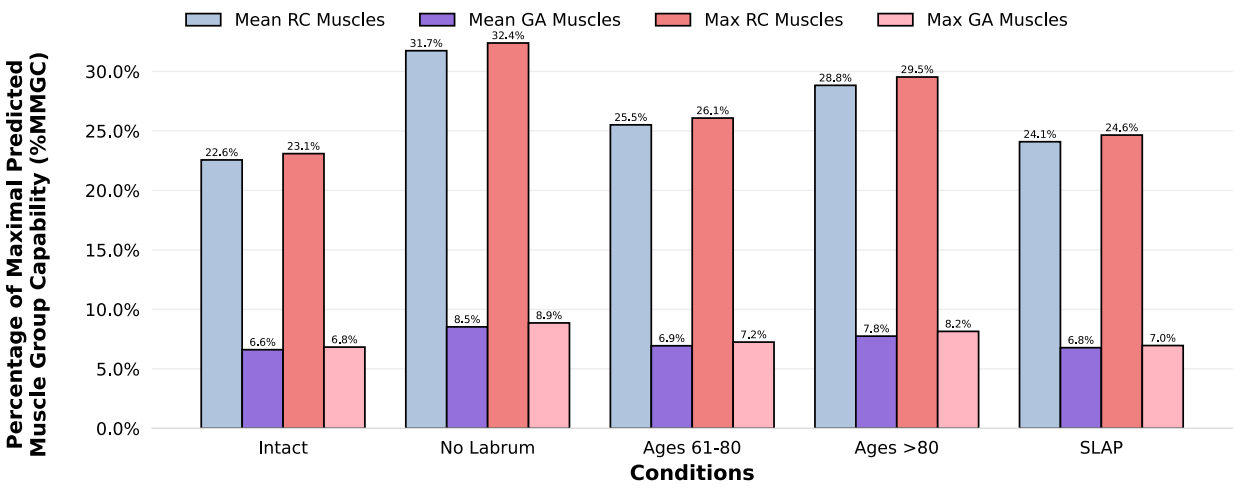

Figure 21. Mean and maximum percentages of maximal predicted muscle group capability (%MMGC) of rotator cuff (RC) muscles and glenohumeral articulating (GA) muscles during isometric external rotation under certain simulated conditions.

Table 8. Mean glenohumeral joint contact forces and task costs during isometric external rotation under certain simulated conditions.

Condition	ASF(+)/PSF(-) (N)	SSF(+)/ISF(-) (N)	RSF (N)	JCF (N)	Cost (N^3cm^6)
Intact	-258.26	-269.45	373.29	1446.01	858395
No Labrum	-273.73	-288.33	397.66	1929.91	2067089
Ages 61–80	-263.65	-275.95	381.73	1603.09	1144145
Ages >80	-269.28	-282.81	390.59	1778.23	1574650
SLAP	-261.12	-272.89	377.77	1527.95	996692

Note: ASF = Anterior Joint Shear Force; PSF = Posterior Joint Shear Force; SSF = Superior Joint Shear Force; ISF = Inferior Joint Shear Force; JCF = Joint Compression Force; SLAP = Superior Labrum Antero-to-Posterior Lesion. Cost represents the magnitude of the cost function.

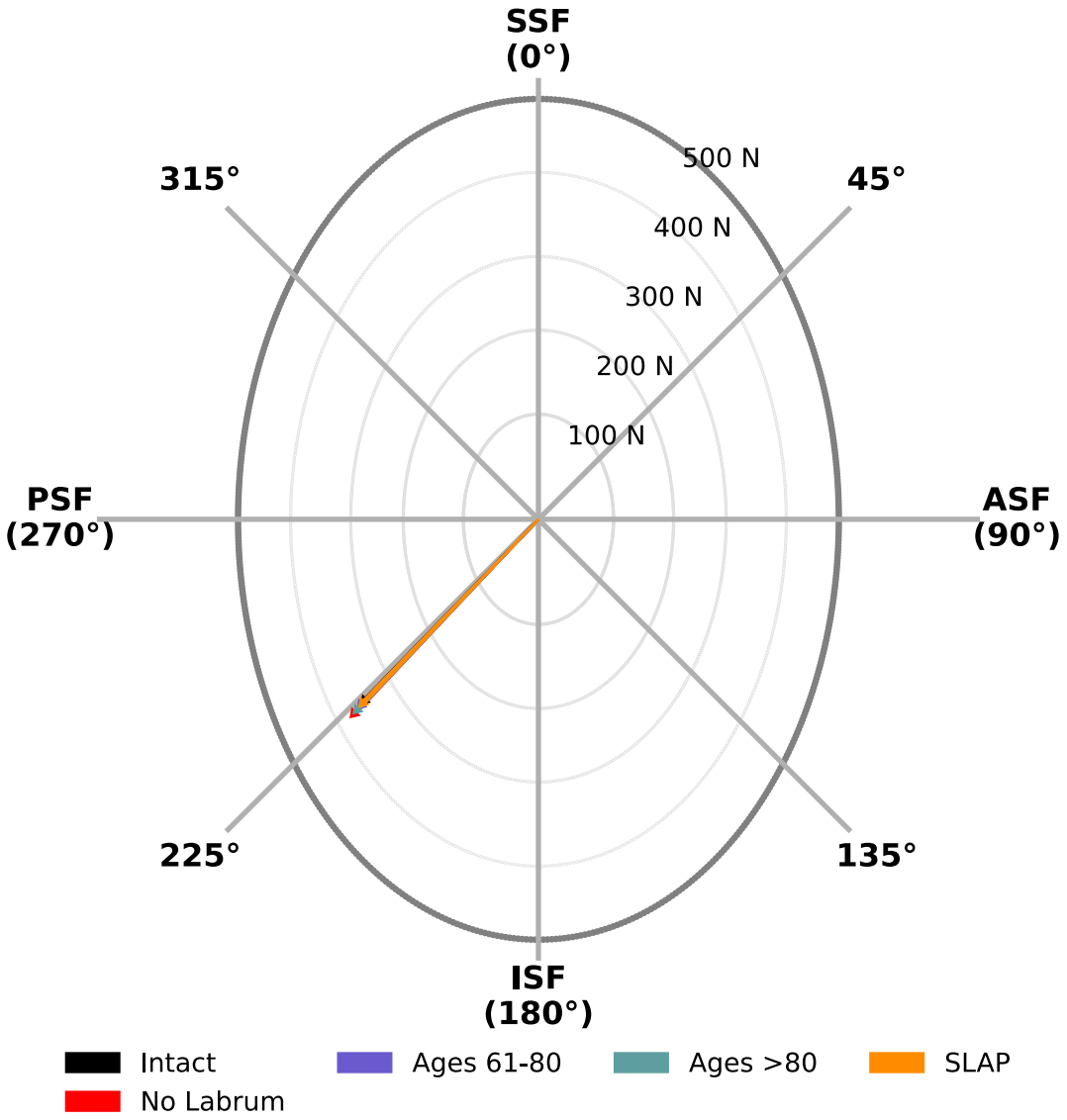

Figure 22. Mean glenohumeral joint resultant shear forces in 8 equally spaced compass directions of the glenoid during isometric external rotation under certain simulated conditions. The length of each arrow represents the magnitude of resultant shear forces under corresponding simulated conditions.

4.3 Isometric Abduction

During isometric abduction, RC muscle activation levels appeared to change under certain simulated conditions. Compared to the intact condition, %MMGCs resulted in 4%–25% increases in no labrum, ages over 60, and SLAP (Figure 23). However, %MMGCs of GH muscles increased only approximately 3% in no labrum even though the task was 4%–26% more demanding under the simulated conditions above (Table 9). After surgical repairs were simulated, activation levels of both muscle groups approximated the intact condition. Moreover, activation levels were twice as high in RC muscles as in GH muscles when performing the isometric abduction under all simulated conditions.

No notable changes emerged in joint shear forces except a minor ~2% decrease in ISFs under the no labrum condition and at ages over 80 (Table 9). Additionally, RSFs were at about 227° under all simulated conditions (Figure 24) with no notable changes in RSF magnitudes (enumerated in Table 9). However, the magnitudes of JCF increased by 7%–21% in no labrum and ages over 60 (Table 9).

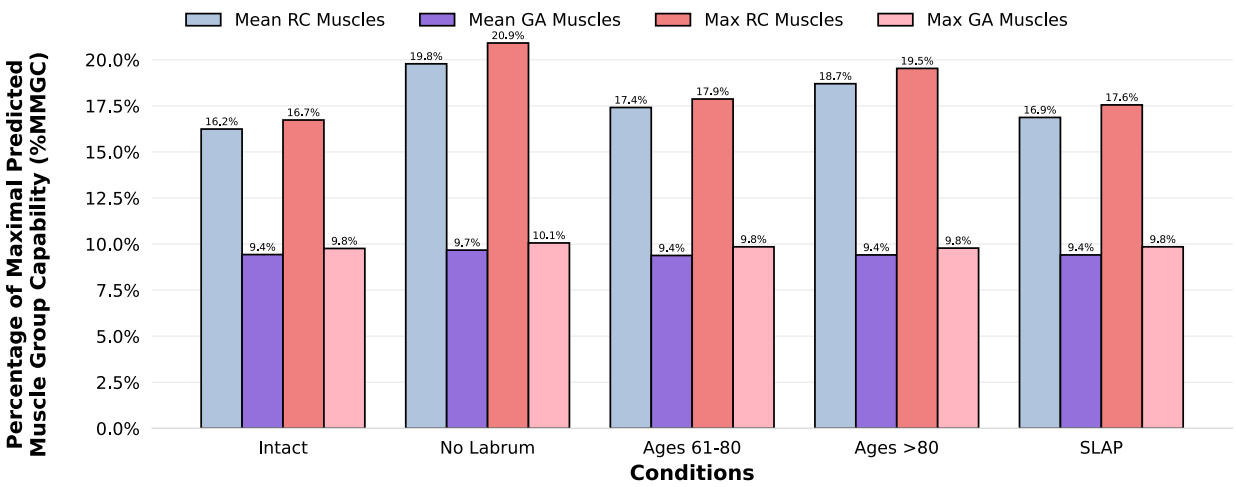

Figure 23. Mean and maximum percentages of maximal predicted muscle group capability (%MMGC) of rotator cuff (RC) muscles and glenohumeral articulating (GA) muscles during isometric abduction under certain simulated conditions.

Table 9. Mean glenohumeral joint contact forces and task costs during isometric abduction under certain simulated conditions.

Condition	ASF(+)/PSF(-) (N)	SSF(+)/ISF(-) (N)	RSF (N)	JCF (N)	Cost (N^3cm^6)
Intact	-197.35	-184.97	270.75	959.5	1605322
No Labrum	-196.17	-181.35	267.52	1164.37	2018015
Ages 61–80	-196.56	-183.46	269.17	1027.73	1728006
Ages >80	-196.24	-182.23	268.14	1102.12	1875961
SLAP	-197.01	-184.24	270.02	995.9	1668255

Note: ASF = Anterior Joint Shear Force; PSF = Posterior Joint Shear Force; SSF = Superior Joint Shear Force; ISF = Inferior Joint Shear Force; JCF = Joint Compression Force; SLAP = Superior Labrum Antero-to-Posterior Lesion. Cost represents the magnitude of the cost function.

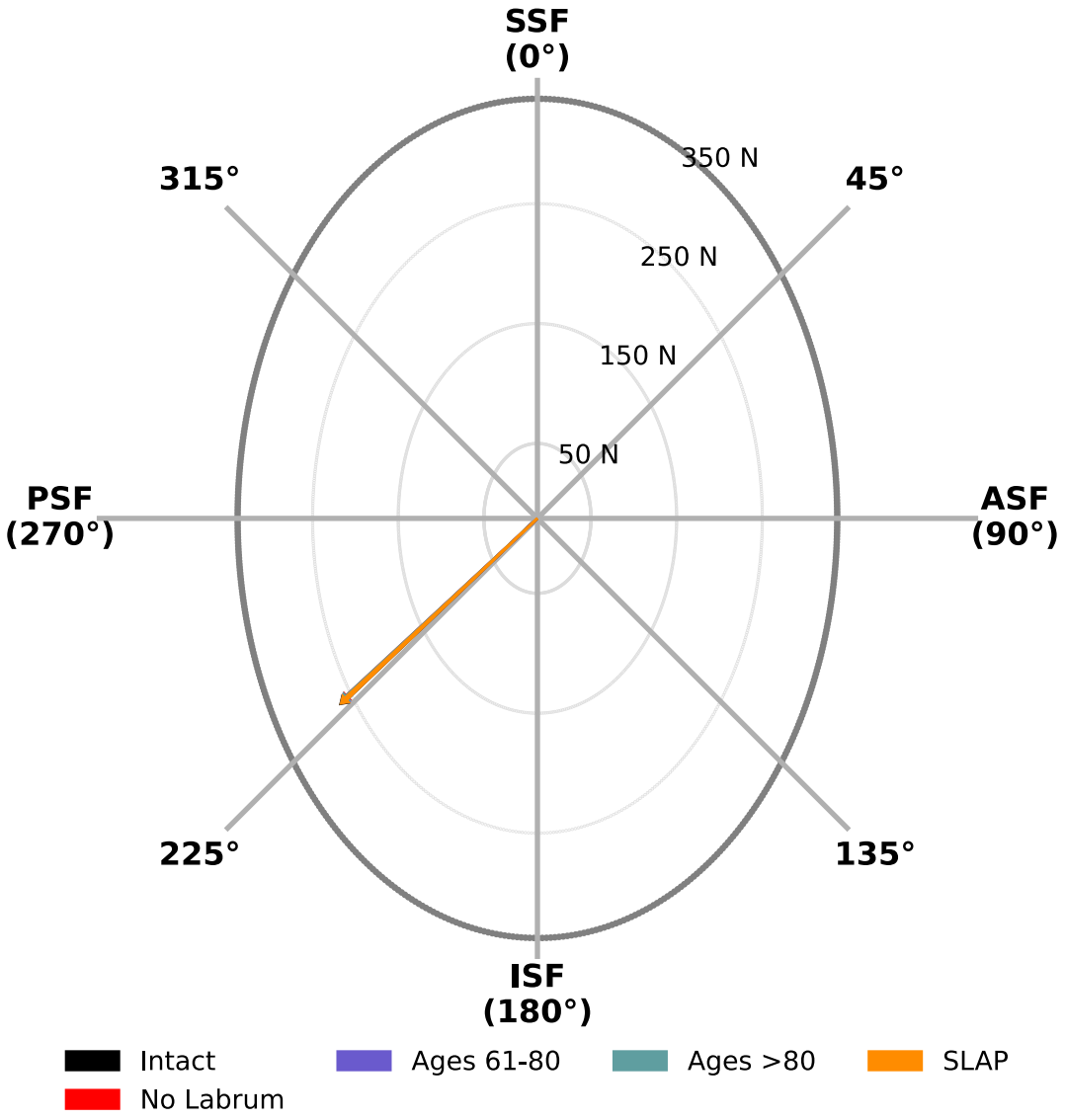

Figure 24. Mean glenohumeral joint resultant shear forces in 8 equally spaced compass directions of the glenoid during isometric abduction under certain simulated conditions. The length of each arrow represents the magnitude of resultant shear forces under corresponding simulated conditions.

4.4 Isometric Adduction

Throughout isometric adduction, %MMGCs in both muscle groups illustrated distinguishable changes under a few simulated conditions. %MMGCs demonstrated 17%–55% reductions in RC muscles and GA muscles %MMGCs increased by 5%–22% in no labrum, ages over 80, and RBKT (Figure 25). Additionally, task costs increased by 13%–49% for these same conditions (Table 10). Subsequently, after the reverse Bankart lesion repair (ReRBKT), the activation level of RC muscles increased by about 111% with an accompanying ~17% decrease in GA muscles %MMGC when compared to BKT. Further, task cost in ReRBKT was 31% lower than in RBKT. Moreover, the task demand in PBB decreased by 19% and RC muscle %MMGCs were about 10% higher with an approximate 10.5% decrease in GA muscles (Figure 25). No major changes in %MMGCs occurred after other surgical techniques were simulated. Under all simulated conditions, %MMGCs in GA muscles were 4–10 times more than in RC muscles.

Substantial changes in joint contact forces occurred for these same simulated conditions. When compared to the intact condition, PSFs decreased by 9%–22% with 7%– 67% decreases in superior joint shear forces (SSFs) in no labrum, at ages over 80, and RBKT (Table 10). Similarly, RSFs were reduced by 8%–39%. Furthermore, PSF increased by 18% along with a 23% increase in SSF, resulting in a 20% increase in RSF in PBB. In addition, JCFs increased by 6%–23% in no labrum, ages over 80 and RBKT, and decreased by 14% in PBB (Table 10). Finally, notable changes in RSF directions existed only for the no labrum and RBKT simulations, by 24° and 16.5°, respectively (Figure 26).

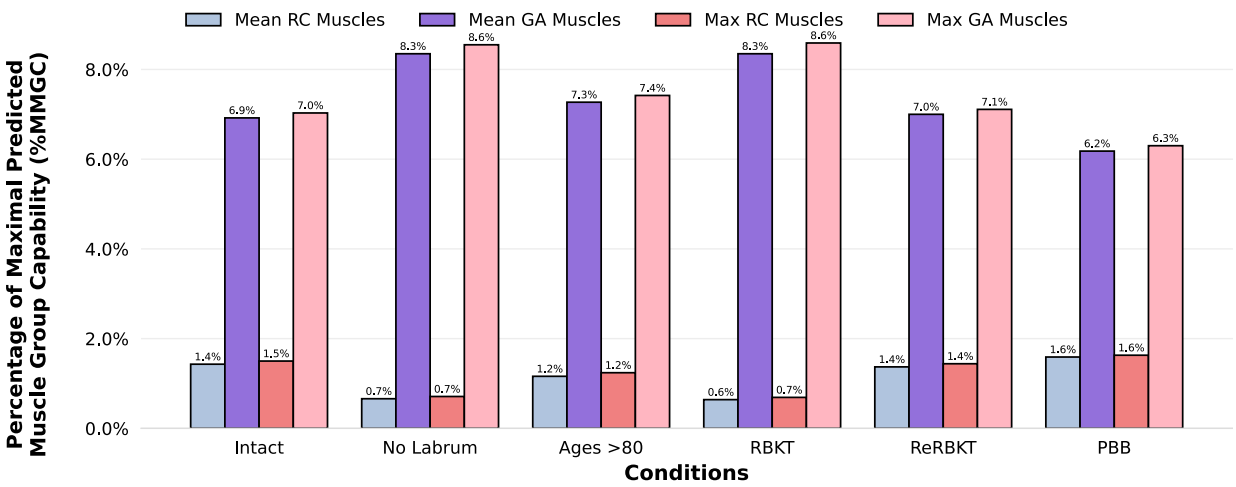

Figure 25. Mean and maximum percentages of maximal predicted muscle group capability (%MMGC) of rotator cuff (RC) muscles and glenohumeral articulating (GA) muscles during isometric adduction under certain simulated conditions.

Table 10. Mean glenohumeral joint contact forces and task costs during isometric adduction under certain simulated conditions.

Condition	ASF(+)/PSF(-) (N)	SSF(+)/ISF(-) (N)	RSF (N)	JCF (N)	Cost (N^3cm^6)
Intact	-107.33	+117.03	158.83	467.69	44233
No Labrum	-88.98	+38.81	97.13	565.27	63637
Ages >80	-98.26	+108.48	146.4	497.8	50003
RBKT	-83.79	+50.46	97.87	574.25	65992
ReRBKT	-105.4	+115.26	156.22	474.27	45383
PBB	-126.12	+143.55	191.09	403.6	36031

Note: ASF = Anterior Joint Shear Force; PSF = Posterior Joint Shear Force; SSF = Superior Joint Shear Force; ISF = Inferior Joint Shear Force; JCF = Joint Compression Force; RBKT = Reverse Bankart Lesion; ReRBKT = Repaired Reverse Bankart Lesion; PBB = Posterior Bone Block. Cost represents the magnitude of the cost function.

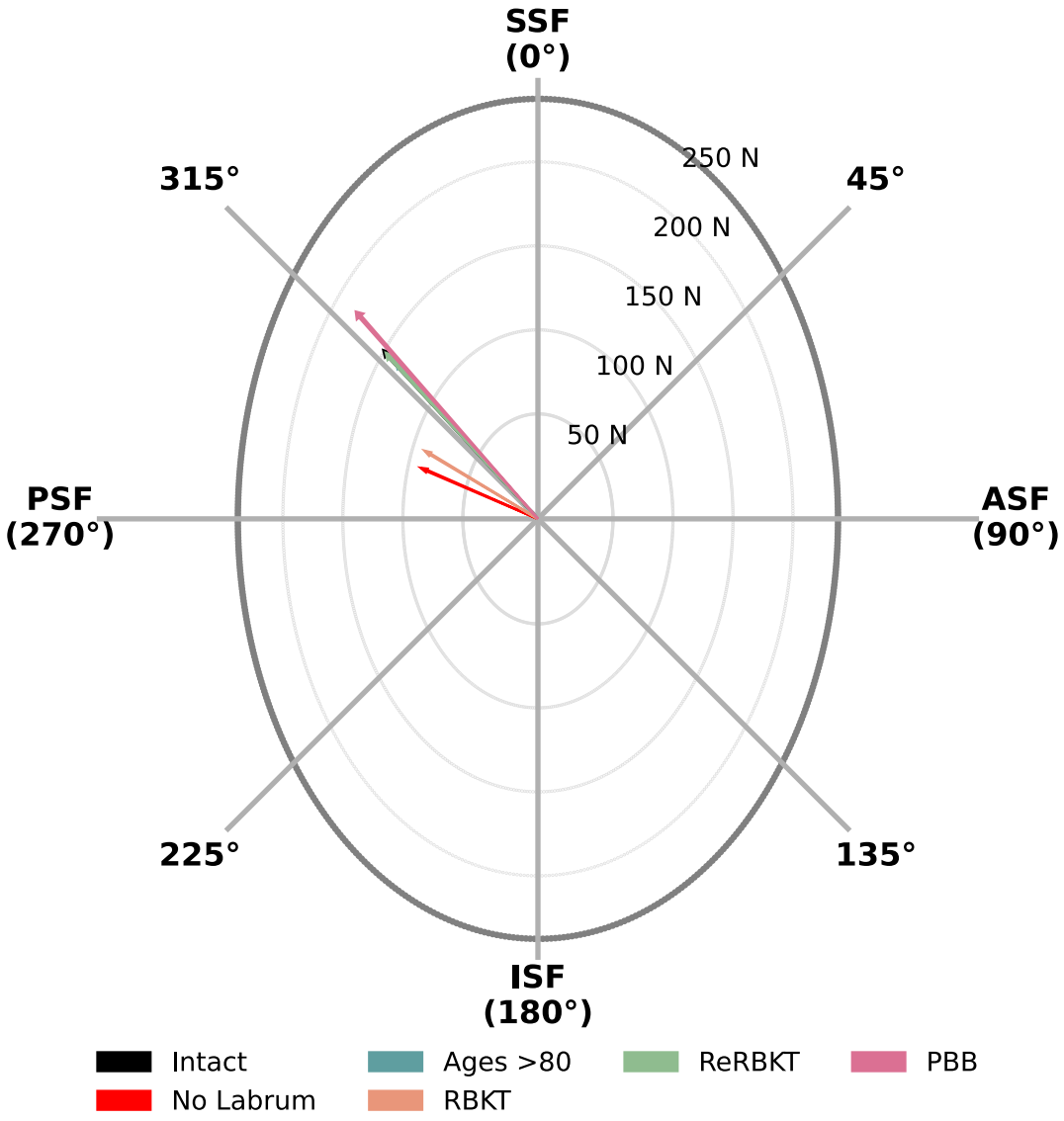

Figure 26. Mean glenohumeral joint resultant shear forces in 8 equally spaced compass directions of the glenoid during isometric adduction under certain simulated conditions. The length of each arrow represents the magnitude of resultant shear forces under corresponding simulated conditions.

4.5 Isometric Flexion

During isometric flexion, changes occurred in muscle activation levels under certain simulated conditions. When compared to the intact condition, minor 0.3%–3% decreases in %MMGCs existed in RC muscles with 2%–7% increases in GA muscles in no labrum, ages over 80, and RBank (Figure 27). Task costs increased by 2%–5% when performing flexion for the same conditions (Table 11). However, in PBB, the task cost decreased by 4% while RC muscle %MMGCs increased by about 3% with an approximate 7% drop in GA muscle activation levels (Figure 27). No major changes appeared in other simulated repaired conditions. Further, the activation levels of RC muscles were 1.5 times lower than GA muscles under all simulated conditions.

Joint contact forces showed substantial changes when compared to the intact condition among these highlighted conditions. PSFs decreased by 10%–27% and SSFs decreased by 32%–102% (Table 11). Hence, 12%–31% reductions in RSFs occurred, with ~20° change in direction for no labrum and RBKT (Figure 28). However, PSF increased by 23% with a 97% increase in SSF in PBB. Consequently, RSF increased by 34% with a 10.4° change from the intact condition. In addition, JCFs increased by 2%-6% in no labrum, ages over 80 and RBKT (Table 11). Further, in PBB, JCF decreased by 6% compared to the intact condition.

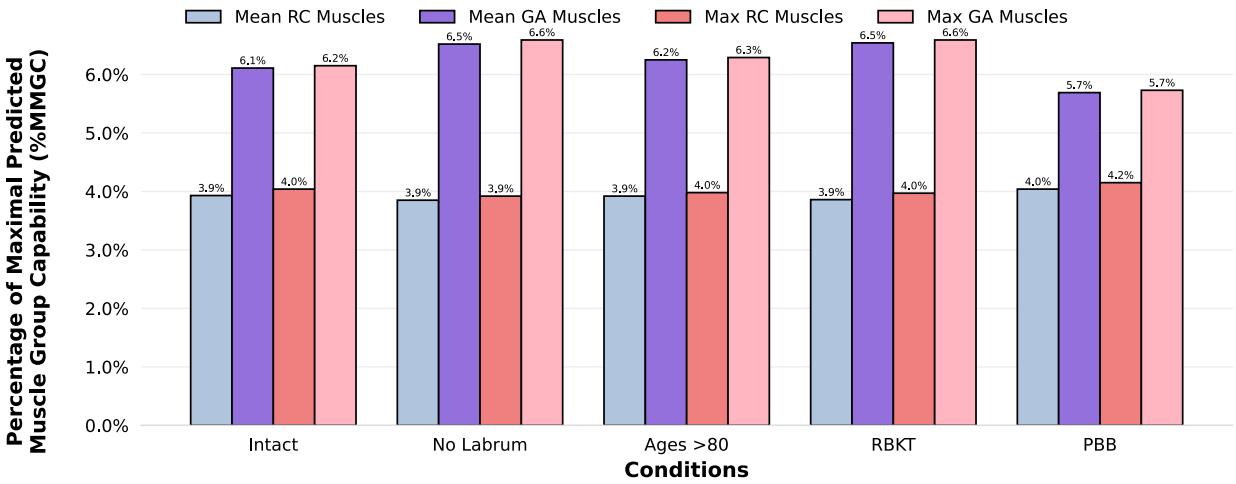

Figure 27. Mean and maximum percentages of maximal predicted muscle group capability (%MMGC) of rotator cuff (RC) muscles and glenohumeral articulating (GA) muscles during isometric flexion under certain simulated conditions.

Table 11. Mean glenohumeral joint contact forces and task costs during isometric flexion under certain simulated conditions.

Condition	ASF(+)/PSF(-) (N)	SSF(+)/ISF(-) (N)	RSF (N)	JCF (N)	Cost (N^3cm^6)
Intact	-95.1	+35.31	101.54	429.88	117359
No Labrum	-75.21	-0.12	75.23	453.03	122234
Ages >80	-85.44	+24.16	88.9	438.96	119444
RBKT	-69.51	-0.73	69.6	455.74	123410
PBB	-116.97	+69.65	136.19	404.97	113239

Note: ASF = Anterior Joint Shear Force; PSF = Posterior Joint Shear Force; SSF = Superior Joint Shear Force; ISF = Inferior Joint Shear Force; JCF = Joint Compression Force; RBKT = Reverse Bankart Lesion; PBB = Posterior Bone Block. Cost represents the magnitude of the cost function.

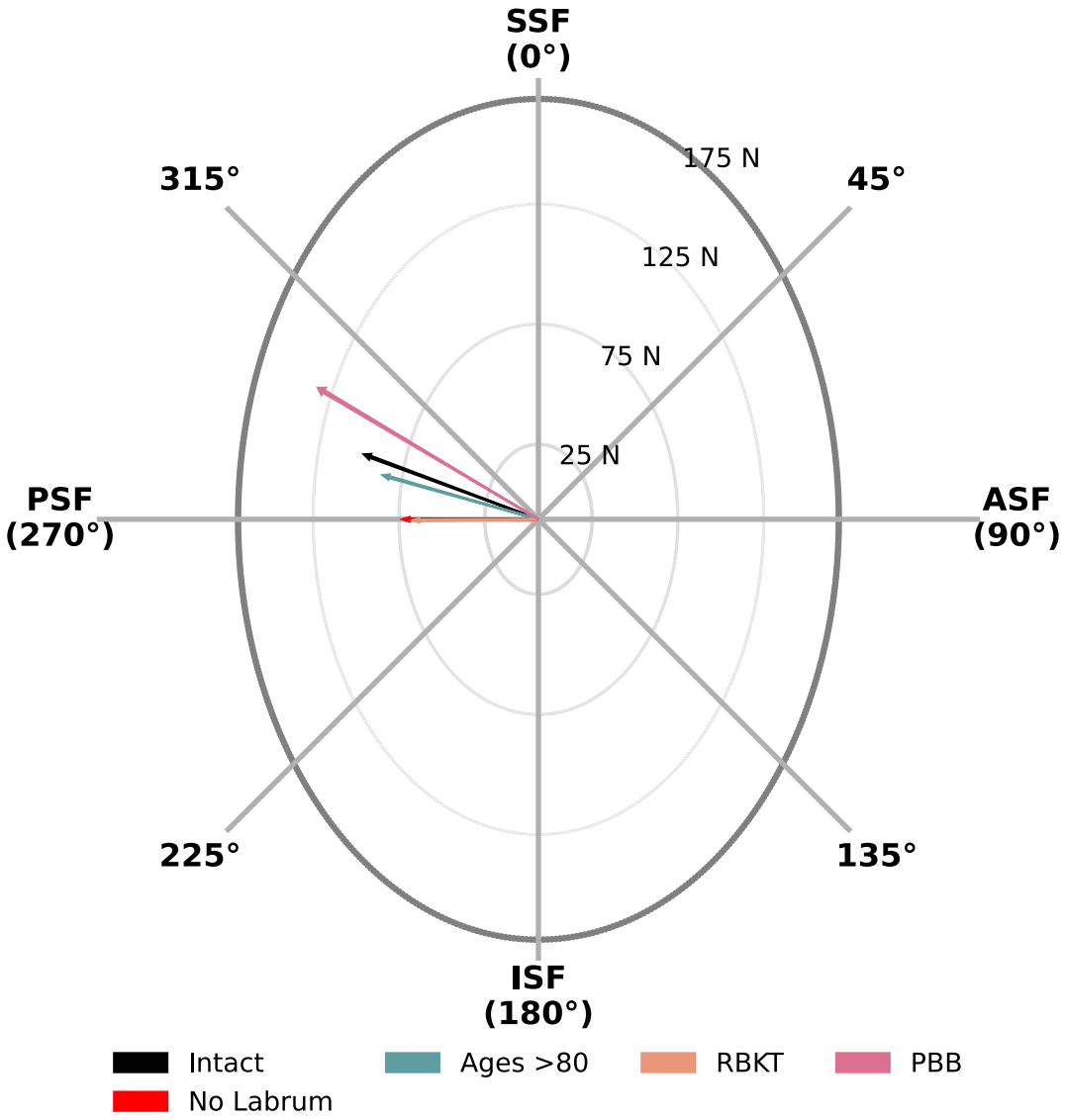

Figure 28. Mean glenohumeral joint resultant shear forces in 8 equally spaced compass directions of the glenoid during isometric flexion under certain simulated conditions. The length of each arrow represents the magnitude of resultant shear forces under corresponding simulated conditions.

4.6 Isometric Extension

In the isometric extension, similar changes occurred in %MMGCs under several conditions. Compared to the intact condition, RC muscle %MMGCs exhibited 9%-39% reductions with GA muscle %MMGCs increased by 4%–13% in no labrum, ages over 80 and RBKT (Figure 29). Concurrently, task costs increased by 6%–26% under these same conditions (Table 12). On the other hand, increases of 23%–31% occurred in RC muscle %MMGCs along with GA muscle %MMGCs were lowered by 2%–14% in Bankart lesion (BKT) and PBB conditions. Further, task demands in PBB decreased by 11%. In addition, the activation levels of GA muscles were 2–4 times higher than in RC muscles throughout the task.

Under the above-simulated conditions, joint contact forces had distinguishable changes compared to the intact condition. PSFs decreased by 15%–82% in no labrum, ages >80 and RBKT (Table 12); increased by 43% and 92% in BKT and PBB, respectively. Moreover, SSFs decreased by 4%–21% in no labrum, ages >80, BKT and RBKT where a 2% increase existed for PBB. Consequently, RSFs decreased by 7%–27% in no labrum, ages over 80, BKT and RBKT, with a 21% increase in PBB. Further, the direction of RSFs had 5.7°–18.1° changes (Figure 30). In addition, JCFs decreased by 8% in PBB compared to the intact condition (Table 12).

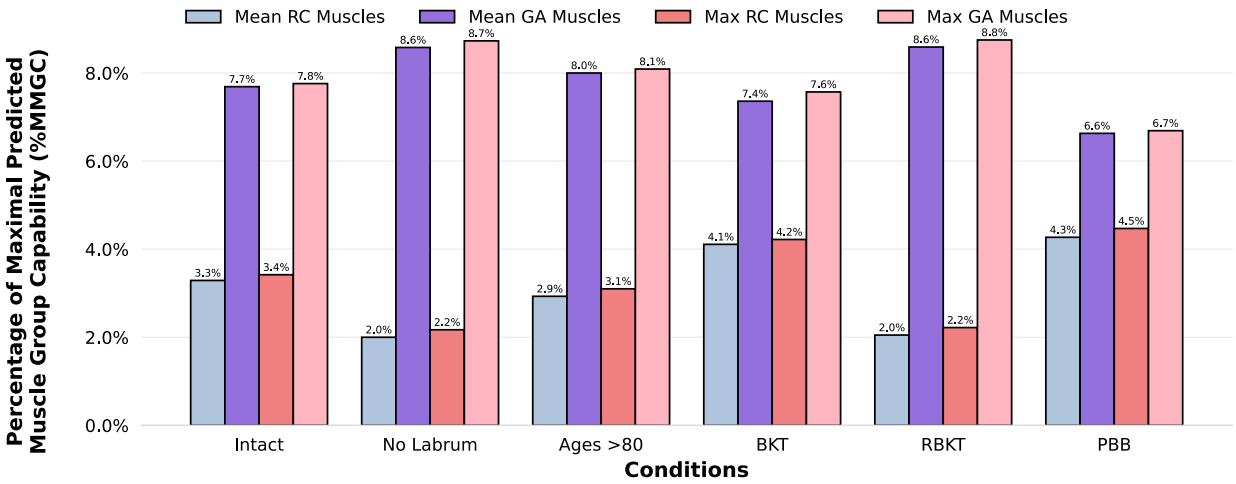

Figure 29. Mean and maximum percentages of maximal predicted muscle group capability (%MMGC) of rotator cuff (RC) muscles and glenohumeral articulating (GA) muscles during isometric extension under certain simulated conditions.

Table 12. Mean glenohumeral joint contact forces and task costs during isometric extension under certain simulated conditions.

Condition	ASF(+)/PSF(-) (N)	SSF(+)/ISF(-) (N)	RSF (N)	JCF (N)	Cost (N^3cm^6)
Intact	-65.39	+148.07	161.92	475.05	88108
No Labrum	-11.89	+120.42	121.15	473.22	109677
Ages >80	-46.62	+142.44	149.92	479.67	93064
BKT	-93.63	+116.45	149.59	481.31	95836
RBKT	-12.62	+117.8	118.64	475.86	110790
PBB	-125.87	+150.41	196.2	437.87	78630

Note: ASF = Anterior Joint Shear Force; PSF = Posterior Joint Shear Force; SSF = Superior Joint Shear Force; ISF = Inferior Joint Shear Force; JCF = Joint Compression Force; BKT = Bankart Lesion; RBKT = Reverse Bankart Lesion; PBB = Posterior Bone Block. Cost represents the magnitude of the cost function.

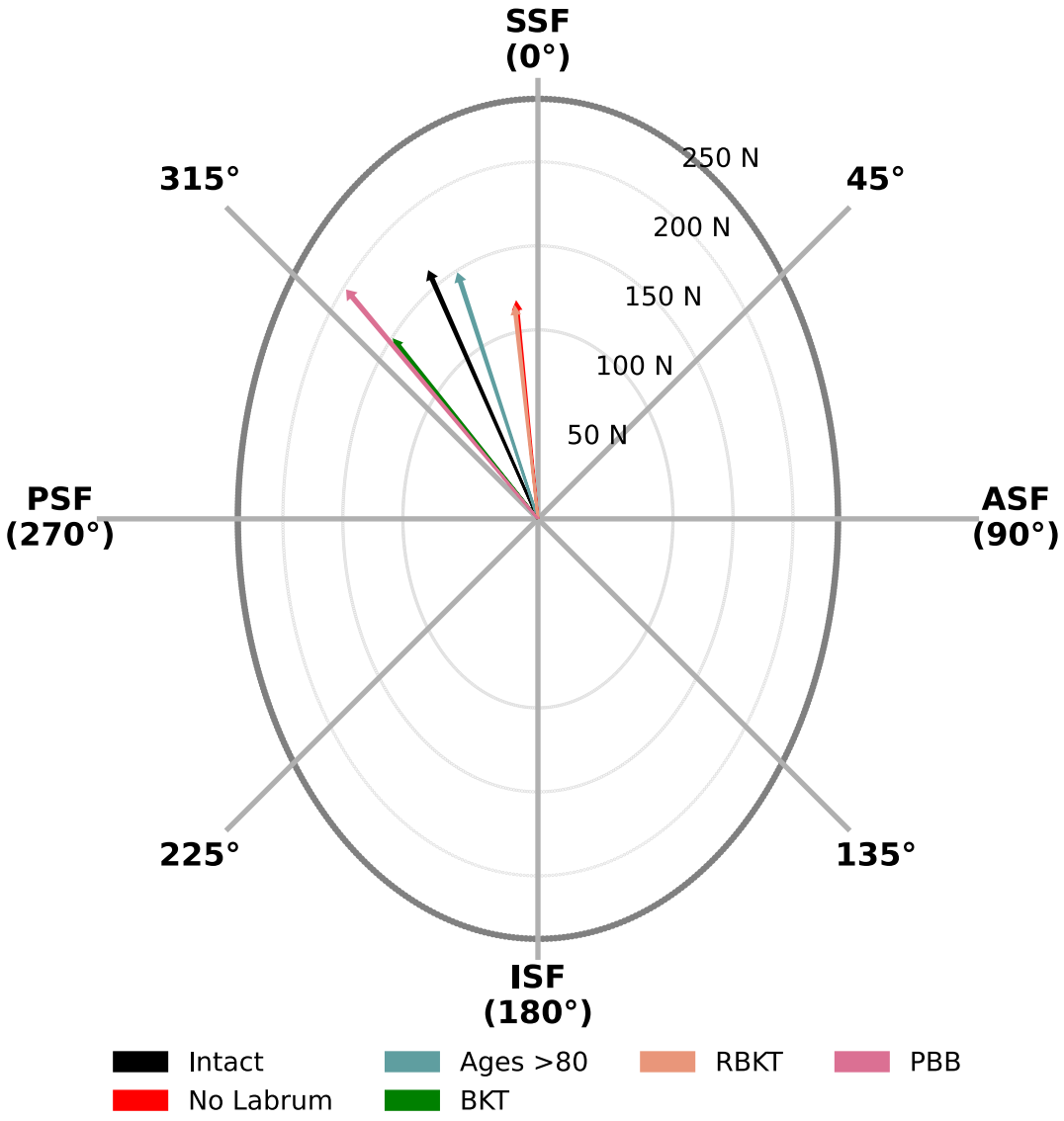

Figure 30. Mean glenohumeral joint resultant shear forces in 8 equally spaced compass directions of the glenoid during isometric extension under certain simulated conditions. The length of each arrow represents the magnitude of resultant shear forces under corresponding simulated conditions.

4.7 Grooming

During grooming, changes in %MMGCs occurred in both muscle groups when compared to the intact condition. Mean %MMGCs increased slightly by 0.5%–6% in both muscle groups in no labrum and ages over 60 (Figure 31). However, peak %MMGCs in RC muscles increased by 11%–30% along with 6%–20% increases in task costs for these conditions (Table 13). In PBB, a 3% increase in RC muscle %MMGC accompanied a 0.8%–4% decrease in GA muscle %MMGC, as a result of a 3% decrease in task costs. %MMGCs had no notable change to the intact condition in both muscle groups in other surgical simulations. Further, the activation levels of both muscle groups were at similar levels throughout the task.

When compared to the intact condition, substantial changes in joint contact forces emerged under certain simulated conditions. With no labrum, PSF decreased by 5% with a 23% decrease in SSF (Table 13) which resulted in a 4% decrease in RSF with a 3.5° change from the intact condition (Figure 32). In SLAP, increases of 0.2% in PSF and 13% in SSF occurred. As a result, RSF decreased by 0.4% with a 2.8° change from the intact condition. Moreover, in RBKT, PSF decreased by 6% along with a 38% decrease in SSF, resulting in a 5% decrease in RSF with a 5.2° change from the intact condition. Additionally, PSF increased by 6% with a 65% increase in SSF. As a result, RSF in PBB increased by 2.2% with an 11.1° shift compared to the intact condition. Furthermore, JCFs increased by 3%–11% in no labrum, ages over 60 and RBKT (Table 13).

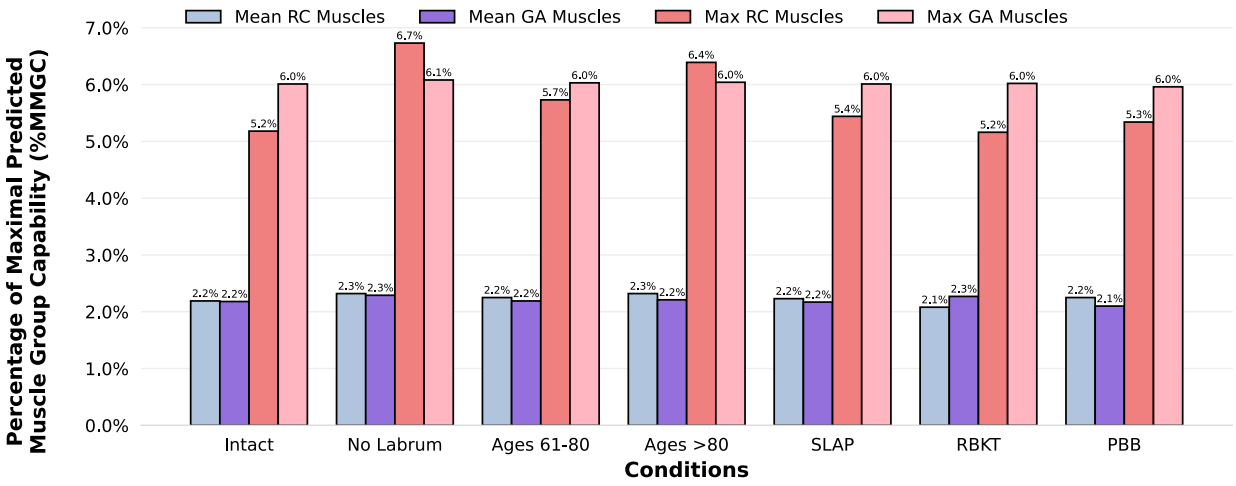

Figure 31. Mean and maximum percentages of maximal predicted muscle group capability (%MMGC) of rotator cuff (RC) muscles and glenohumeral articulating (GA) muscles during grooming under certain simulated conditions.

Table 13. Mean glenohumeral joint contact forces and task costs during grooming under certain simulated conditions.

Condition	ASF(+)/PSF(-) (N)	SSF(+)/ISF(-) (N)	RSF (N)	JCF (N)	Cost (N^3cm^6)
Intact	-75.16	+10.76	85.88	139.05	12612
No Labrum	-71.62	+8.3	82.31	154.28	15182
Ages 61–80	-74.65	+11.17	85.11	143.06	13319
Ages >80	-74.2	+11.66	84.53	147.89	14174
BKT	-75.06	+10.84	85.77	138.94	12616
RBKT	-70.54	+6.67	81.76	142.63	12766
PBB	-79.56	+17.76	87.77	137.53	12261

Note: ASF = Anterior Joint Shear Force; PSF = Posterior Joint Shear Force; SSF = Superior Joint Shear Force; ISF = Inferior Joint Shear Force; JCF = Joint Compression Force; BKT = Bankart Lesion; RBKT = Reverse Bankart Lesion; PBB = Posterior Bone Block. Cost represents the magnitude of the cost function.

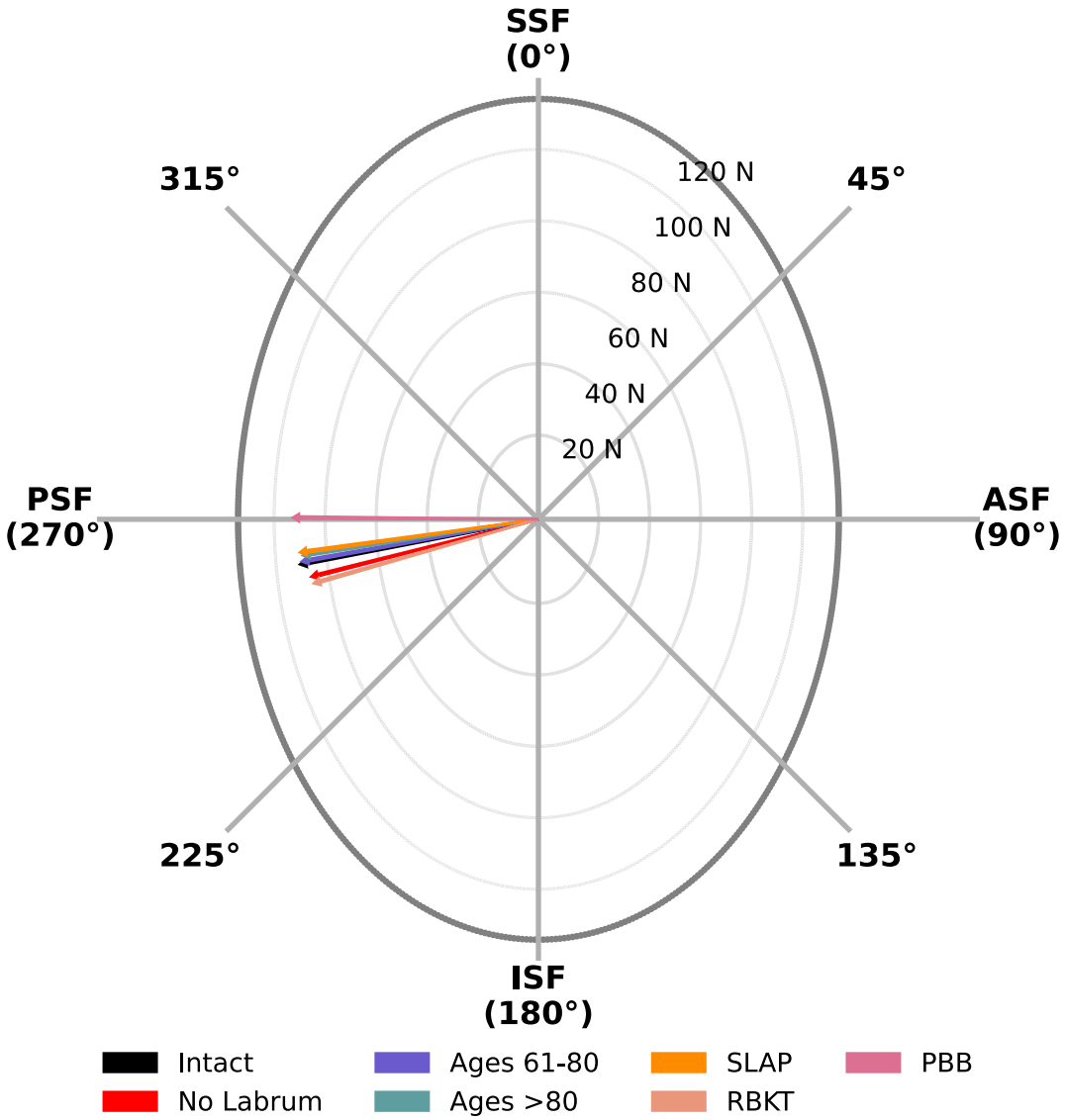

Figure 32. Mean glenohumeral joint resultant shear forces in 8 equally spaced compass directions of the glenoid during grooming under certain simulated conditions. The length of each arrow represents the magnitude of resultant shear forces under corresponding simulated conditions.

4.8 One-Arm Row

Throughout one-arm row, %MMGCs in both muscle groups differed for some simulated conditions. When comparing no labrum to the intact condition, 2% (15%) and 9% (18%) increases occurred in mean (and maximum) %MMGC in RC and GA muscles (Figure 33), respectively. Task demands increased by 46% (Table 14). In ages over 80, task cost increased by 17% which was associated with a 9% increase in maximum RC muscle %MMGC and a 4% increase in mean GA muscle %MMGC. Furthermore, with a 25% increase in task cost in RBKT, maximum RC muscle %MMGC increased by 8% with a 14% increase in maximum GA muscle %MMGC. However, mean RC and GA muscle %MMGCs decreased by 9% and 8% in PBB, along with a 30% decrease in task cost. In other simulated repaired conditions, the %MMGCs of both muscle groups were not noticeably changed compared to the intact condition. Additionally, RC muscle levels were about 1.5–2 times greater than GA muscle levels throughout the task.

Similar patterns were observed in joint contact forces for these conditions. PSF decreased by 4%–17% in no labrum, ages over 60 and RBKT with 33%–178% increases in ISF (Table 14). These changes resulted in 4%–10% decreases in RSF with 3.6°–19.3° shifts toward the posteroinferior direction (Figure 34). However, in PBB, PSF increased by 7% and VSF shifted and increased by 176% superiorly. Furthermore, RSF increased by 9.16% with a 15.4° shift in direction toward the posterosuperior direction. In addition, compared to the intact condition, JCF increased by 4% in no labrum and decreased by 6% in PBB (Table 14).

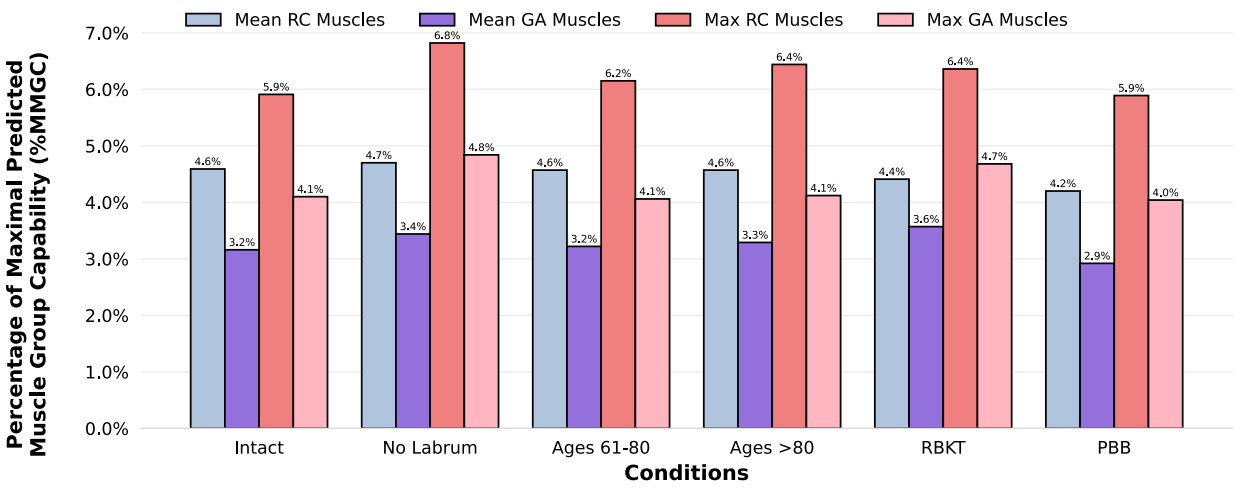

Figure 33. Mean and maximum percentages of maximal predicted muscle group capability (%MMGC) of rotator cuff (RC) muscles and glenohumeral articulating (GA) muscles during one-arm row under certain simulated conditions.

Table 14. Mean glenohumeral joint contact forces and task costs during one-arm row under certain simulated conditions.

Condition	ASF(+)/PSF(-) (N)	SSF(+)/ISF(-) (N)	RSF (N)	JCF (N)	Cost (N^3cm^6)
Intact	-92.58	-14.66	97.07	250.5	42678
No Labrum	-79.93	-28.49	87.33	261.06	62311
Ages 61–80	-88.76	-19.51	93.34	249.63	46159
Ages >80	-86.11	-21.09	90.86	250.99	49786
RBKT	-76.57	-40.69	89.5	250.04	53190
PBB	-99.2	+11.16	105.96	234.74	29814

Note: ASF = Anterior Joint Shear Force; PSF = Posterior Joint Shear Force; SSF = Superior Joint Shear Force; ISF = Inferior Joint Shear Force; JCF = Joint Compression Force; RBKT = Reverse Bankart Lesion; PBB = Posterior Bone Block. Cost represents the magnitude of the cost function.

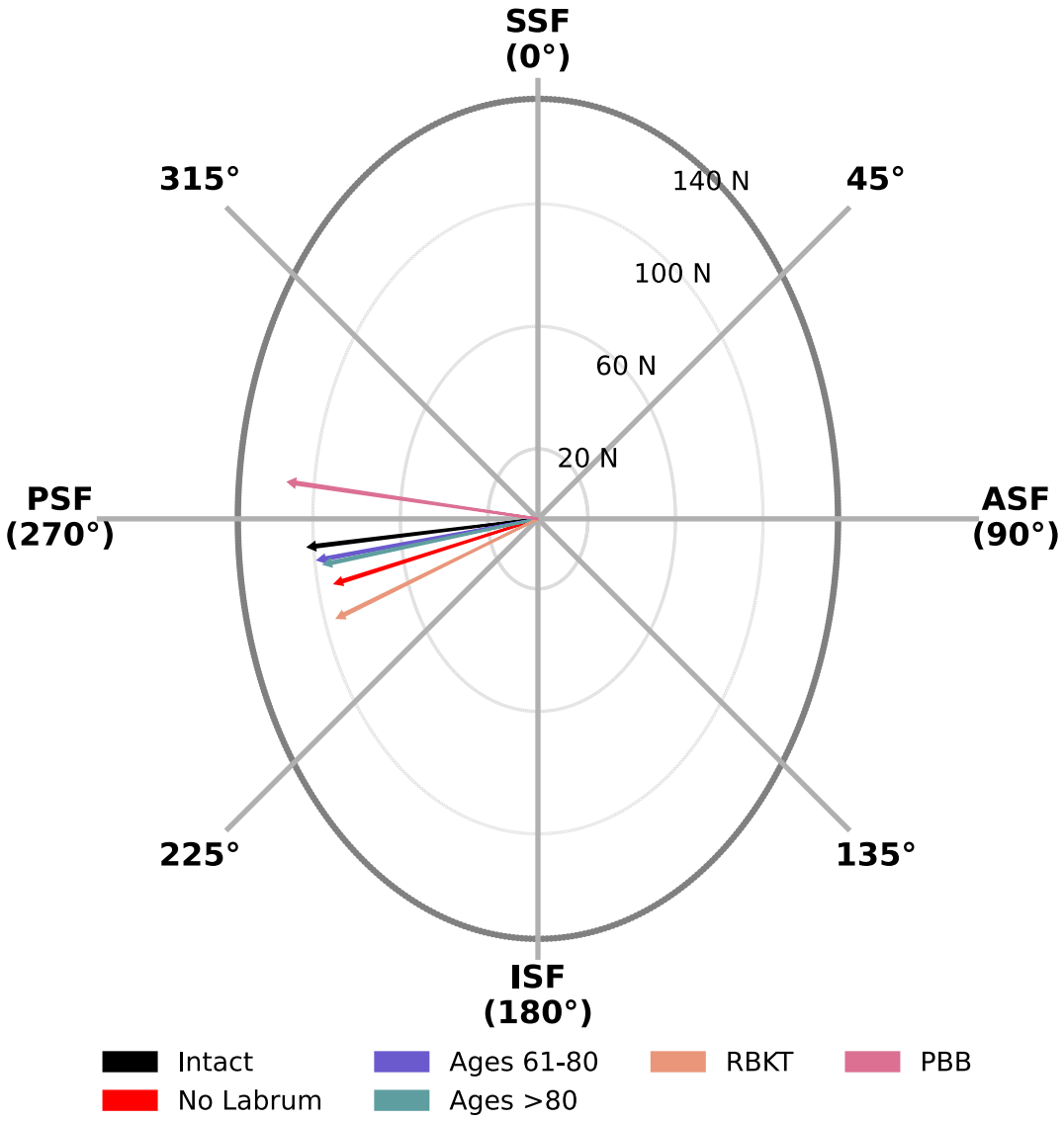

Figure 34. Mean glenohumeral joint resultant shear forces in 8 equally spaced compass directions of the glenoid during one-arm row under certain simulated conditions. The length of each arrow represents the magnitude of resultant shear forces under corresponding simulated conditions.

4.9 One-Arm Chest Press

During one-arm chest press, substantial changes in maximum muscle activation levels occurred in both muscle groups compared to the intact condition. Maximum RC muscle activation levels increased by 5%–13% in no labrum, ages over 80 and RBKT (Figure 35). Maximum GA muscle %MMGCs increased by 5%–17% (Figure 35), along with task costs raised by 6%–42% (Table 15). However, a 6% and 5% decrease occurred in the maximum RC and GA muscle %MMGCs in PBB, respectively. The task cost decreased by 16% in PBB. After other simulated repairs, %MMGCs and task costs approximated the intact condition. Further, GA muscle %MMGCs were approximately 1.25–2 times lower than RC muscle %MMGCs throughout the task under all simulated conditions.

Compared to the intact condition, distinguishable changes in joint contact forces occurred under some simulated conditions. Specifically, there were 6%–33% decreases in PSFs, along with 18%–111% decreases in SSFs in no labrum, ages over 60 and RBKT (Table 15). As a result, RSFs were reduced by 8%–30% under the mentioned conditions. In PBB, PSF increased by 18% with a 53% increase in SSF. Hence, RSF increased by 19% in PBB. However, notable changes of 5.5°–22.1° in RSF directions occurred only for no labrum, RBKT and PBB (Figure 36). Additionally, JCF increased by 2%–5% in no labrum, ages over 80 and RBKT, whereas in PBB, JCF decreased by 4% (Table 15).

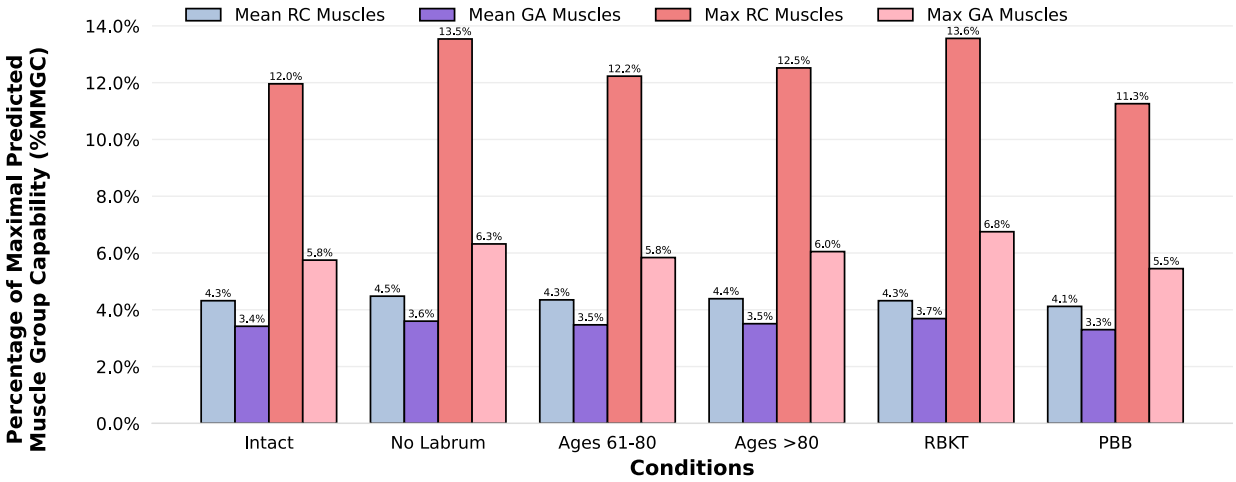

Figure 35. Mean and maximum percentages of maximal predicted muscle group capability (%MMGC) of rotator cuff (RC) muscles and glenohumeral articulating (GA) muscles during one-arm chest press under certain simulated conditions.

Table 15. Mean glenohumeral joint contact forces and task costs during one-arm chest press under certain simulated conditions.

Condition	ASF(+)/PSF(-) (N)	SSF(+)/ISF(-) (N)	RSF (N)	JCF (N)	Cost (N^3cm^6)
Intact	-38.38	+19.92	55.2	254.02	77760
No Labrum	-26.74	+5.2	38.72	267.02	110191
Ages 61–80	-36.18	+16.42	50.93	256.02	82344
Ages >80	-34.03	+13.12	47.42	259.42	87084
RBKT	-25.75	-2.19	40.66	263.07	106233
PBB	-45.24	+30.54	65.58	243.99	65122

Note: ASF = Anterior Joint Shear Force; PSF = Posterior Joint Shear Force; SSF = Superior Joint Shear Force; ISF = Inferior Joint Shear Force; JCF = Joint Compression Force; RBKT = Reverse Bankart Lesion; PBB = Posterior Bone Block. Cost represents the magnitude of the cost function.

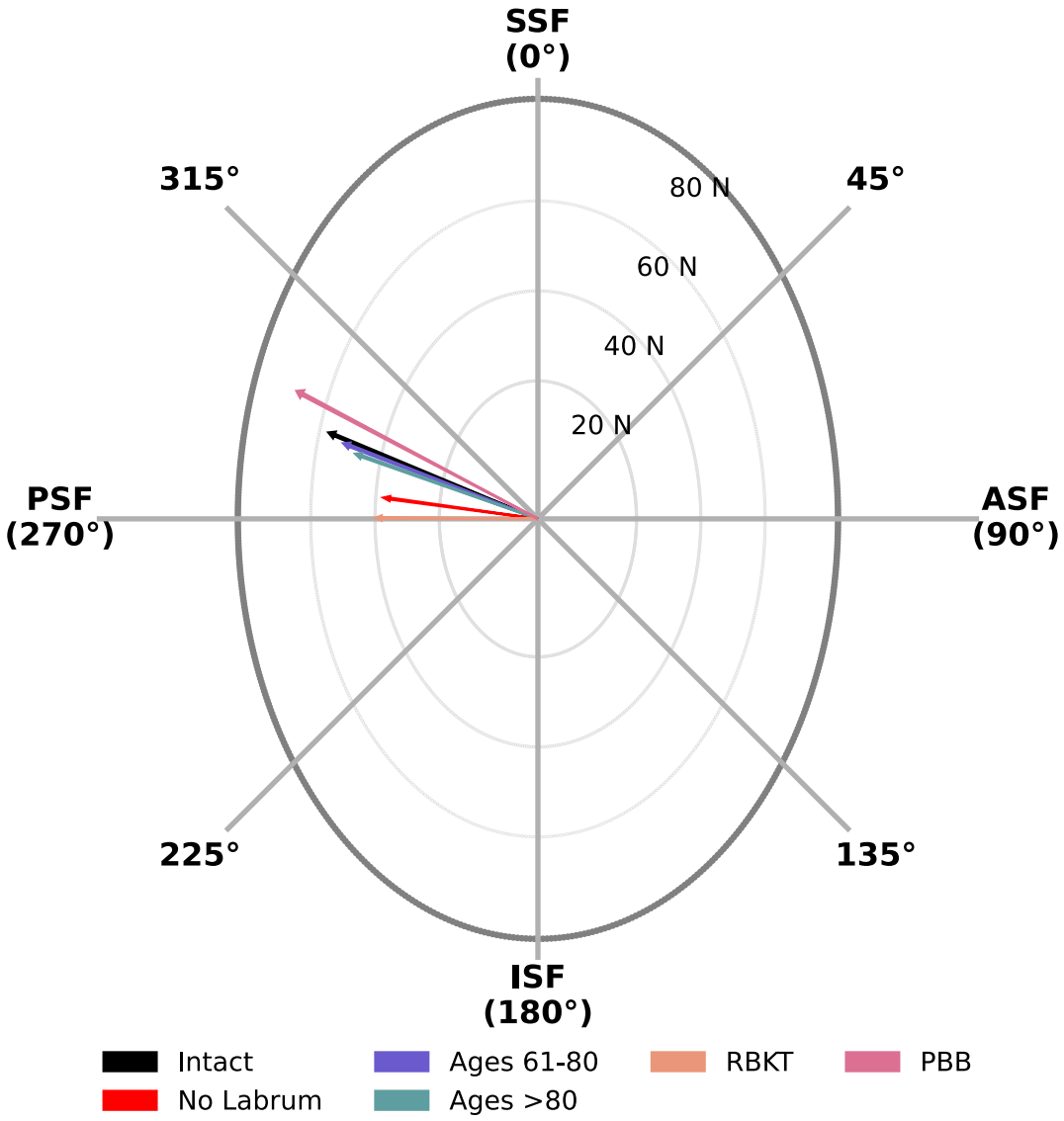

Figure 36. Mean glenohumeral joint resultant shear forces in 8 equally spaced compass directions of the glenoid during one-arm chest press under certain simulated conditions. The length of each arrow represents the magnitude of resultant shear forces under corresponding simulated conditions.

4.10 One-Arm Face Pull

Throughout one-arm face pull, minor changes in muscle activation levels occurred for certain simulated conditions. Compared to the intact condition, mean RC muscle %MMGC decreased by 26% and 27% for no labrum and RBKT, respectively (Figure 37). Similarly, mean GA muscle %MMGC increased by 10% in no labrum and RBKT. Task costs increased by 10.38%–11.67% for these conditions (Table 16). No major changes in %MMGCs occurred in other surgical techniques. Additionally, activation levels were twice as high in GA muscles as in RC muscles under all simulated conditions.

Substantial changes in joint contact forces existed for certain simulated conditions. Compared to the intact condition, PSFs decreased 6%–25% in no labrum, ages over 80 and RBKT (Table 16). SSFs were decreased by 10%–81%, and thus, RSFs decreased by 5%–18% for the same conditions. On the other hand, in PBB, PSF increased by 7% with a 9% increase in SSF. As a result, RSF increased by 6% in PBB. Further, small changes of 2.4°–3.5° in RSF directions occurred for no labrum, BKT, RBKT and PBB (Figure 38). In addition, minor changes in JCFs occurred in no labrum, ages over 80, RBKT and PBB (Table 16).

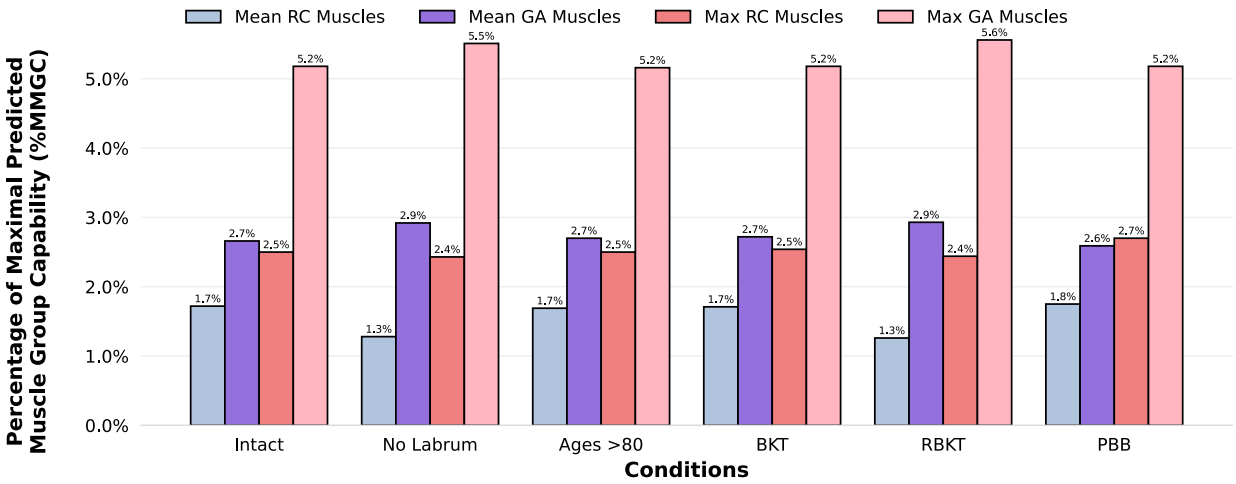

Figure 37. Mean and maximum percentages of maximal predicted muscle group capability (%MMGC) of rotator cuff (RC) muscles and glenohumeral articulating (GA) muscles during one-arm face pull under certain simulated conditions.

Table 16. Mean glenohumeral joint contact forces and task costs during one-arm face pull under certain simulated conditions.

Condition	ASF(+)/PSF(-) (N)	SSF(+)/ISF(-) (N)	RSF (N)	JCF (N)	Cost (N^3cm^6)
Intact	-50.26	+22.37	64.72	214.56	6138
No Labrum	-38.44	+4.31	53.88	219.9	6775
Ages >80	-47.47	+20.1	61.46	216.78	6189
BKT	-49.9	+17.04	60.4	216.16	6223
RBKT	-37.9	+4.18	53.04	220.31	6854
PBB	-53.96	+24.32	68.29	210.26	6107

Note: ASF = Anterior Joint Shear Force; PSF = Posterior Joint Shear Force; SSF = Superior Joint Shear Force; ISF = Inferior Joint Shear Force; JCF = Joint Compression Force; BKT = Bankart Lesion; RBKT = Reverse Bankart Lesion; PBB = Posterior Bone Block. Cost represents the magnitude of the cost function.

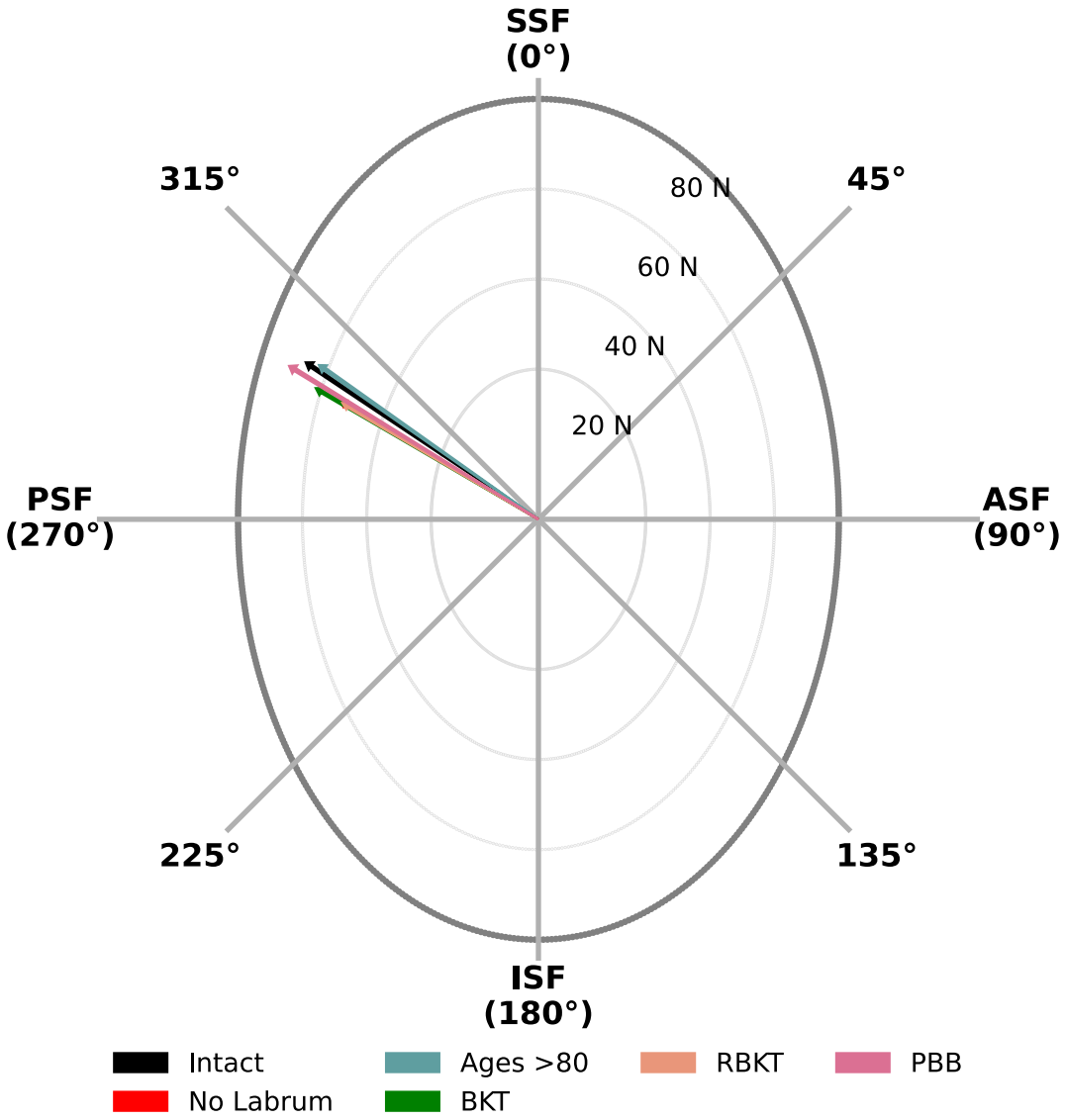

Figure 38. Mean glenohumeral joint resultant shear forces in 8 equally spaced compass directions of the glenoid during one-arm face pull under certain simulated conditions. The length of each arrow represents the magnitude of resultant shear forces under corresponding simulated conditions.

4.11 Box Lifting

During box lifting, activation levels of RC muscles experienced minor changes under certain simulated conditions. Compared to the intact condition, 3%–11% increases of mean RC muscle %MMGCs occurred in no labrum, ages over 60 and PBB (Figure 39). Further, maximum RC muscle %MMGCs increased by 25% and 20% in no labrum and ages over 80, respectively. However, no substantial changes existed for GA muscle %MMGCs (Figure 39). Task costs increased by 3%, 7% and 11% in ages 41–60, ages over 80 and no labrum, respectively (Table 17). %MMGCs in both muscle groups returned to a similar level as in intact condition after surgical repairs, except PBB. Throughout the task, both muscle group activation levels were at similar levels under all simulated conditions.

Major changes in joint contact forces occurred in some simulated conditions compared to the intact condition. ISFs demonstrated 14% and 25% increases in no labrum and RBKT, respectively (Table 17); 11% and 55% decreases in SLAP and PBB, respectively. PSFs decreased by 15% and 12% in no labrum and RBKT, respectively (Table 17); 1% and 19% increases in SLAP and PBB, respectively. Only minor magnitude changes of 1%–5% in RSFs occurred in the above conditions (Table 17). Furthermore, RSF directions shifted by 3.5°–21.5° across the simulations (Figure 40). Additionally, JCFs showed a 2%–6% increase in no labrum, ages over 60, SLAP and PBB (Table 17). However, in RBKT, JCF decreased by 5%.

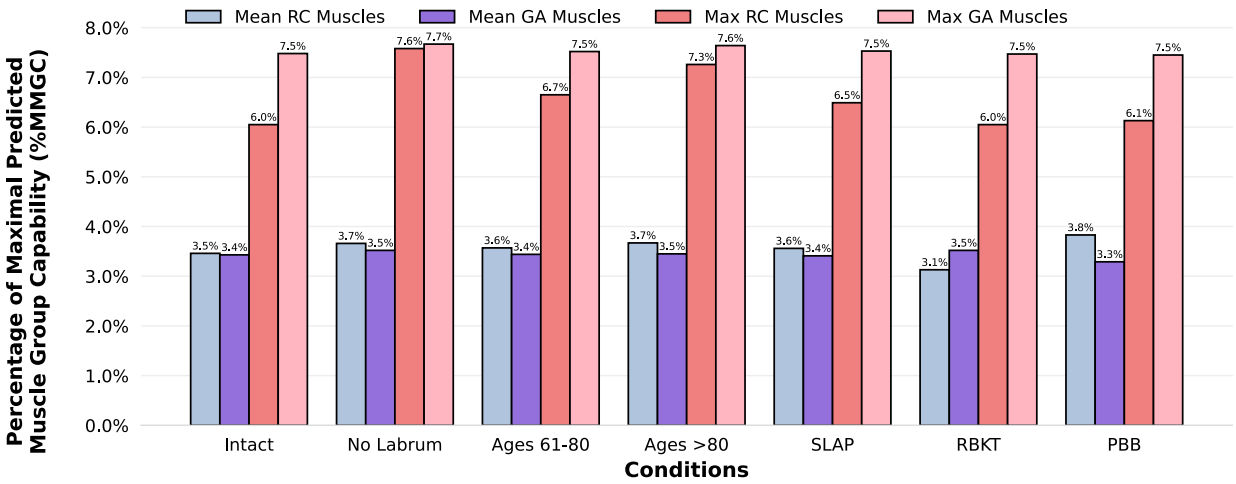

Figure 39. Mean and maximum percentages of maximal predicted muscle group capability (%MMGC) of rotator cuff (RC) muscles and glenohumeral articulating (GA) muscles during box lifting under certain simulated conditions.

Table 17. Mean glenohumeral joint contact forces and task costs during box lifting under certain simulated conditions.

Condition	ASF(+)/PSF(-) (N)	SSF(+)/ISF(-) (N)	RSF (N)	JCF (N)	Cost (N^3cm^6)
Intact	-68.32	-36.21	88.09	274.49	62298
No Labrum	-58.11	-41.12	83.91	290.58	69430
Ages 61–80	-66.32	-34.88	86.64	281.73	64214
Ages >80	-64.11	-34.22	85.1	288.35	66367
SLAP	-69.07	-32.35	87.17	280.22	62939
RBKT	-60.24	-45.13	86.59	260.87	63618
PBB	-81.17	-16.26	90.73	290.3	60644

Note: ASF = Anterior Joint Shear Force; PSF = Posterior Joint Shear Force; SSF = Superior Joint Shear Force; ISF = Inferior Joint Shear Force; JCF = Joint Compression Force; SLAP = Superior Labrum Antero-to-Posterior Lesion; RBKT = Reverse Bankart Lesion; PBB = Posterior Bone Block. Cost represents the magnitude of the cost function.

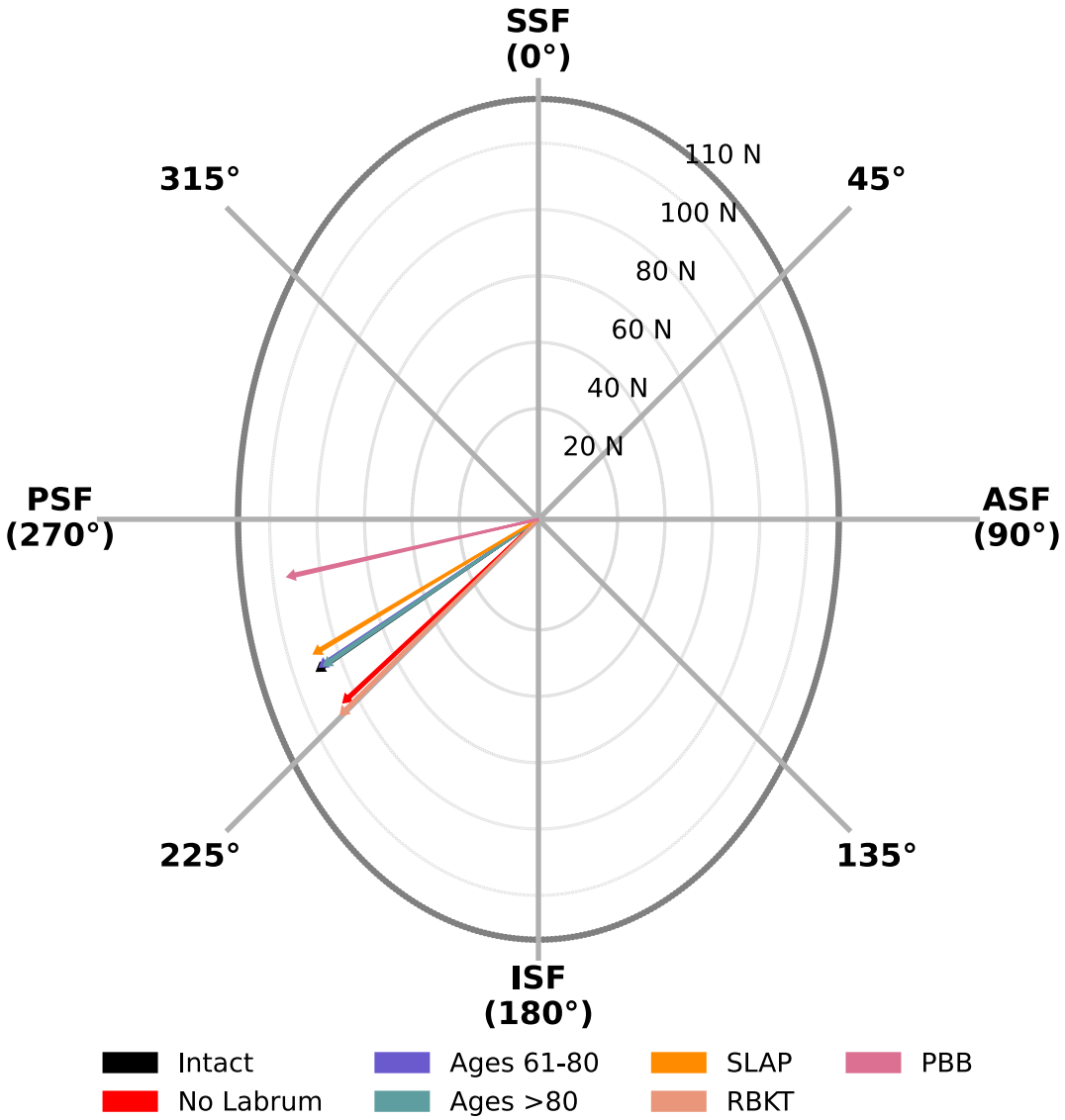

Figure 40. Mean glenohumeral joint resultant shear forces in 8 equally spaced compass directions of the glenoid during box lifting under certain simulated conditions. The length of each arrow represents the magnitude of resultant shear forces under corresponding simulated conditions.

4.12 Weight Relief

Throughout weight relief, only RC muscles changed markedly in terms of %MMGCs compared to the intact condition. Maximum RC muscle %MMGCs increased by 6%–17% in no labrum and ages over 60 (Figure 41). Moreover, task demands also increased by 5%–20% for these conditions (Table 18). Further, maximum RC muscle %MMGCs decreased by 10% and 8% in RBKT and PBB, respectively. Task costs had small changes. %MMGCs approximated the intact condition in both muscle groups in other simulated repaired conditions. However, no major changes in %MMGCs occurred in GA muscles (Figure 41). Additionally, the maximum %MMGCs in RC muscles were about 1.5 times greater than in GA muscles under all simulated conditions.

Similarly, notable joint shear forces (JSFs) changes accompanied the noted conditions. In no labrum, PSF decreased by 7% with a 1% increase in ISF (Table 18). In ages over 80, PSF decreased by 2% and ISF decreased by 7%. In RBKT, PSF decreased by 3% with a 18% increase in ISF. RSFs decreased by 1%–5% (Table 18). In addition, PSF increased by 3% and ISF decreased by 13% in PBB. Hence, RSF in PBB increased by 2%. Further, RSF directions changed by 1.1°–14.1° (Figure 42). Additionally, in no labrum and RBKT, JCFs decreased by 1% and 8%, respectively (Table 18). However, JCFs increased by 2%–4% in ages over 60, SLAP and PBB when compared to the intact condition.

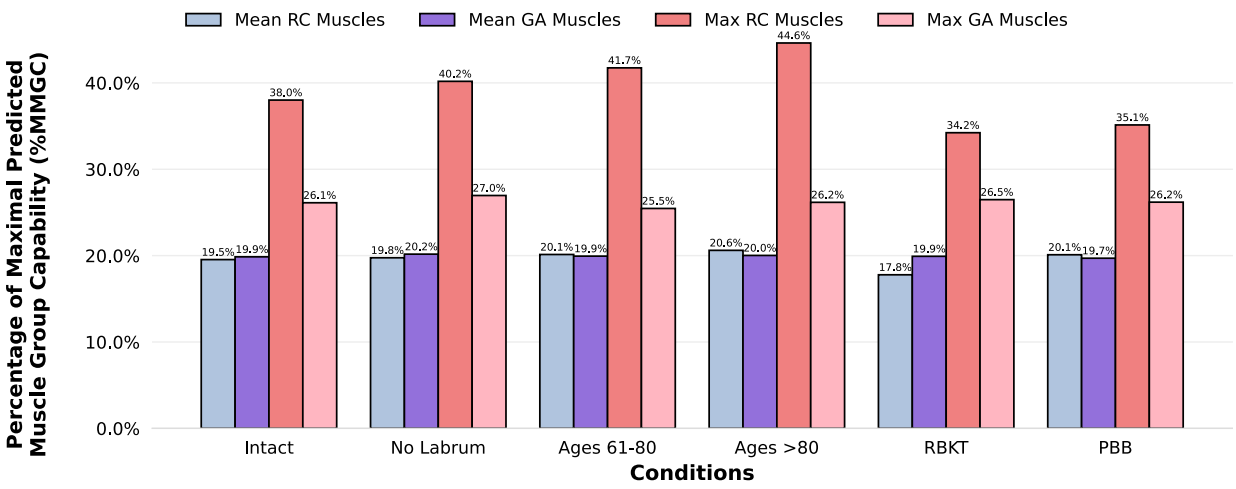

Figure 41. Mean and maximum percentages of maximal predicted muscle group capability (%MMGC) of rotator cuff (RC) muscles and glenohumeral articulating (GA) muscles during weight relief under certain simulated conditions.

Table 18. Mean glenohumeral joint contact forces and task costs during weight relief under simulated conditions.

Condition	ASF(+)/PSF(-) (N)	SSF(+)/ISF(-) (N)	RSF (N)	JCF (N)	Cost (N^3cm^6)
Intact	-819.99	-286.32	973.76	1495.52	6418759
No Labrum	-764.81	-289.4	921.58	1479.67	7720594
Ages 61–80	-810.72	-274.79	964.74	1526.04	6741778
Ages >80	-802.07	-266.9	956.78	1550.95	7087570
RBKT	-795.28	-337.59	959.31	1380.59	6594869
PBB	-841.43	-249.37	996.05	1533.46	6151790

Note: ASF = Anterior Joint Shear Force; PSF = Posterior Joint Shear Force; SSF = Superior Joint Shear Force; ISF = Inferior Joint Shear Force; JCF = Joint Compression Force; RBKT = Reverse Bankart Lesion; PBB = Posterior Bone Block. Cost represents the magnitude of the cost function.

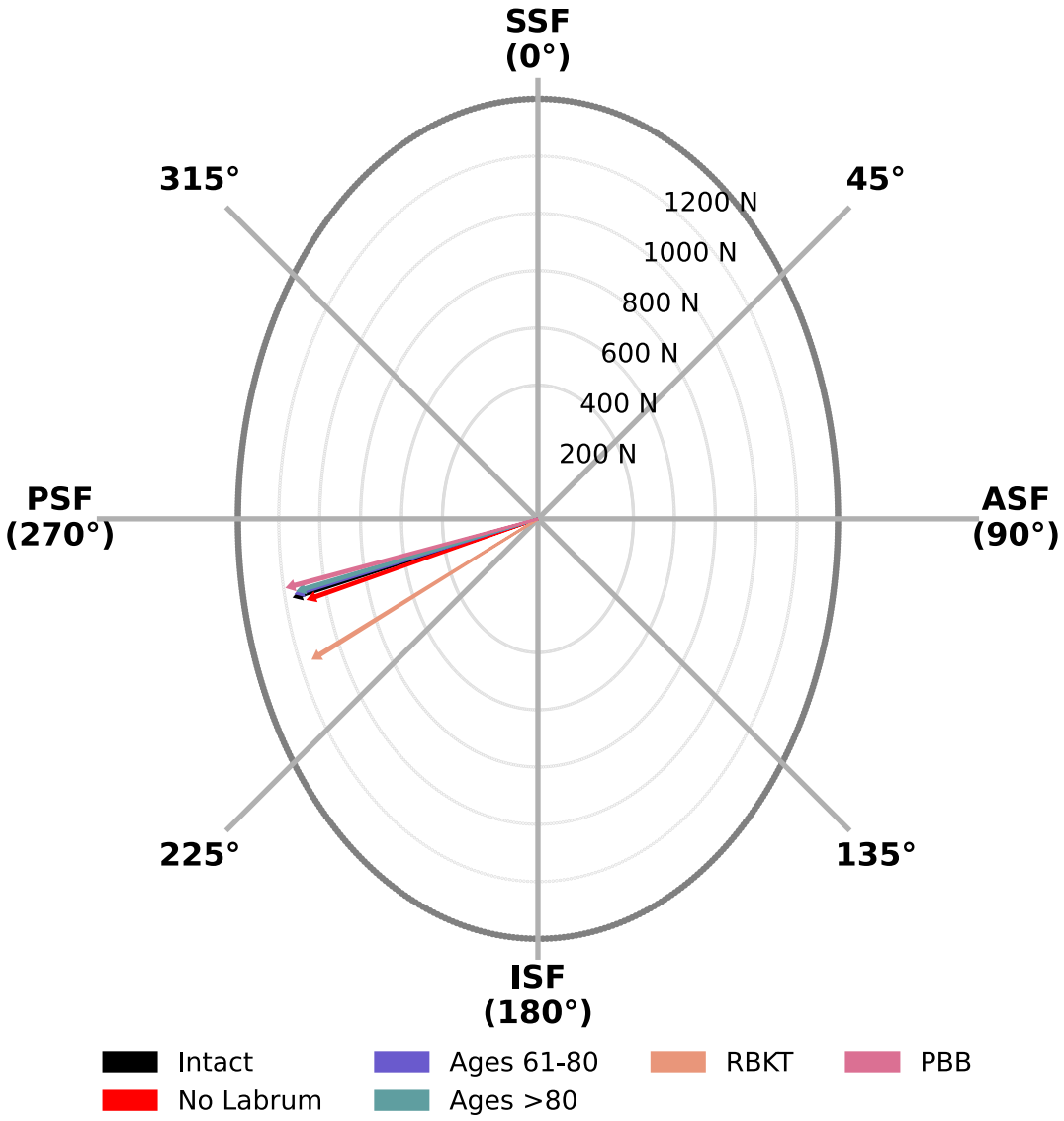

Figure 42. Mean glenohumeral joint resultant shear forces in 8 equally spaced compass directions of the glenoid during weight relief under certain simulated conditions. The length of each arrow represents the magnitude of resultant shear forces under corresponding simulated conditions.

V. Discussion

The primary goal of this study was to determine how muscle activation strategies changed with simulated intact and compromised labral statuses when performing various tasks. Fundamentally, %MMGCs and task costs typically but not universally increased in simulated compromised labral conditions, especially for those labral conditions with no labrum or in older age groups. This highlights the contribution of the glenoid labrum to GH joint stability and its link to changes in muscle activations. RC muscle %MMGCs were greater than in GA muscles in tasks with higher mechanical costs, emphasizing the role of RC muscles as key GH joint stabilizers. In addition, arthroscopic surgical approaches improved GH joint stability and resulted in decreased muscle activation levels compared to compromised situations, indicating a positive impact on overall GH joint stability. Finally, JSF results featured minimal changes in the directions of the RSF between simulated conditions in more demanding activities. Yet, redirections of JSF occurred in tasks with lower mechanical costs. As discussed later, distinct compensations emerged in response to the compromised labra and depended somewhat on the overall task cost. The highlighted compensatory strategies represent the potential responses of individuals with labral deficiencies when performing these tasks. Hence, potential muscle fatigue can be anticipated and related to the subsequent possibility of secondary damage resulting from the adopted muscle recruitment strategies.

5.1 Aging Effects

%MMGCs increased fairly consistently when isometric exercises and functional tasks were simulated without a labrum and in older adults. The stability of the GH joint was substantially weakened if the labrum was completely removed, prompting additional muscle activation with increased joint compression forces (Lippitt & Matsen, 1993; Thompson et al., 1996). Hence, lower shear forces. This supports the reports of Lippitt and Matsen (1993), who stressed the function of the glenoid labrum in providing joint stability (Section 2.1). As a result of the severity of the condition, the removal of a labrum was expected to result in the highest activation levels of both muscle groups when comparing simulated conditions, which indeed occurred in all task simulations. Similarly, age-related alterations in the labrum also impaired intrinsic GH joint stability leading to increased muscle activation of both muscle groups to provide stabilizing forces. Decreased GH joint stability with increasing age appeared to increase muscular demands across all tasks, previously highlighted by Pfahler et al. (2003) and illustrated in Table 5. The increase in %MMGCs in both muscle groups was lower in degenerated labra because conditions were less severe compared to no labrum condition. However, this does not explain why conditions with degenerated labra had a higher muscle activation level than conditions with torn labra.

5.2 Lesion Location Impacts on Muscle Activities

The variations in %MMGCs in degenerated did not result solely from varying the severities of the simulated conditions as simulated by decreasing stability ratios; rather, the location of the labrum or the area of degeneration also mattered. Three prevalent labrum lesions were also simulated by modifying the GH joint stability constraints, which were based on the

findings of earlier cadaveric humeral translation studies (Black et al., 1999; Clavert, 2015; Kleiner et al., 2016; Panossian et al., 2005; Patzer et al., 2012; Wellmann et al., 2011). As illustrated in Table 4, lesions were represented as more severe labrum destruction in the respective directions compared to degenerated labra. However, %MMGCs of both muscle groups were higher in degenerated labra which suggested that the severity of the damage was not the only factor that could potentially raise muscle demands. Tissue degeneration caused less severe focal damage to the labrum, but it impacted all directions and influenced the overall system's capacity and flexibility to redirect GH joint translational forces (discussed in Section 5.2). The aging effects in this study agree with Pfahler et al. (2003) and even demonstrated a greater conceptual risk of muscle fatigue compared to conditions with torn labra. Additionally, the decline in muscular mass and strength associated with aging may exacerbate the aging impacts shown in this study (Hughes et al., 1999). As age-dependent changes in muscle mass and strength were not simulated in this study, further investigations should consider and may more fulsomely illustrate the functional outcomes of aging effects on the glenoid labrum.

5.3 Compensatory Rotator Cuff Muscle Strategies

To reiterate, the main goal of this study was to identify variations in muscle recruitment between simulated labral conditions. RC muscles are activated to a larger extent than GA muscles in more physically demanding activities. The stabilization of the GH joint required a significant contribution from the RC muscles (supporting concepts of Mulla et al., 2020). Due to the anatomical arrangement of RC muscles, they establish force couples around the shoulder joint to balance anterior and posterior muscular forces while compressing the humeral head into the glenoid (Lippitt & Matsen, 1993; Thompson et al., 1996). The concavity of the GH joint

conceptually diminishes when the integrity and structure of the labrum are impaired. Thus, support from the RC muscles logically would become more crucial for preserving the GH joint stability through the concavity-compression mechanism. This compression mechanism was computationally confirmed in this study, particularly for several activities with substantial task demands, i.e., isometric external rotation, isometric abduction, and weight relief lifting. For higher physical task demands, and compromised labral conditions, the GH joint required stabilization generated by increased RC activity. This increase would compress the humeral head into the glenoid, enhancing GH joint stabilization.

The joint stability level was preserved through the predicted additional RC muscle force, which reduced the ratio of the amplitudes of GH joint shear to compression force under higher-demand circumstances when performing the above challenging activities. Eq. 6 illustrated the relationship between joint shear force and joint compression force and showed how improving concavity compression restricts humeral head motion in loose GH joints. Hence, this should prevent or lessen the likelihood of joint dislocation. The aforementioned high-cost tasks findings also suggested that the direction of the GH joint shear force was confined and limited within a range of 2.5° in the majority of simulated labral conditions. This constraint on the direction of joint translational force was more prominent in simulations of isometric exercises, such as external rotation and abduction, in which the variation in joint shear force direction between simulated conditions was minimal (±0.2°). This notable restriction in humeral movements highlighted the possible difficulty that patients with a compromised labrum may have while performing external rotation or elevation with an increased risk of muscle fatigue, which aligns with the conclusions of Aranha et al. (2022). Additionally, for most simulations, scenarios with no labrum or a degenerated labrum resulted in a larger reduction of GH joint shear force

magnitude than other conditions. This supports the findings on the significance of the glenoid labrum and its changes with aging, which further implies why RC muscles are more susceptible to muscle fatigue in this vulnerable group, especially during external rotation and abduction.

5.4 Effectiveness of Surgical Treatments

There are ongoing discussions over the best treatments for injured labra since labrum lesions require sophisticated management and care (Horner et al., 2018; Lafosse & Boyle, 2010; Wu et al., 2021). When comparing treatment outcomes between conservative and operational approaches, Zughaib et al. (2017) revealed substantial improvements in the quality of life of patients with labrum tears or tissue degeneration following surgical treatments. Current simulation results suggest that reductions in the activation level of RC muscles in physically demanding tasks after surgical approaches were achieved, indicating improvement in intrinsic stability. Since muscle groups were less engaged during activities with lower task costs, the amount of reduction in muscle level was less compared to more challenging tasks. The simulations of arthroscopic surgical repairs in this study were derived from earlier mechanical investigations (Black et al., 1999; Panossian et al., 2005; Patzer et al., 2012; Wellmann et al., 2011). These studies revealed that surgical repairs preserved the integrity of the GH joint by restoring the stability level of the joint to a state that is nearly identical to an intact condition. Thus, the amount of muscular stabilization required was decreased, relieving the RC muscles.

Bone augmentations further diminished potential muscle overuse by further stabilizing the GH joint, in the event that arthroscopic repairs failed (Kleiner et al., 2016; Wellmann et al., 2011). The directions of joint shear force were between 220°–255° in physically demanding tasks under all simulated conditions, which was where the bone graft was placed in the posterior

bone block procedure (Levigne et al., 2005). Therefore, a greater reduction in muscle activation level was anticipated after a posterior bone block was simulated. Not only did posterior bone block lower the muscle demands, but it also reduced the mechanical cost of all activities, as quantified by the cost function. This evidence supports reports by Wellmann et al. (2011) and Lafosse et al. (2012) investigations on the efficacy of the arthroscopic posterior bone block technique. Hence, this technique should be considered in the future while treating posterior labrum lesions. Even though this study did not evaluate the functional outcomes from non-operative approaches, the simulated mechanical benefits that arthroscopic operations provide compared to torn labra point to the benefits of undergoing early surgical procedures. In addition, future studies should consider the variations between individuals to better simulate and highlight the advantages of each surgical technique on individuals.

5.5 Potential Shoulder Pathologies

GH joint instability, as instigated by simulated compromised labral statuses, induced an increase in RC muscle activity to compensate and try to preserve GH joint stability through the compression mechanism, which may in turn increase the likelihood of muscle fatigue in RC muscles. This may potentially precipitate other shoulder pathologies. According to Aranha et al. (2022), performing external rotation and abduction potentially increases the risk of fatigue in supraspinatus and infraspinatus, which was confirmed in the current study. Further research is needed to better understand the nature of the link between the risk of fatigue and muscular demands. Muscular fatigue of these RC muscles may disturb the scapulohumeral balance at the GH joint and compromise its stability. The imbalance of rotator cuff muscle forces possesses the potential for GH joint dislocation and subluxation (Gaudet et al., 2018; Lippitt & Matsen, 1993).

Furthermore, under weakened labral circumstances, the increased activation level in RC muscles places persistent stress on the muscle tendons which may promote over-stimulation of tendon cells and result in a continuous loss of collagen (Arnoczky et al., 2007). According to Evanko and Vogel (1993) and Wang et al. (2003), this over-stimulation of tendon cells triggers the inflammatory response and eventually leads to tendinitis or tendinopathy. Consequently, these weakened tendon cells caused by degeneration and microdamage as a result of muscle overuse might result in rotator cuff tears and worsen the damage in the glenoid labrum (Gallagher & Schall, 2017). Additionally, muscular fatigue of the RC muscles can compromise consistent stabilization forces at the GH joint resulting in potential superior and anterior translation of the humeral head. This humeral translation can cause encroachment into the limited subacromial space which may cause functional impingement, tendon damage, altered kinematics, or osteoarthritis (Chopp & Dickerson, 2012; Dickerson et al., 2011; Lang et al., 2019; Page, 2011; Werner et al., 2004).

5.6 Relevance and Implications

This study discovered a correlation between the quality of the glenoid labrum and the variations in muscle recruitments which helped identify potential muscle overload when performing physically demanding tasks. This information can advise clinicians about the challenges that patients with defective labrum may face when performing challenging tasks, especially during shoulder external rotation and abduction (Aranha et al., 2022; Gaudet et al., 2018). Moreover, the findings of this study demonstrated the efficacy of surgical management and the advantages of early surgical treatments, which also showed benefits in treating degenerated labra in older adults (Zughaib et al., 2017). Further, given that linkages between

tissue overuse and potential shoulder pathologies exist, all this information can be used as a guideline for occupational injury prevention. This study demonstrated the challenges and risk of injury in RC muscles, especially supraspinatus and infraspinatus (Aranha et al., 2022), in performing external rotation and abduction which exceeded the median threshold (10%–14% load level) described in Jonsson (1978). Moreover, the muscle activation levels were further exceeding the threshold level in conditions with a defective labrum, suggesting that labrum lesions or degeneration may put individuals at a higher risk of fatigue if performed high-cost tasks in a full workday even though the magnitudes of change were between 2%–8% (Jonsson, 1988; La Delfa et al., 2022). Therefore, the duration of tasks involved in these postures and the applied force should be reduced (in concord with Alenabi et al., 2019; Brookham et al., 2010; Whittaker et al., 2022). Additionally, this information uncovered potential complications associated with improper care of labrum injuries and degenerations. Beyond this, the addressed compensatory muscle techniques from this study could serve as an advisory to physiotherapists to emphasize the advantages of early degenerated labra treatments in older adults in an attempt to improve function outcomes and prevent secondary injuries or other shoulder pathologies.

5.7 Limitations

5.7.1 Clinical Joint Stiffness

Although the connection between muscle activations and labral quality was examined in this study, several limitations influenced the findings. First, the experimental kinematic data, which was used as inputs for the SLAM model, was collected from one healthy male. The study was focused on the mechanical changes between various labral conditions; however, potential changes in clinical joint stiffness were not addressed. This study simulated all isometric and dynamic tasks using the same motion data. Hence, the postures and movement patterns remained for all labral conditions, which may not fully reflect reality in the clinical population. Different kinematics with restricted ROM have been observed in clinical populations and vulnerable groups when performing ADLs due to discomfort and the challenging nature of some tasks (Brookham et al., 2018; Hall et al., 2011; Lang et al., 2019). Therefore, patients with damaged or degenerated labra demonstrate analogous kinematic changes when performing the experimental tasks. Thus, the compensatory responses of the system may mispresent some changes. However, it was logistically challenging to accurately collect, model, or simulate the possible spectrum of variations in movement patterns in the clinical population. There is a scarcity of research to support and emphasize the movement variations in patients under various labral statuses. However, this does not preclude the value of this study as an initial investigation into the mechanical outcomes and relationships among labral conditions. Furthermore, the movement tasks that were evaluated in this study include mainly isometric and dynamic movements which did not require full ROM. Additionally, it was infeasible to identify and recruit participants to represent all the interested labral conditions of this study. Therefore, clinical joint stiffness emulation was not included.

5.7.2 Variation in Muscular Mass and Strength

A second notable limitation was the lack of variation in muscular mass and strength. The SLAM model was used in this study to predict muscle force contributions in scenarios with healthy, defected or repaired labra. The glenoid stability constraints were modified to simulate various situations, however, without muscle size and strength were held constant. This was intentional to isolate the stability ratios as modified variables. Although the results identified the impact of simulated age-related labral degeneration on muscular responses, age-related declines in muscle strength and mass were not illustrated (Hughes et al., 1999; Volpi et al., 2004). The aging effects on muscle activation levels may be underestimated since the muscular mass and strength were modelled as in a young, healthy individual, which likely does not match the aged population. However, the primary purpose of this study was to investigate how labral quality influences muscle activations. Alterations were focused on glenoid stability constraints to ensure that changes in muscle recruitment were directly attributable to the variations in GH joint stability level as described. Further, due to a knowledge gap in estimating the loss of muscle mass with aging, it was decided to not model variations in muscle mass. For a similar reason, this study was unable to examine the efficacy of conservative labral treatments since it was difficult to reliably estimate the gains in muscle mass and strength after non-operative treatments for this population. Therefore, future development of a muscle strength generation model can be beneficial to better represent the system responses by taking individual variations in muscular mass and strength into account.

5.8 Future Directions

This study offers the theoretical foundation for a better understanding of the effects of aging and associated muscle compensatory strategies associated with variations in labrum quality, but future research may be able to improve on this early work. Assessment of a condition-matched reference population would assist in providing more fidelic kinematic inputs of the symptomatic groups which may further aid in determining the specific compensatory muscle strategies in the clinical population. The current research would also be furthered by expanding the experimental tasks to include a wider range of activities including more difficult functional activities and isometric exercises performed at various arm elevation angles. These may present greater directional or overall challenges to the compromised system and be more effective in illustrating the multidirectional and anisotropic function of the GH joint stabilizers and the compression mechanism of the RC muscles (Aranha et al., 2022; Chopp-Hurley et al., 2016). Further, simulating isometric tasks with different arm elevation angles may more fully explore the complex relationship between the balance of postural-dependent stabilizing forces and muscle force responses. Finally, sources of patient-to-patient variation could be addressed in future investigations to clarify individual differences in scapular rhythm and muscular mass associated with individuals' injury and the aging impacts on kinematics and muscle tissue quality (Hughes et al., 1999). These considerations may provide additional insight into different populations rather than a generalized concept while also more fully illustrating the compensatory muscle strategies in patients. A third benefit may be increasing the specific fidelity of SLAM implementation through targeted parameter modification, i.e., individual variation in muscle attachment sites and bone dimensions.

VI. Conclusions

This study illustrated the aging effects and potential compensatory muscle strategies that patients with defective glenoid labrum may encounter through biomechanical model simulations. This study was the first to explore a mechanical link between the quality of the labrum and the activations of shoulder muscles on a large scale and to correlate and predict the likelihood of increased muscular demands in the clinical population when performing certain activities. The stabilization role of the rotator cuff muscles was underlined by the results, which also confirmed the theorized benefits of some surgical approaches for damaged glenoid labrum. Future investigations may clarify aspects of these mechanical links by considering the inter-individual variations in shoulder functions, kinematics, bony morphology, and muscular mass.

REFERENCES

Alashkham, A., Alraddadi, A., & Soames, R. (2020). Age related morphometric changes of the glenoid labrum. *Anatomy*, *14*(3), 177–184. https://doi.org/10.2399/ana.20.821264

Alenabi, T., Whittaker, R. L., Kim, S. Y., & Dickerson, C. R. (2019). Arm posture influences on regional supraspinatus and infraspinatus activation in isometric arm elevation efforts. *Journal of Electromyography and Kinesiology*, *44*, 108–116. https://doi.org/10.1016/j.jelekin.2018.12.005

Ando, A., Sugaya, H., Takahashi, N., Kawai, N., Hagiwara, Y., & Itoi, E. (2012). Arthroscopic Management of Selective Loss of External Rotation after Surgical Stabilization of Traumatic Anterior Glenohumeral Instability: Arthroscopic Restoration of Anterior Transverse Sliding Procedure. *Arthroscopy: The Journal of Arthroscopic and Related Surgery*, *28*(6), 749–753. https://doi.org/10.1016/j.arthro.2011.11.003

Aranha, L., Eapen, C., Patel, V. D., Prabhakar, A. J., & Hariharan, K. (2022). Muscle fatigue response of rotator cuff muscles in different postures. *Archives of Orthopaedic and Trauma Surgery*, *143*, 3191–3199. https://doi.org/10.1007/s00402-022-04650-8

Arnoczky, S. P., Lavagnino, M., & Egerbacher, M. (2007). The mechanobiological aetiopathogenesis of tendinopathy: Is it the over-stimulation or the under-stimulation of tendon cells? *International Journal of Experimental Pathology*, *88*(4), 217–226. https://doi.org/10.1111/j.1365-2613.2007.00548.x

Bents, E., Brady, P. C., Adams, C. R., Tokish, J. M., Higgins, L. D., & Denard, P. J. (2017). Patient-Reported Outcomes of Knotted and Knotless Glenohumeral Labral Repairs Are Equivalent. *American Journal of Orthopedics*, *46*(6), 279–283.

Bigliani, L. U., Codd, T. P., Connor, P. M., Levine, W. N., Littlefield, M. A., & Hershon, S. J. (1997). Shoulder Motion and Laxity in the Professional Baseball Player. *The American Journal of Sports Medicine*, *25*(5), 609–613. https://doi.org/10.1177/036354659702500504

Black, K. P., Schneider, D. J., Yu, J. R., & Jacobs, C. R. (1999). Biomechanics of the Bankart Repair: The Relationship Between Glenohumeral Translation and Labral Fixation Site. *The American Journal of Sports Medicine*, *27*(3), 339–344. https://doi.org/10.1177/03635465990270031201

Brookham, R. L., Cudlip, A. C., & Dickerson, C. R. (2018). Examining upper limb kinematics and dysfunction of breast cancer survivors in functional dynamic tasks. *Clinical Biomechanics*, *55*, 86–93. https://doi.org/10.1016/j.clinbiomech.2018.04.010

Brookham, R. L., & Dickerson, C. R. (2016). Comparison of humeral rotation co-activation of breast cancer population and healthy shoulders. *Journal of Electromyography and Kinesiology*, *29*, 100–106. https://doi.org/10.1016/j.jelekin.2015.07.002

Brookham, R. L., Middlebrook, E. E., Grewal, T. jaskirat, & Dickerson, C. R. (2011). The utility of an empirically derived co-activation ratio for muscle force prediction through optimization. *Journal of Biomechanics*, *44*(8), 1582–1587. https://doi.org/10.1016/j.jbiomech.2011.02.077

Brookham, R. L., Wong, J. M., & Dickerson, C. R. (2010). Upper limb posture and submaximal hand tasks influence shoulder muscle activity. *International Journal of Industrial Ergonomics*, *40*(3), 337–344. https://doi.org/10.1016/j.ergon.2009.11.006

Burkhart, S. S., & Morgan, C. D. (1998). The Peel-Back Mechanism: Its Role in Producing and Extending Posterior Type II SLAP Lesions and Its Effect on SLAP Repair Rehabilitation. *Arthroscopy: The Journal of Arthroscopic and Related Surgery*, *14*(6), 637–640.

Chaffin, D. B. (1997). Development of computerized human static strength simulation model for job design. *Human Factors and Ergonomics In Manufacturing*, *7*(4), 305–322. https://doi.org/10.1002/(sici)1520-6564(199723)7:4<305::aid-hfm3>3.0.co;2-7

Chalmers, P. N., Erickson, B. J., D'Angelo, J., Ma, K., & Romeo, A. A. (2019). Epidemiology of Shoulder Surgery Among Professional Baseball Players. *American Journal of Sports Medicine*, *47*(5), 1068–1073. https://doi.org/10.1177/0363546519832525

Charlton, I. W., & Johnson, G. R. (2001). Application of spherical and cylindrical wrapping algorithms in a musculoskeletal model of the upper limb. *Journal of Biomechanics*, *34*(9), 1209–1216. https://doi.org/https://doi.org/10.1016/S0021-9290(01)00074-4

Chopp, J. N., & Dickerson, C. R. (2012). Resolving the contributions of fatigue-induced migration and scapular reorientation on the subacromial space: An orthopaedic geometric simulation analysis. *Human Movement Science*, *31*(2), 448–460. https://doi.org/10.1016/j.humov.2011.09.005

Chopp-Hurley, J. N., Brookham, R. L., & Dickerson, C. R. (2016). Identification of potential compensatory muscle strategies in a breast cancer survivor population: A combined computational and experimental approach. *Clinical Biomechanics*, *40*, 63–67. https://doi.org/10.1016/j.clinbiomech.2016.10.015

Clauser, C. E., Mcconville, J. T., & Young, J. W. (1969). Weight, volume, and center of mass of segments of the human body. *Medicine*.

Clavert, P. (2015). Glenoid labrum pathology. *Orthopaedics and Traumatology: Surgery and Research*, *101*(1), S19–S24. https://doi.org/10.1016/j.otsr.2014.06.028

Collins, J. J. (1995). The redundant nature of locomotor optimization laws. *Journal of Biomechanics*, *28*(3), 251–267. https://doi.org/https://doi.org/10.1016/0021-9290(94)00072-C

Crall, T. S., Bishop, J. A., Guttman, D., Kocher, M., Bozic, K., & Lubowitz, J. H. (2012). Cost-Effectiveness Analysis of Primary Arthroscopic Stabilization Versus Nonoperative Treatment for First-Time Anterior Glenohumeral Dislocations. *Arthroscopy: Journal of Arthroscopic and Related Surgery*, *28*(12), 1755–1765. https://doi.org/10.1016/j.arthro.2012.05.885

Crowninshield, R. D., & Brand, R. A. (1981). A physiologically based criterion of muscle force prediction in locomotion. *Journal of Biomechanics*, *14*(11), 793–801. https://doi.org/https://doi.org/10.1016/0021-9290(81)90035-X

DeFroda, S. F., Goyal, D., Patel, N., Gupta, N., & Mulcahey, M. K. (2018). Shoulder Instability in the Overhead Athlete. *Current Sports Medicine Reports*, *17*(9), 308–314. https://journals.lww.com/acsm-csmr/Fulltext/2018/09000/Shoulder_Instability_in_the_Overhead_Athlete.10.aspx

DeFroda, S. F., Perry, A. K., Bodendorfer, B. M., & Verma, N. N. (2021). Evolving Concepts in the Management of Shoulder Instability. *Indian Journal of Orthopaedics*, *55*(2), 285–298. https://doi.org/10.1007/s43465-020-00348-4

Dickerson, C. R., Chaffin, D. B., & Hughes, R. E. (2007). A mathematical musculoskeletal shoulder model for proactive ergonomic analysis. *Computer Methods in Biomechanics and Biomedical Engineering*, *10*(6), 389–400. https://doi.org/10.1080/10255840701592727

Dickerson, C. R., Chopp, J. N., & Borgs, S. P. (2011). Simulation of fatigue-initiated subacromial impingement: Clarifying mechanisms. *Procedia IUTAM*, *2*, 35–57. https://doi.org/10.1016/j.piutam.2011.04.005

Dul, J., Johnson, G. E., Shiavi, R., & Townsend, M. A. (1984). Muscular synergism—II. A minimum-fatigue criterion for load sharing between synergistic muscles. *Journal of Biomechanics*, *17*(9), 675–684. https://doi.org/https://doi.org/10.1016/0021-9290(84)90121-0

Dul, J., Townsend, M. A., Shiavi, R., & Johnson, G. E. (1984). Muscular synergism—I. On criteria for load sharing between synergistic muscles. *Journal of Biomechanics*, *17*(9), 663–673. https://doi.org/https://doi.org/10.1016/0021-9290(84)90120-9

Dumont, G. D., Russell, R. D., & Robertson, W. J. (2011). Anterior shoulder instability: A review of pathoanatomy, diagnosis and treatment. *Current Reviews in Musculoskeletal Medicine*, *4*(4), 200–207. https://doi.org/10.1007/s12178-011-9092-9

Ebaugh, D., Spinelli, B., & Schmitz, K. H. (2011). Shoulder impairments and their association with symptomatic rotator cuff disease in breast cancer survivors. *Medical Hypotheses*, *77*(4), 481–487. https://doi.org/https://doi.org/10.1016/j.mehy.2011.06.015

Edwards, S. L., Lee, J. A., Bell, J. E., Packer, J. D., Ahmad, C. S., Levine, W. N., Bigliani, L. U., & Blaine, T. A. (2010). Nonoperative treatment of superior labrum anterior posterior tears: Improvements in pain, function, and quality of life. *American Journal of Sports Medicine*, *38*(7), 1458–1461. https://doi.org/10.1177/0363546510370937

Evanko, S. P., & Vogel, K. G. (1993). Proteoglycan Synthesis in Fetal Tendon Is Differentially Regulated by Cyclic Compression in Vitro. *Archives of Biochemistry and Biophysics*, *307*(1), 153–164. https://doi.org/https://doi.org/10.1006/abbi.1993.1574

Fleisig, G. S., Andrews, J. R., Dillman, C. J., & Escamilla, R. F. (1995). Kinetics of Baseball Pitching with Implications About Injury Mechanisms. *The American Journal of Sports Medicine*, *23*(2), 233–239. https://doi.org/10.1177/036354659502300218

Fortenbaugh, D., Fleisig, G. S., & Andrews, J. R. (2009). Baseball Pitching Biomechanics in Relation to Injury Risk and Performance. *Sports Health*, *1*(4), 314–320. https://doi.org/10.1177/1941738109338546

Gallagher, S., & Schall, M. C. (2017). Musculoskeletal disorders as a fatigue failure process: evidence, implications and research needs. *Ergonomics*, *60*(2), 255–269. https://doi.org/10.1080/00140139.2016.1208848

Gaudet, S., Tremblay, J., & Dal Maso, F. (2018). Evolution of muscular fatigue in periscapular and rotator cuff muscles during isokinetic shoulder rotations. *Journal of Sports Sciences*, *36*(18), 2121–2128. https://doi.org/10.1080/02640414.2018.1440513

Gowan, I. D., Jobe, F. W., Tibone, J. E., Perry, J., & Moynes, D. R. (1984). A comparative electromyographic analysis of the shoulder during pitching professional versus amateur pitchers. *The American Journal of Sports Medicine*, *15*(6).

Gulotta, L. V., Lobatto, D., Delos, D., Coleman, S. H., & Altchek, D. W. (2014). Anterior shoulder capsular tears in professional baseball players. *Journal of Shoulder and Elbow Surgery*, *23*(8). https://doi.org/10.1016/j.jse.2013.11.027

Hall, L. C., Middlebrook, E. E., & Dickerson, C. R. (2011). Analysis of the influence of rotator cuff impingements on upper limb kinematics in an elderly population during activities of daily living. *Clinical Biomechanics*, *26*(6), 579–584. https://doi.org/10.1016/j.clinbiomech.2011.02.006

Högfors, C., Peterson, B., Sigholm, G., & Herberts, P. (1991). Biomechanical model of the human shoulder joint—II. The shoulder rhythm. *Journal of Biomechanics*, *24*(8), 699–709. https://doi.org/https://doi.org/10.1016/0021-9290(91)90334-J

Högfors, C., Sigholm, G., & Herberts, P. (1987). Biomechanical model of the human shoulder—I. Elements. *Journal of Biomechanics*, *20*(2), 157–166. https://doi.org/https://doi.org/10.1016/0021-9290(87)90307-1

Horner, N. S., Moroz, P. A., Bhullar, R., Habib, A., Simunovic, N., Wong, I., Bedi, A., & Ayeni, O. R. (2018). Open versus arthroscopic Latarjet procedures for the treatment of shoulder instability: A systematic review of comparative studies. *BMC Musculoskeletal Disorders*, *19*(1). https://doi.org/10.1186/s12891-018-2188-2

Howarth, S. J., & Callaghan, J. P. (2010). Quantitative assessment of the accuracy for three interpolation techniques in kinematic analysis of human movement. *Computer Methods in Biomechanics and Biomedical Engineering*, *13*(6), 847–855. https://doi.org/10.1080/10255841003664701

Howell, S. M., & Galinat, B. J. (1987). The Glenoid-Labral Socket: A Constrained Articular Surface. *Clinical Orthopaedics and Related Research*, *243*, 122–125.

Hu, T., Kühn, J., & Haddadin, S. (2020). Forward and inverse dynamics modeling of human shoulder-arm musculoskeletal system with scapulothoracic constraint. *Computer Methods in Biomechanics and Biomedical Engineering*, *23*(11), 785–803. https://doi.org/10.1080/10255842.2020.1764945

Hughes, R. E., Johnson, M. E., O'driscoll, S. W., & An, K.-N. (1999). Age-Related Changes in Normal Isometric Shoulder Strength. In *THE AMERICAN JOURNAL OF SPORTS MEDICINE* (Vol. 27, Issue 5).

Imam, M. A., Shehata, M. S. A., Martin, A., Attia, H., Sinokrot, M., Bahbah, E. I., Gwilym, S., Jacob, J., Narvani, A. A., & Meyer, D. C. (2020). Bankart Repair Versus Latarjet Procedure for Recurrent Anterior Shoulder Instability: A Systematic Review and Meta-analysis of 3275 Shoulders. *The American Journal of Sports Medicine*, *49*(7), 1945–1953. https://doi.org/10.1177/0363546520962082

Jakobsen, B. W., Johannsen, H. V., Suder, P., & Søjbjerg, J. O. (2007). Primary Repair Versus Conservative Treatment of First-Time Traumatic Anterior Dislocation of the Shoulder: A Randomized Study With 10-Year Follow-up. *Arthroscopy: Journal of Arthroscopic and Related Surgery*, *23*(2), 118–123. https://doi.org/10.1016/j.arthro.2006.11.004

Jonsson, B. (1978). Quantitative electromyographic evaluation of muscular load during work. *Scandinavian Journal of Rehabilitation Medicine. Supplement*, *6*, 69–74.

Jonsson, B. (1988). The static load component in muscle work. *Eur J Appl Physiol*, *57*, 305–310.

Karlsson, D., & Peterson, B. (1992). Towards a model for force predictions in the human shoulder. *Journal of Biomechanics*, *25*(2), 189–199. https://doi.org/https://doi.org/10.1016/0021-9290(92)90275-6

Kleiner, M. T., Payne, W. B., McGarry, M. H., Tibone, J. E., & Lee, T. Q. (2016). Biomechanical Comparison of the Latarjet Procedure with and without Capsular Repair. *CiOS Clinics in Orthopedic Surgery*, *8*(1), 84–91. https://doi.org/10.4055/cios.2016.8.1.84

Knapik, D. M., Kolaczko, J. G., Gillespie, R. J., Salata, M. J., & Voos, J. E. (2020). Complications and Return to Activity After Arthroscopic Repair of Isolated Type II SLAP Lesions: A Systematic Review Comparing Knotted Versus Knotless Suture Anchors. *Orthopaedic Journal of Sports Medicine*, *8*(4). https://doi.org/10.1177/2325967120911361

Kreitner, K. F., Botchen, K., Rude, J., Bittinger, F., Krummenauer, F., & Thelen, M. (1998). Superior labrum and labral-bicipital complex: MR imaging with pathologic-anatomic and histologic correlation. *American Journal of Roentgenology*, *170*(3), 599–605. https://doi.org/10.2214/ajr.170.3.9490937

La Delfa, N. J., Whittaker, R. L., Lockley, R. M. E., Fournier, D. E., & Dickerson, C. R. (2022). The sensitivity of shoulder muscle fatigue to vertical hand location during complex manual force exertions. *International Journal of Industrial Ergonomics*, *88*. https://doi.org/10.1016/j.ergon.2022.103272

Ladd, L. M., Crews, M., & Maertz, N. A. (2021). Glenohumeral Joint Instability: A Review of Anatomy, Clinical Presentation, and Imaging. *Clinics in Sports Medicine*, *40*(4), 585–599. https://doi.org/10.1016/j.csm.2021.05.001

Lafosse, L., & Boyle, S. (2010). Arthroscopic Latarjet procedure. *Journal of Shoulder and Elbow Surgery*, *19*, 2–12. https://doi.org/10.1016/j.jse.2009.12.010

Lafosse, L., Franceschi, G., Kordasiewicz, B., Andrews, W. J., & Schwartz, D. (2012). Arthroscopic posterior bone block: Surgical technique. *Musculoskeletal Surgery*, *96*(3), 205–212. https://doi.org/10.1007/s12306-012-0220-5

Lang, A. E., Dickerson, C. R., Kim, S. Y., Stobart, J., & Milosavljevic, S. (2019). Impingement pain affects kinematics of breast cancer survivors in work-related functional tasks. *Clinical Biomechanics*, *70*, 223–230. https://doi.org/10.1016/j.clinbiomech.2019.10.001

Levigne, C., Garret, J., & Walch, G. (2005). Posterior Bone Block for Posterior Instability. *Techniques in Shoulder and Elbow Surgery*, *6*(1), 26–35.

Li, X., Lin, T. J., Jager, M., Price, M. D., Deangelis, N. A., Busconi, B. D., & Brown, M. A. (2010). Management of type II superior labrum anterior posterior lesions: a review of the literature. *Orthopedic Reviews*, *2*(6), 16–22. https://doi.org/10.4081/or.2010.e6

Linderman, S. E., Johnson, J. E., Anderson, D. D., & Patterson, B. M. (2021). Influence of subscapularis stiffness with glenosphere lateralization on physiological external rotation limits after reverse shoulder arthroplasty. *Journal of Shoulder and Elbow Surgery*, *30*(11), 2629–2637. https://doi.org/10.1016/j.jse.2021.04.039

Lippitt, S., & Matsen, F. (1993). Mechanisms of glenohumeral joint stability. *Clinical Orthopaedics and Related Research*, *291*(291), 20–28. https://doi.org/10.1097/00003086-199306000-00004

Makhsous, M., Hok, C., Siemienski, A., & Peterson, B. (1999). Total shoulder and relative muscle strength in the scapular plane. *Journal of Biomechanics*, *32*, 1213–1220.

Matache, B. A., Hurley, E. T., Kanakamedala, A. C., Jazrawi, L. M., Virk, M., Strauss, E. J., & Campbell, K. A. (2021). Knotted Versus Knotless Anchors for Labral Repair in the Shoulder: A Systematic Review. *Arthroscopy: Journal of Arthroscopic and Related Surgery*, *37*(4), 1314–1321. https://doi.org/10.1016/j.arthro.2020.11.056

Mihata, T., Gates, J., Mcgarry, M. H., Lee, J., Kinoshita, M., & Lee, T. Q. (2007). Effect of Rotator Cuff Muscle Imbalance on Forceful Internal Impingement and Peel-Back of the Superior Labrum A Cadaveric Study and the. *The American Journal of Sports Medicine*, *37*(11). https://doi.org/10.1177/0363546509337450

Mihata, T., Lee, Y. S., McGarry, M. H., Abe, M., & Lee, T. Q. (2004). Excessive humeral external rotation results in increased shoulder laxity. *American Journal of Sports Medicine*, *32*(5), 1278–1285. https://doi.org/10.1177/0363546503262188

Miniaci, A., Mascia, A. T., Salonen, D. C., & Becker, E. J. (2002). Magnetic Resonance Imaging of the Shoulder in Asymptomatic Professional Baseball Pitchers. *The American Journal of Sports Medicine*, *30*(1).

Mulla, D. M., Hodder, J. N., Maly, M. R., Lyons, J. L., & Keir, P. J. (2020). Glenohumeral stabilizing roles of the scapulohumeral muscles: Implications of muscle geometry. *Journal of Biomechanics*, *100*. https://doi.org/10.1016/j.jbiomech.2019.109589

Mutlu, S., Mahıroğullari, M., Güler, O., Uçar, B. Y., Mutlu, H., Sönmez, G., & Mutlu, H. (2013). Anterior Glenohumeral Instability: Classification of Pathologies of Anteroinferior Labroligamentous Structures Using MR Arthrography. *Advances in Orthopedics*, *2013*, 1–4. https://doi.org/10.1155/2013/473194

Nigg, B. M., & Herzog, W. (1994). *Biomechanics of the Musculo-Skeletal System*.

Nussbaum, M. A., & Zhang, X. (2000). Heuristics for locating upper extremity joint centres from a reduced set of surface markers. *Human Movement Science*, *19*, 797–816. www.elsevier.com/locate/humov

Owens, B. D., Agel, J., Mountcastle, S. B., Cameron, K. L., & Nelson, B. J. (2009). Incidence of glenohumeral instability in collegiate athletics. *American Journal of Sports Medicine*, *37*(9), 1750–1754. https://doi.org/10.1177/0363546509334591

Owens, B. D., Cameron, K. L., Peck, K. Y., DeBerardino, T. M., Nelson, B. J., Taylor, D. C., Tenuta, J., & Svoboda, S. J. (2015). Arthroscopic versus open stabilization for anterior shoulder subluxations. *Orthopaedic Journal of Sports Medicine*, *3*(1), 1–4. https://doi.org/10.1177/2325967115571084

Owens, B. D., Nelson, B. J., Duffey, M. L., Mountcastle, S. B., Taylor, D. C., Cameron, K. L., Campbell, S., & DeBerardino, T. M. (2010). Pathoanatomy of first-time, traumatic, anterior

glenohumeral subluxation events. *Journal of Bone and Joint Surgery*, *92*(7), 1605–1611. https://doi.org/10.2106/JBJS.I.00851

Page, P. (2011). Shoulder muscle imbalance and subacromial impingement syndrome in overhead athletes. *The International Journal of Sports Physical Therapy*, *6*(1), 51–58.

Panossian, V. R., Mihata, T., Tibone, J. E., Fitzpatrick, M. J., McGarry, M. H., & Lee, T. Q. (2005). Biomechanical analysis of isolated type II SLAP lesions and repair. *Journal of Shoulder and Elbow Surgery*, *14*(5), 529–534. https://doi.org/https://doi.org/10.1016/j.jse.2004.11.002

Patzer, T., Habermeyer, P., Hurschler, C., Bobrowitsch, E., Wellmann, M., Kircher, J., & Schofer, M. D. (2012). The influence of superior labrum anterior to posterior (SLAP) repair on restoring baseline glenohumeral translation and increased biceps loading after simulated SLAP tear and the effectiveness of SLAP repair after long head of biceps tenotomy. *Journal of Shoulder and Elbow Surgery*, *21*(11), 1580–1587. https://doi.org/10.1016/j.jse.2011.11.005

Péan, F., Favre, P., & Goksel, O. (2022). Computational analysis of subscapularis tears and pectoralis major transfers on muscular activity. *Clinical Biomechanics*, *92*. https://doi.org/10.1016/j.clinbiomech.2021.105541

Pfahler, M., Haraida, S., Schulz, C., Anetzberger, H., Refior, H. J., Bauer, G. S., & Bigliani, L. U. (2003). Age-related changes of the glenoid labrum in normal shoulders. *Journal of Shoulder and Elbow Surgery*, *12*(1), 40–52. https://doi.org/https://doi.org/10.1067/mse.2003.3

Prilutsky, B. I., & Zatsiorsky, V. M. (2002). Optimization-based models of muscle coordination. *Exercise and Sport Sciences Reviews*, *30*(1), 32–38. https://doi.org/10.1097/00003677-200201000-00007

Prodromos, C. C., Ferry, J. A., Schiller, A. L., Zarins, B., & From, M. (1990). Histological Studies of the Glenoid Labrum from Fetal Life to Old Age. *The Journal of Bone and Joint Surgery*.

Robinson, C. M., Howes, J., Murdoch, H., Will, E., & Graham, C. (2006). Functional Outcome and Risk of Recurrent Instability After Primary Traumatic Anterior Shoulder Dislocation in Young Patients. *The Journal of Bone and Joint Surgery*, *88-A*(11), 2326–2336.

Snyder, S. J., Karzel, R. P., Pizzo, W. Del, Ferkel, R. D., & Friedman, M. J. (1990). SLAP Lesions of the Shoulder. *Arthroscopy: The Journal of Arthroscopic and Related Surgery*, *6*(4), 21–279.

Thompson, W. O., Debski, R. E., Boardman, N. D., Taskiran, E., Warner, J. J. P., Fu, F. H., & Woo, S. L.-Y. (1996). A Biomechanical Analysis of Rotator Cuff Deficiency in a Cadaveric Model. *The American Journal of Sports Medicine*, *24*(3), 286–292. https://doi.org/10.1177/036354659602400307

Townsend, H., Jobe, F. W., Pink, M., & Perry, J. (1991). Electromyographic analysis of the glenohumeral muscles during a baseball rehabilitation program. *The American Journal of Sports Medicine*, *19*(3), 264–272. https://doi.org/10.1177/036354659101900309

van der Helm, F. C. T. (1994). Analysis of the kinematic and dynamic behavior of the shoulder mechanism. *Journal of Biomechanics*, *27*(5), 527–550. https://doi.org/https://doi.org/10.1016/0021-9290(94)90064-7

Vaughan, C. L., Davis, B. L., & O'Connor, J. C. (1992). *Dynamics of Human Gait*.

Volpi, E., Nazemi, R., & Fujita, S. (2004). Muscle tissue changes with aging. *Curr Opin Clin Nutr Metab Care*, *7*(4), 405–410.

Wang, J. H. C., Jia, F., Yang, G., Yang, S., Campbell, B. H., Stone, D., & Woo, S. L. Y. (2003). Cyclic Mechanical Stretching of Human Tendon Fibroblasts Increases the Production of Prostaglandin E 2 and Levels of Cyclooxygenase Expression: A Novel In Vitro Model Study. *Connective Tissue Research*, *44*(42067), 128–133. https://doi.org/10.1080/03008200390223909

Wellmann, M., Bobrowitsch, E., Khan, N., Patzer, T., Windhagen, H., Petersen, W., & Bohnsack, M. (2011). Biomechanical effectiveness of an arthroscopic posterior bankart repair versus an open bone block procedure for posterior shoulder instability. *American Journal of Sports Medicine*, *39*(4), 796–803. https://doi.org/10.1177/0363546510389991

Werner, C. M. L., Nyffeler, R. W., Jacob, H. A. C., & Gerber, C. (2004). The effect of capsular tightening on humeral head translations. *Journal of Orthopaedic Research*, *22*(1), 194–201. https://doi.org/https://doi.org/10.1016/S0736-0266(03)00137-2

Wheeler, J. H., Ryan, J. B., Arciero, R. A., & Molinari, R. N. (1989). Arthroscopic versus nonoperative treatment of acute shoulder dislocations in young athletes. *Arthroscopy: The Journal of Arthroscopic & Related Surgery*, *5*(3), 213–217. https://doi.org/https://doi.org/10.1016/0749-8063(89)90174-6

Whittaker, R. L., Alenabi, T., Kim, S. Y., & Dickerson, C. R. (2022). Regional Electromyography of the Infraspinatus and Supraspinatus Muscles During Standing Isometric External Rotation Exercises. *Sports Health*, *14*(5), 725–732. https://doi.org/10.1177/19417381211043849

Wood, J. E., Meek, S. G., & Jacobsen, S. C. (1989). Quantitation of human shoulder anatomy for prosthetic arm control—I. Surface modelling. *J. Biomechanics*, *22*(3), 273–292.

Wood, V. J. C., Sabick, M. B., Pfeiffer, R. P., Kuhlman, S. M., Christensen, J. H., & Curtin, M. J. (2011). Glenohumeral muscle activation during provocative tests designed to diagnose superior labrum anterior-posterior lesions. *American Journal of Sports Medicine*, *39*(12), 2670–2678. https://doi.org/10.1177/0363546511419822

Wu, I. T., Desai, V. S., Mangold, D. R., Camp, C. L., Barlow, J. D., Sanchez-Sotelo, J., Dahm, D. L., & Krych, A. J. (2021). Comparable clinical outcomes using knotless and knot-tying anchors for arthroscopic capsulolabral repair in recurrent anterior glenohumeral instability at mean 5-year follow-up. *Knee Surgery, Sports Traumatology, Arthroscopy*, *29*(7), 2077–2084. https://doi.org/10.1007/s00167-020-06057-7

Zatsiorsky, V., & Seluyanov, V. (1985). Estimation of the mass and inertia characteristics of the human body by means of the best predictive regression equations. *Biomechanics IX-B*, 233–239. https://www.scopus.com/inward/record.uri?eid=2-s2.0-0001396993&partnerID=40&md5=8929f2def312ae5131bc11134620207e

Zughaib, M., Robbins, C. B., Miller, B. S., & Gagnier, J. J. (2017). Outcomes in patients with glenoid labral lesions: A cohort study. *BMJ Open Sport and Exercise Medicine*, *2*(1). https://doi.org/10.1136/bmjsem-2016-000209

Appendix A: Percentages of Maximal Predicted Muscle Group Capability and Costs, By Task

Table A-1. Mean and maximum percentages of maximal predicted muscle group capability and mean task costs during isometric internal rotation under all simulated conditions.

Condition	RC Muscles %MMGC (%)				GA Muscles %MMGC (%)				Cost (N^3cm^6)	
	Mean	%Change	Max	%Change	Mean	%Change	Max	%Change	Mean	%Change
Intact	11.84		12		6.72		6.89		566733	
No Labrum	12.19	+2.96	12.33	+2.75	7.19	+6.99	7.35	+6.68	605959	+6.92
Ages 41–60	11.84	0	11.97	-0.25	6.72	0	6.92	+0.44	566724	0
Ages 61–80	11.98	+1.18	12.17	+1.42	6.68	-0.6	6.81	-1.16	576228	+1.68
Ages >80	12.12	+2.36	12.33	+2.75	6.67	-0.74	6.8	-1.31	587393	+3.65
SLAP	11.91	+0.59	12.03	+0.25	6.64	-1.19	6.81	-1.16	569526	+0.49
BKT	11.84	0	12	0	6.72	0	6.86	-0.44	566737	0
RBKT	11.73	-0.93	11.88	-1	7.2	+7.14	7.37	+6.97	573644	+1.22
ReSLAP	11.82	-0.17	12	0	6.74	+0.3	6.93	+0.58	565676	-0.19
ReBKT	11.84	0	12.04	+0.33	6.72	0	6.85	-0.58	566758	0
ReRBKT	11.85	+0.08	12.05	+0.42	6.76	+0.6	6.93	+0.58	567701	+0.17
LTJ	11.84	0	12.05	+0.42	6.72	0	6.88	-0.15	566752	0
PBB	11.79	-0.42	11.94	-0.5	6.66	-0.89	6.89	0	561932	-0.85

Note: %MMGC = Percentage of Maximal Predicted Muscle Group Capability; RC = Rotator Cuff; GA = Glenohumeral Articulating; SLAP = Superior Labrum Antero-to-Posterior Lesion; BKT = Bankart Lesion; RBKT = Reverse Bankart Lesion; ReSLAP = Repaired Superior Labrum Antero-to-Posterior Lesion; ReBKT = Repaired Bankart Lesion; ReRBKT = Repaired Reverse Bankart Lesion; LTJ = Latarjet; PBB = Posterior Bone Block. Cost represents the magnitude of the cost function.

Table A-2. Mean and maximum percentages of maximal predicted muscle group capability and mean task costs during isometric external rotation under all simulated conditions.

Condition	RC Muscles %MMGC (%)				GA Muscles %MMGC (%)				Cost (N^3cm^6)	
	Mean	%Change	Max	%Change	Mean	%Change	Max	%Change	Mean	%Change
Intact	22.56		23.09		6.61		6.83		858395	
No Labrum	31.74	+40.69	32.39	+40.28	8.53	+29.05	8.86	+29.72	2067089	+140.81
Ages 41–60	22.56	0	23.06	-0.13	6.61	0	6.82	-0.15	858395	0
Ages 61–80	25.51	+13.08	26.08	+12.95	6.94	+4.99	7.25	+6.15	1144145	+33.29
Ages >80	28.83	+27.79	29.53	+27.89	7.75	+17.25	8.15	+19.33	1574650	+83.44
SLAP	24.09	+6.78	24.65	+6.76	6.78	+2.57	6.96	+1.9	996692	+16.11
BKT	22.56	0	23.07	-0.09	6.61	0	6.84	+0.15	858420	0
RBKT	22.56	0	23.07	-0.09	6.61	0	6.87	+0.59	858380	0
ReSLAP	22	-2.48	22.52	-2.47	6.55	-0.91	6.76	-1.02	812975	-5.29
ReBKT	22.56	0	23.06	-0.13	6.61	0	6.81	-0.29	858395	0
ReRBKT	22.56	0	23.11	+0.09	6.61	0	6.88	+0.73	858400	0
LTJ	22.56	0	23.07	-0.09	6.61	0	6.78	-0.73	858385	0
PBB	22.56	0	23.08	-0.04	6.61	0	6.86	+0.44	858403	0

Note: %MMGC = Percentage of Maximal Predicted Muscle Group Capability; RC = Rotator Cuff; GA = Glenohumeral Articulating; SLAP = Superior Labrum Antero-to-Posterior Lesion; BKT = Bankart Lesion; RBKT = Reverse Bankart Lesion; ReSLAP = Repaired Superior Labrum Antero-to-Posterior Lesion; ReBKT = Repaired Bankart Lesion; ReRBKT = Repaired Reverse Bankart Lesion; LTJ = Latarjet; PBB = Posterior Bone Block. Cost represents the magnitude of the cost function.

Table A-3. Mean and maximum percentages of maximal predicted muscle group capability and mean task costs during isometric abduction under all simulated conditions.

Condition	RC Muscles %MMGC (%)				GA Muscles %MMGC (%)				Cost (N^3cm^6)	
	Mean	%Change	Max	%Change	Mean	%Change	Max	%Change	Mean	%Change
Intact	16.24		16.73		9.43		9.76		1605322	
No Labrum	19.78	+21.8	20.91	+24.99	9.67	+2.55	10.06	+3.07	2018015	+25.71
Ages 41–60	16.24	0	16.77	+0.24	9.43	0	9.74	-0.2	1605297	0
Ages 61–80	17.41	+7.2	17.87	+6.81	9.38	-0.53	9.85	+0.92	1728006	+7.64
Ages >80	18.7	+15.15	19.53	+16.74	9.41	-0.21	9.78	+0.2	1875961	+16.86
SLAP	16.87	+3.88	17.55	+4.9	9.41	-0.21	9.85	+0.92	1668255	+3.92
BKT	16.24	0	16.73	0	9.43	0	9.78	+0.2	1605399	0
RBKT	16.24	0	16.66	-0.42	9.43	0	9.79	+0.31	1605365	0
ReSLAP	16.01	-1.42	16.41	-1.91	9.44	+0.11	9.91	+1.54	1583028	-1.39
ReBKT	16.24	0	16.65	-0.48	9.43	0	9.87	+1.13	1605430	+0.01
ReRBKT	16.23	-0.06	16.78	+0.3	9.43	0	9.76	0	1605354	0
LTJ	16.24	0	16.84	+0.66	9.43	0	9.78	+0.2	1605356	0
PBB	16.24	0	17.04	+1.85	9.43	0	9.78	+0.2	1605389	0

Note: %MMGC = Percentage of Maximal Predicted Muscle Group Capability; RC = Rotator Cuff; GA = Glenohumeral Articulating; SLAP = Superior Labrum Antero-to-Posterior Lesion; BKT = Bankart Lesion; RBKT = Reverse Bankart Lesion; ReSLAP = Repaired Superior Labrum Antero-to-Posterior Lesion; ReBKT = Repaired Bankart Lesion; ReRBKT = Repaired Reverse Bankart Lesion; LTJ = Latarjet; PBB = Posterior Bone Block. Cost represents the magnitude of the cost function.

Table A-4. Mean and maximum percentages of maximal predicted muscle group capability and mean task costs during isometric adduction under all simulated conditions.

Condition	RC Muscles %MMGC (%)				GA Muscles %MMGC (%)				Cost (N^3cm^6)	
	Mean	%Change	Max	%Change	Mean	%Change	Max	%Change	Mean	%Change
Intact	1.43		1.5		6.92		7.03		44233	
No Labrum	0.66	-53.85	0.71	-52.67	8.35	+20.66	8.55	+21.62	63637	+43.87
Ages 41–60	1.43	0	1.49	-0.67	6.92	0	7.04	+0.14	44233	0
Ages 61–80	1.3	-9.09	1.38	-8	7.1	+2.6	7.21	+2.56	47002	+6.26
Ages >80	1.16	-18.88	1.24	-17.33	7.27	+5.06	7.42	+5.55	50003	+13.04
SLAP	1.43	0	1.49	-0.67	6.92	0	7.04	+0.14	44233	0
BKT	1.43	0	1.51	+0.67	6.92	0	7.03	0	44232	0
RBKT	0.64	-55.24	0.69	-54	8.35	+20.66	8.59	+22.19	65992	+49.19
ReSLAP	1.43	0	1.5	0	6.92	0	7.06	+0.43	44233	0
ReBKT	1.43	0	1.49	-0.67	6.92	0	7.04	+0.14	44233	0
ReRBKT	1.37	-4.2	1.44	-4	7	+1.16	7.11	+1.14	45383	+2.6
LTJ	1.43	0	1.5	0	6.92	0	7.03	0	44233	0
PBB	1.59	+11.19	1.63	+8.67	6.18	-10.69	6.3	-10.38	36031	-18.54

Note: %MMGC = Percentage of Maximal Predicted Muscle Group Capability; RC = Rotator Cuff; GA = Glenohumeral Articulating; SLAP = Superior Labrum Antero-to-Posterior Lesion; BKT = Bankart Lesion; RBKT = Reverse Bankart Lesion; ReSLAP = Repaired Superior Labrum Antero-to-Posterior Lesion; ReBKT = Repaired Bankart Lesion; ReRBKT = Repaired Reverse Bankart Lesion; LTJ = Latarjet; PBB = Posterior Bone Block. Cost represents the magnitude of the cost function.

Table A-5. Mean and maximum percentages of maximal predicted muscle group capability and mean task costs during isometric flexion under all simulated conditions.

Condition	RC Muscles %MMGC (%)				GA Muscles %MMGC (%)				Cost (N^3cm^6)	
	Mean	%Change	Max	%Change	Mean	%Change	Max	%Change	Mean	%Change
Intact	3.93		4.04		6.11		6.15		117359	
No Labrum	3.85	-2.04	3.92	-2.97	6.52	+6.71	6.59	+7.15	122234	+4.15
Ages 41–60	3.93	0	4.04	0	6.1	-0.16	6.15	0	117360	0
Ages 61–80	3.92	-0.25	4	-0.99	6.18	+1.15	6.22	+1.14	118417	+0.9
Ages >80	3.92	-0.25	3.98	-1.49	6.25	+2.29	6.29	+2.28	119444	+1.78
SLAP	3.92	-0.25	4	-0.99	6.1	-0.16	6.15	0	117360	0
BKT	3.93	0	4.01	-0.74	6.1	-0.16	6.15	0	117359	0
RBKT	3.86	-1.78	3.97	-1.73	6.54	+7.04	6.59	+7.15	123410	+5.16
ReSLAP	3.93	0	4	-0.99	6.1	-0.16	6.14	-0.16	117360	0
ReBKT	3.93	0	3.99	-1.24	6.11	0	6.15	0	117356	0
ReRBKT	3.92	-0.25	3.99	-1.24	6.14	+0.49	6.19	+0.65	117768	+0.35
LTJ	3.92	-0.25	4.01	-0.74	6.11	0	6.15	0	117361	0
PBB	4.04	+2.8	4.15	+2.72	5.69	-6.87	5.73	-6.83	113239	-3.51

Note: %MMGC = Percentage of Maximal Predicted Muscle Group Capability; RC = Rotator Cuff; GA = Glenohumeral Articulating; SLAP = Superior Labrum Antero-to-Posterior Lesion; BKT = Bankart Lesion; RBKT = Reverse Bankart Lesion; ReSLAP = Repaired Superior Labrum Antero-to-Posterior Lesion; ReBKT = Repaired Bankart Lesion; ReRBKT = Repaired Reverse Bankart Lesion; LTJ = Latarjet; PBB = Posterior Bone Block. Cost represents the magnitude of the cost function.

Table A-6. Mean and maximum percentages of maximal predicted muscle group capability and mean task costs during isometric extension under all simulated conditions.

Condition	RC Muscles %MMGC (%)				GA Muscles %MMGC (%)				Cost (N^3cm^6)	
	Mean	%Change	Max	%Change	Mean	%Change	Max	%Change	Mean	%Change
Intact	3.29		3.42		7.69		7.76		88108	
No Labrum	2	-39.21	2.17	-36.55	8.58	+11.57	8.73	+12.5	109677	+24.48
Ages 41–60	3.3	+0.3	3.41	-0.29	7.69	0	7.76	0	88107	0
Ages 61–80	3.15	-4.26	3.26	-4.68	7.84	+1.95	7.92	+2.06	90547	+2.77
Ages >80	2.93	-10.94	3.1	-9.36	8	+4.03	8.09	+4.25	93064	+5.62
SLAP	3.3	+0.3	3.41	-0.29	7.69	0	7.75	-0.13	88108	0
BKT	4.11	+24.92	4.22	+23.39	7.36	-4.29	7.57	-2.45	95836	+8.77
RBKT	2.05	-37.69	2.22	-35.09	8.59	+11.7	8.75	+12.76	110790	+25.74
ReSLAP	3.3	+0.3	3.4	-0.58	7.69	0	7.77	+0.13	88108	0
ReBKT	3.26	-0.91	3.38	-1.17	7.71	+0.26	7.79	+0.39	89037	+1.05
ReRBKT	3.36	+2.13	3.48	+1.75	7.64	-0.65	7.69	-0.9	85786	-2.64
LTJ	3.36	+2.13	3.47	+1.46	7.64	-0.65	7.69	-0.9	86380	-1.96
PBB	4.27	+29.79	4.47	+30.7	6.63	-13.78	6.69	-13.79	78630	-10.76

Note: %MMGC = Percentage of Maximal Predicted Muscle Group Capability; RC = Rotator Cuff; GA = Glenohumeral Articulating; SLAP = Superior Labrum Antero-to-Posterior Lesion; BKT = Bankart Lesion; RBKT = Reverse Bankart Lesion; ReSLAP = Repaired Superior Labrum Antero-to-Posterior Lesion; ReBKT = Repaired Bankart Lesion; ReRBKT = Repaired Reverse Bankart Lesion; LTJ = Latarjet; PBB = Posterior Bone Block. Cost represents the magnitude of the cost function.

Table A-7. Mean and maximum percentages of maximal predicted muscle group capability and mean task costs during grooming under all simulated conditions.

Condition	RC Muscles %MMGC (%)				GA Muscles %MMGC (%)				Cost (N^3cm^6)	
	Mean	%Change	Max	%Change	Mean	%Change	Max	%Change	Mean	%Change
Intact	2.19		5.18		2.18		6.01		12612	
No Labrum	2.32	+5.94	6.73	+29.92	2.29	+5.05	6.08	+1.16	15182	+20.38
Ages 41–60	2.19	0	5.17	-0.19	2.18	0	6.01	0	12614	+0.02
Ages 61–80	2.25	+2.74	5.73	+10.62	2.19	+0.46	6.03	+0.33	13319	+5.61
Ages >80	2.32	+5.94	6.39	+23.36	2.21	+1.38	6.04	+0.5	14174	+12.39
SLAP	2.23	+1.83	5.44	+5.02	2.17	-0.46	6.01	0	12920	+2.44
BKT	2.19	0	5.11	-1.35	2.18	0	6	-0.17	12616	+0.03
RBKT	2.08	-5.02	5.16	-0.39	2.27	+4.13	6.02	+0.17	12766	+1.22
ReSLAP	2.18	-0.46	5.01	-3.28	2.18	0	6.01	0	12492	-0.95
ReBKT	2.18	-0.46	5.17	-0.19	2.18	0	6.01	0	12613	+0.01
ReRBKT	2.19	0	5.16	-0.39	2.19	+0.46	6.02	+0.17	12623	+0.09
LTJ	2.19	0	5.15	-0.58	2.18	0	6.01	0	12615	+0.02
PBB	2.25	+2.74	5.34	+3.09	2.1	-3.67	5.96	-0.83	12261	-2.78

Note: %MMGC = Percentage of Maximal Predicted Muscle Group Capability; RC = Rotator Cuff; GA = Glenohumeral Articulating; SLAP = Superior Labrum Antero-to-Posterior Lesion; BKT = Bankart Lesion; RBKT = Reverse Bankart Lesion; ReSLAP = Repaired Superior Labrum Antero-to-Posterior Lesion; ReBKT = Repaired Bankart Lesion; ReRBKT = Repaired Reverse Bankart Lesion; LTJ = Latarjet; PBB = Posterior Bone Block. Cost represents the magnitude of the cost function.

Table A-8. Mean and maximum percentages of maximal predicted muscle group capability and mean task costs during one-arm row under all simulated conditions.

Condition	RC Muscles %MMGC (%)				GA Muscles %MMGC (%)				Cost (N^3cm^6)	
	Mean	%Change	Max	%Change	Mean	%Change	Max	%Change	Mean	%Change
Intact	4.59		5.91		3.16		4.1		42678	
No Labrum	4.7	+2.4	6.82	+15.4	3.44	+8.86	4.84	+18.05	62311	+46
Ages 41–60	4.59	0	5.89	-0.34	3.16	0	4.06	-0.98	42674	-0.01
Ages 61–80	4.57	-0.44	6.15	+4.06	3.22	+1.9	4.06	-0.98	46159	+8.16
Ages >80	4.57	-0.44	6.44	+8.97	3.29	+4.11	4.12	+0.49	49786	+16.65
SLAP	4.6	+0.22	5.89	-0.34	3.15	-0.32	4.1	0	42681	+0.01
BKT	4.59	0	5.88	-0.51	3.16	0	4.12	+0.49	42726	+0.11
RBKT	4.41	-3.92	6.36	+7.61	3.57	+12.97	4.68	+14.15	53190	+24.63
ReSLAP	4.58	-0.22	5.89	-0.34	3.16	0	4.11	+0.24	42674	-0.01
ReBKT	4.59	0	5.91	0	3.16	0	4.11	+0.24	42682	+0.01
ReRBKT	4.58	-0.22	6.01	+1.69	3.19	+0.95	4.07	-0.73	43883	+2.82
LTJ	4.59	0	5.91	0	3.16	0	4.07	-0.73	42662	-0.04
PBB	4.2	-8.5	5.89	-0.34	2.92	-7.59	4.04	-1.46	29814	-30.14

Note: %MMGC = Percentage of Maximal Predicted Muscle Group Capability; RC = Rotator Cuff; GA = Glenohumeral Articulating; SLAP = Superior Labrum Antero-to-Posterior Lesion; BKT = Bankart Lesion; RBKT = Reverse Bankart Lesion; ReSLAP = Repaired Superior Labrum Antero-to-Posterior Lesion; ReBKT = Repaired Bankart Lesion; ReRBKT = Repaired Reverse Bankart Lesion; LTJ = Latarjet; PBB = Posterior Bone Block. Cost represents the magnitude of the cost function.

Table A-9. Mean and maximum percentages of maximal predicted muscle group capability and mean task costs during one-arm chest press under all simulated conditions.

Condition	RC Muscles %MMGC (%)				GA Muscles %MMGC (%)				Cost (N^3cm^6)	
	Mean	%Change	Max	%Change	Mean	%Change	Max	%Change	Mean	%Change
Intact	4.32		11.96		3.42		5.75		77760	
No Labrum	4.48	+3.7	13.54	+13.21	3.6	+5.26	6.32	+9.91	110191	+41.71
Ages 41–60	4.31	-0.23	11.96	0	3.42	0	5.75	0	77761	0
Ages 61–80	4.35	+0.69	12.23	+2.26	3.47	+1.46	5.84	+1.57	82344	+5.9
Ages >80	4.39	+1.62	12.52	+4.68	3.51	+2.63	6.05	+5.22	87084	+11.99
SLAP	4.32	0	11.96	0	3.42	0	5.75	0	77766	+0.01
BKT	4.36	+0.93	12.58	+5.18	3.43	+0.29	5.77	+0.35	82495	+6.09
RBKT	4.32	0	13.56	+13.38	3.69	+7.89	6.75	+17.39	106233	+36.62
ReSLAP	4.31	-0.23	11.96	0	3.42	0	5.76	+0.17	77755	-0.01
ReBKT	4.32	0	12.05	+0.75	3.42	0	5.75	0	78320	+0.72
ReRBKT	4.29	-0.69	11.65	-2.59	3.44	+0.58	5.77	+0.35	77236	-0.67
LTJ	4.3	-0.46	11.74	-1.84	3.42	0	5.76	+0.17	76581	-1.52
PBB	4.12	-4.63	11.26	-5.85	3.3	-3.51	5.45	-5.22	65122	-16.25

Note: %MMGC = Percentage of Maximal Predicted Muscle Group Capability; RC = Rotator Cuff; GA = Glenohumeral Articulating; SLAP = Superior Labrum Antero-to-Posterior Lesion; BKT = Bankart Lesion; RBKT = Reverse Bankart Lesion; ReSLAP = Repaired Superior Labrum Antero-to-Posterior Lesion; ReBKT = Repaired Bankart Lesion; ReRBKT = Repaired Reverse Bankart Lesion; LTJ = Latarjet; PBB = Posterior Bone Block. Cost represents the magnitude of the cost function.

Table A-10. Mean and maximum percentages of maximal predicted muscle group capability and mean task costs during one-arm face pull under all simulated conditions.

Condition	RC Muscles %MMGC (%)				GA Muscles %MMGC (%)				Cost (N^3cm^6)	
	Mean	%Change	Max	%Change	Mean	%Change	Max	%Change	Mean	%Change
Intact	1.72		2.5		2.66		5.18		6138	
No Labrum	1.28	-25.58	2.43	-2.8	2.92	+9.77	5.51	+6.37	6775	+10.38
Ages 41–60	1.72	0	2.5	0	2.66	0	5.18	0	6138	0
Ages 61–80	1.71	-0.58	2.49	-0.4	2.68	+0.75	5.18	0	6160	+0.36
Ages >80	1.69	-1.74	2.5	0	2.7	+1.5	5.16	-0.39	6189	+0.83
SLAP	1.72	0	2.5	0	2.66	0	5.18	0	6138	0
BKT	1.71	-0.58	2.54	+1.6	2.72	+2.26	5.18	0	6223	+1.38
RBKT	1.26	-26.74	2.44	-2.4	2.93	+10.15	5.56	+7.34	6854	+11.67
ReSLAP	1.72	0	2.5	0	2.66	0	5.18	0	6138	0
ReBKT	1.72	0	2.46	-1.6	2.66	0	5.18	0	6145	+0.11
ReRBKT	1.72	0	2.58	+3.2	2.64	-0.75	5.18	0	6122	-0.26
LTJ	1.72	0	2.56	+2.4	2.64	-0.75	5.18	0	6126	-0.2
PBB	1.75	+1.74	2.7	+8	2.59	-2.63	5.18	0	6107	-0.51

Note: %MMGC = Percentage of Maximal Predicted Muscle Group Capability; RC = Rotator Cuff; GA = Glenohumeral Articulating; SLAP = Superior Labrum Antero-to-Posterior Lesion; BKT = Bankart Lesion; RBKT = Reverse Bankart Lesion; ReSLAP = Repaired Superior Labrum Antero-to-Posterior Lesion; ReBKT = Repaired Bankart Lesion; ReRBKT = Repaired Reverse Bankart Lesion; LTJ = Latarjet; PBB = Posterior Bone Block. Cost represents the magnitude of the cost function.

Table A-11. Mean and maximum percentages of maximal predicted muscle group capability and mean task costs during box lifting under all simulated conditions.

Condition	RC Muscles %MMGC (%)				GA Muscles %MMGC (%)				Cost (N^3cm^6)	
	Mean	%Change	Max	%Change	Mean	%Change	Max	%Change	Mean	%Change
Intact	3.46		6.05		3.43		7.48		62298	
No Labrum	3.66	+5.78	7.58	+25.29	3.52	+2.62	7.67	+2.54	69430	+11.45
Ages 41–60	3.47	+0.29	6	-0.83	3.44	+0.29	7.51	+0.4	62290	-0.01
Ages 61–80	3.57	+3.18	6.65	+9.92	3.44	+0.29	7.52	+0.53	64214	+3.08
Ages >80	3.67	+6.07	7.26	+20	3.45	+0.58	7.64	+2.14	66367	+6.53
SLAP	3.56	+2.89	6.49	+7.27	3.41	-0.58	7.53	+0.67	62939	+1.03
BKT	3.47	+0.29	6.04	-0.17	3.43	0	7.53	+0.67	62295	0
RBKT	3.13	-9.54	6.05	0	3.52	+2.62	7.47	-0.13	63618	+2.12
ReSLAP	3.42	-1.16	5.91	-2.31	3.44	+0.29	7.53	+0.67	61980	-0.51
ReBKT	3.46	0	6.02	-0.5	3.44	+0.29	7.47	-0.13	62285	-0.02
ReRBKT	3.42	-1.16	6.02	-0.5	3.45	+0.58	7.48	0	62394	+0.15
LTJ	3.46	0	6.01	-0.66	3.44	+0.29	7.54	+0.8	62295	0
PBB	3.83	+10.69	6.13	+1.32	3.29	-4.08	7.45	-0.4	60644	-2.65

Note: %MMGC = Percentage of Maximal Predicted Muscle Group Capability; RC = Rotator Cuff; GA = Glenohumeral Articulating; SLAP = Superior Labrum Antero-to-Posterior Lesion; BKT = Bankart Lesion; RBKT = Reverse Bankart Lesion; ReSLAP = Repaired Superior Labrum Antero-to-Posterior Lesion; ReBKT = Repaired Bankart Lesion; ReRBKT = Repaired Reverse Bankart Lesion; LTJ = Latarjet; PBB = Posterior Bone Block. Cost represents the magnitude of the cost function.

Table A-12. Mean and maximum percentages of maximal predicted muscle group capability and mean task costs during weight relief under all simulated conditions.

Condition	RC Muscles %MMGC (%)				GA Muscles %MMGC (%)				Cost (N^3cm^6)	
	Mean	%Change	Max	%Change	Mean	%Change	Max	%Change	Mean	%Change
Intact	19.54		38.01		19.86		26.12		6418759	
No Labrum	19.75	+1.07	40.18	+5.71	20.17	+1.56	26.96	+3.22	7720594	+20.28
Ages 41–60	19.53	-0.05	37.76	-0.66	19.86	0	26.09	-0.11	6419440	+0.01
Ages 61–80	20.13	+3.02	41.74	+9.81	19.94	+0.4	25.46	-2.53	6741778	+5.03
Ages >80	20.61	+5.48	44.62	+17.39	20.02	+0.81	26.17	+0.19	7087570	+10.42
SLAP	20.08	+2.76	39.74	+4.55	19.87	+0.05	25.61	-1.95	6508734	+1.4
BKT	19.5	-0.2	37.68	-0.87	19.85	-0.05	26.19	+0.27	6419099	+0.01
RBKT	17.78	-9.01	34.23	-9.94	19.92	+0.3	26.48	+1.38	6594869	+2.74
ReSLAP	19.33	-1.07	37.36	-1.71	19.84	-0.1	26.32	+0.77	6383720	-0.55
ReBKT	19.51	-0.15	37.8	-0.55	19.87	+0.05	26.1	-0.08	6418212	-0.01
ReRBKT	19.39	-0.77	38.19	+0.47	19.88	+0.1	26.07	-0.19	6463282	+0.69
LTJ	19.46	-0.41	37.77	-0.63	19.86	0	26.42	+1.15	6419388	+0.01
PBB	20.1	+2.87	35.13	-7.58	19.7	-0.81	26.19	+0.27	6151790	-4.16

Note: %MMGC = Percentage of Maximal Predicted Muscle Group Capability; RC = Rotator Cuff; GA = Glenohumeral Articulating; SLAP = Superior Labrum Antero-to-Posterior Lesion; BKT = Bankart Lesion; RBKT = Reverse Bankart Lesion; ReSLAP = Repaired Superior Labrum Antero-to-Posterior Lesion; ReBKT = Repaired Bankart Lesion; ReRBKT = Repaired Reverse Bankart Lesion; LTJ = Latarjet; PBB = Posterior Bone Block. Cost represents the magnitude of the cost function.

Appendix B: Glenohumeral Joint Contact Forces, By Task

Table B-1. Mean and direction of glenohumeral joint contact forces during isometric internal rotation under all simulated conditions.

Condition	ASF(+)/PSF(-) (N)		SSF(+)/ISF(-) (N)		Resultant Shear Force (N)				JCF (N)	
	Mean	%Change	Mean	%Change	Mean	%Change	Direction	Change	Mean	%Change
Intact	-181.91		-100.38		207.8		241.1°		928.36	
No Labrum	-137.38	+24.48	-117.8	-17.35	180.99	-12.9	229.4°	-11.7°	941.37	+1.4
Ages 41–60	-181.89	+0.01	-100.47	-0.09	207.82	+0.01	241.1°	0°	928.35	0
Ages 61–80	-172.22	+5.33	-81.34	+18.97	190.49	-8.33	244.7°	+3.6°	927.73	-0.07
Ages >80	-163.77	+9.97	-64.71	+35.53	176.19	-15.21	248.5°	+7.4°	927.89	-0.05
SLAP	-180.68	+0.68	-84.25	+16.07	199.42	-4.03	245°	+3.9°	926.49	-0.2
BKT	-181.87	+0.02	-100.53	-0.15	207.83	+0.01	241.1°	0°	928.31	-0.01
RBKT	-167.92	+7.69	-175.17	-74.51	242.7	+16.79	223.8°	-17.3°	940.07	+1.26
ReSLAP	-182.82	-0.5	-106.08	-5.68	211.39	+1.73	239.9°	-1.2°	928.87	+0.05
ReBKT	-181.88	+0.02	-100.46	-0.08	207.81	0	241.1°	0°	928.32	0
ReRBKT	-179.56	+1.29	-104.58	-4.18	207.82	+0.01	239.8°	-1.3°	929.3	+0.1
LTJ	-181.85	+0.03	-100.6	-0.22	207.85	+0.02	241.1°	0°	928.31	-0.01
PBB	-197.62	-8.64	-86.34	+13.99	215.76	+3.83	246.4°	+5.3°	926.67	-0.18

Note: ASF = Anterior Joint Shear Force; PSF = Posterior Joint Shear Force; SSF = Superior Joint Shear Force; ISF = Inferior Joint Shear Force; JCF = Joint Compression Force; SLAP = Superior Labrum Antero-to-Posterior Lesion; BKT = Bankart Lesion; RBKT = Reverse Bankart Lesion; ReSLAP = Repaired Superior Labrum Antero-to-Posterior Lesion; ReBKT = Repaired Bankart Lesion; ReRBKT = Repaired Reverse Bankart Lesion; LTJ = Latarjet; PBB = Posterior Bone Block.

Table B-2. Mean and direction of glenohumeral joint contact forces during isometric external rotation under all simulated conditions.

Condition	ASF(+)/PSF(-) (N)		SSF(+)/ISF(-) (N)		Resultant Shear Force (N)				JCF (N)	
	Mean	%Change	Mean	%Change	Mean	%Change	Direction	Change	Mean	%Change
Intact	-258.26		-269.45		373.29		223.8°		1446.01	
No Labrum	-273.73	-5.99	-288.33	-7.01	397.66	+6.53	223.5°	-0.3°	1929.91	+33.46
Ages 41–60	-258.27	0	-269.46	0	373.31	+0.01	223.8°	0°	1446.08	0
Ages 61–80	-263.65	-2.09	-275.95	-2.41	381.73	+2.26	223.7°	-0.1°	1603.09	+10.86
Ages >80	-269.28	-4.27	-282.81	-4.96	390.59	+4.63	223.6°	-0.2°	1778.23	+22.97
SLAP	-261.12	-1.11	-272.89	-1.28	377.77	+1.2	223.7°	-0.1°	1527.95	+5.67
BKT	-258.26	0	-269.45	0	373.29	0	223.8°	0°	1446	0
RBKT	-258.27	0	-269.46	0	373.32	+0.01	223.8°	0°	1446.1	+0.01
ReSLAP	-257.2	+0.41	-268.18	+0.47	371.65	-0.44	223.8°	0°	1416.06	-2.07
ReBKT	-258.27	0	-269.46	0	373.32	+0.01	223.8°	0°	1446.09	+0.01
ReRBKT	-258.26	0	-269.45	0	373.3	0	223.8°	0°	1446.03	0
LTJ	-258.27	0	-269.46	0	373.31	+0.01	223.8°	0°	1446.08	0
PBB	-258.23	+0.01	-269.42	+0.01	373.26	-0.01	223.8°	0°	1445.87	-0.01

Note: ASF = Anterior Joint Shear Force; PSF = Posterior Joint Shear Force; SSF = Superior Joint Shear Force; ISF = Inferior Joint Shear Force; JCF = Joint Compression Force; SLAP = Superior Labrum Antero-to-Posterior Lesion; BKT = Bankart Lesion; RBKT = Reverse Bankart Lesion; ReSLAP = Repaired Superior Labrum Antero-to-Posterior Lesion; ReBKT = Repaired Bankart Lesion; ReRBKT = Repaired Reverse Bankart Lesion; LTJ = Latarjet; PBB = Posterior Bone Block.

Table B-3. Mean and direction of glenohumeral joint contact forces during isometric abduction under all simulated conditions.

Condition	ASF(+)/PSF(-) (N)		SSF(+)/ISF(-) (N)		Resultant Shear Force (N)				JCF (N)	
	Mean	%Change	Mean	%Change	Mean	%Change	Direction	Change	Mean	%Change
Intact	-197.35		-184.97		270.75		226.7°		959.5	
No Labrum	-196.17	+0.6	-181.35	+1.96	267.52	-1.19	226.9°	+0.2°	1164.37	+21.35
Ages 41–60	-197.29	+0.03	-184.91	+0.03	270.67	-0.03	226.7°	0°	959.21	-0.03
Ages 61–80	-196.56	+0.4	-183.46	+0.82	269.17	-0.58	226.8°	+0.1°	1027.73	+7.11
Ages >80	-196.24	+0.56	-182.23	+1.48	268.14	-0.96	226.9°	+0.2°	1102.12	+14.86
SLAP	-197.01	+0.17	-184.24	+0.39	270.02	-0.27	226.7°	0°	995.9	+3.79
BKT	-197.3	+0.03	-184.93	+0.02	270.69	-0.02	226.7°	0°	959.35	-0.02
RBKT	-197.29	+0.03	-184.92	+0.03	270.68	-0.03	226.7°	0°	959.24	-0.03
ReSLAP	-197.43	-0.04	-185.2	-0.12	270.96	+0.08	226.6°	-0.1°	945.72	-1.44
ReBKT	-197.31	+0.02	-184.93	+0.02	270.69	-0.02	226.7°	0°	959.27	-0.02
ReRBKT	-197.26	+0.05	-184.88	+0.05	270.62	-0.05	226.7°	0°	959.02	-0.05
LTJ	-197.32	+0.02	-184.94	+0.02	270.71	-0.01	226.7°	0°	959.34	-0.02
PBB	-197.33	+0.01	-184.95	+0.01	270.73	-0.01	226.7°	0°	959.44	-0.01

Note: ASF = Anterior Joint Shear Force; PSF = Posterior Joint Shear Force; SSF = Superior Joint Shear Force; ISF = Inferior Joint Shear Force; JCF = Joint Compression Force; SLAP = Superior Labrum Antero-to-Posterior Lesion; BKT = Bankart Lesion; RBKT = Reverse Bankart Lesion; ReSLAP = Repaired Superior Labrum Antero-to-Posterior Lesion; ReBKT = Repaired Bankart Lesion; ReRBKT = Repaired Reverse Bankart Lesion; LTJ = Latarjet; PBB = Posterior Bone Block.

Table B-4. Mean and direction of glenohumeral joint contact forces during isometric adduction under all simulated conditions.

Condition	ASF(+)/PSF(-) (N)		SSF(+)/ISF(-) (N)		Resultant Shear Force (N)				JCF (N)	
	Mean	%Change	Mean	%Change	Mean	%Change	Direction	Change	Mean	%Change
Intact	-107.33		117.03		158.83		317.5°		467.69	
No Labrum	-88.98	+17.1	38.81	-66.84	97.13	-38.85	293.5°	-24°	565.27	+20.86
Ages 41–60	-107.33	0	117.03	0	158.83	0	317.5°	0°	467.69	0
Ages 61–80	-102.79	+4.23	117.03	-3.57	152.68	-3.87	317.7°	+0.2°	482.96	+3.26
Ages >80	-98.26	+8.45	112.85	-7.31	146.4	-7.83	317.8°	+0.3°	497.8	+6.44
SLAP	-107.33	0	108.48	0	158.82	-0.01	317.5°	0°	467.68	0
BKT	-107.33	0	117.03	0	158.83	0	317.5°	0°	467.69	0
RBKT	-83.79	+21.93	50.46	-56.88	97.87	-38.38	301°	-16.5°	574.25	+22.78
ReSLAP	-107.32	+0.01	117.03	0	158.82	-0.01	317.5°	0°	467.66	-0.01
ReBKT	-107.33	0	117.03	0	158.82	-0.01	317.5°	0°	467.67	0
ReRBKT	-105.4	+1.8	115.26	-1.51	156.22	-1.64	317.5°	0°	474.27	+1.41
LTJ	-107.33	0	117.03	0	158.83	0	317.5°	0°	467.69	0
PBB	-126.12	-17.51	143.55	+22.66	191.09	+20.31	318.7°	+1.2°	403.6	-13.7

Note: ASF = Anterior Joint Shear Force; PSF = Posterior Joint Shear Force; SSF = Superior Joint Shear Force; ISF = Inferior Joint Shear Force; JCF = Joint Compression Force; SLAP = Superior Labrum Antero-to-Posterior Lesion; BKT = Bankart Lesion; RBKT = Reverse Bankart Lesion; ReSLAP = Repaired Superior Labrum Antero-to-Posterior Lesion; ReBKT = Repaired Bankart Lesion; ReRBKT = Repaired Reverse Bankart Lesion; LTJ = Latarjet; PBB = Posterior Bone Block.

Table B-5. Mean and direction of glenohumeral joint contact forces during isometric flexion under all simulated conditions.

Condition	ASF(+)/PSF(-) (N)		SSF(+)/ISF(-) (N)		Resultant Shear Force (N)				JCF (N)	
	Mean	%Change	Mean	%Change	Mean	%Change	Direction	Change	Mean	%Change
Intact	-95.1		35.31		101.54		290.4°		429.88	
No Labrum	-75.21	+20.91	-0.12	-100.34	75.23	-25.91	270°	-20.4°	453.03	+5.39
Ages 41–60	-95.09	+0.01	35.29	-0.06	101.52	-0.02	290.4°	0°	429.83	-0.01
Ages 61–80	-90.12	+5.24	29.6	-16.17	94.96	-6.48	288.2°	-2.2°	434.6	+1.1
Ages >80	-85.44	+10.16	24.16	-31.58	88.9	-12.45	285.8°	-4.6°	438.96	+2.11
SLAP	-95.09	+0.01	35.29	-0.06	101.53	-0.01	290.4°	0°	429.86	0
BKT	-95.09	+0.01	35.28	-0.08	101.53	-0.01	290.4°	0°	429.86	0
RBKT	-69.51	+26.91	-0.73	-102.07	69.6	-31.46	269.5°	-20.9°	455.74	+6.02
ReSLAP	-95.1	0	35.29	-0.06	101.53	-0.01	290.4°	0°	429.86	0
ReBKT	-95.1	0	35.27	-0.11	101.52	-0.02	290.4°	0°	429.87	0
ReRBKT	-93.2	+2	32.59	-7.7	98.83	-2.67	289.3°	-1.1°	431.91	+0.47
LTJ	-95.09	+0.01	35.28	-0.08	101.52	-0.02	290.4°	0°	429.85	-0.01
PBB	-116.97	-23	69.65	97.25	136.19	+34.12	300.8°	+10.4°	404.97	-5.79

Note: ASF = Anterior Joint Shear Force; PSF = Posterior Joint Shear Force; SSF = Superior Joint Shear Force; ISF = Inferior Joint Shear Force; JCF = Joint Compression Force; SLAP = Superior Labrum Antero-to-Posterior Lesion; BKT = Bankart Lesion; RBKT = Reverse Bankart Lesion; ReSLAP = Repaired Superior Labrum Antero-to-Posterior Lesion; ReBKT = Repaired Bankart Lesion; ReRBKT = Repaired Reverse Bankart Lesion; LTJ = Latarjet; PBB = Posterior Bone Block.

Table B-6. Mean and direction of glenohumeral joint contact forces during isometric extension under all simulated conditions.

Condition	ASF(+)/PSF(-) (N)		SSF(+)/ISF(-) (N)		Resultant Shear Force (N)				JCF (N)	
	Mean	%Change	Mean	%Change	Mean	%Change	Direction	Change	Mean	%Change
Intact	-65.39		148.07		161.92		336.2°		475.05	
No Labrum	-11.89	+81.82	120.42	-18.67	121.15	-25.18	354.3°	+18.1°	473.22	-0.39
Ages 41–60	-65.39	0	148.09	+0.01	161.94	+0.01	336.2°	0°	475.11	+0.01
Ages 61–80	-55.73	+14.77	145.23	-1.92	155.61	-3.9	339°	+2.8°	478.25	+0.67
Ages >80	-46.62	+28.7	142.44	-3.8	149.92	-7.41	341.9°	+5.7°	479.67	+0.97
SLAP	-65.4	-0.02	148.07	0	161.92	0	336.2°	0°	475.07	0
BKT	-93.63	-43.19	116.45	-21.35	149.59	-7.61	321.2°	-15°	481.31	+1.32
RBKT	-12.62	+80.7	117.8	-20.44	118.64	-26.73	353.8°	+17.6°	475.86	+0.17
ReSLAP	-65.4	-0.02	148.08	+0.01	161.93	+0.01	336.2°	0°	475.09	+0.01
ReBKT	-62.81	+3.95	144.92	-2.13	158	-2.42	336.6°	+0.4°	473.53	-0.32
ReRBKT	-72.42	-10.75	156.89	+5.96	172.85	+6.75	335.2°	-1°	478.04	+0.63
LTJ	-70.94	-8.49	153.63	+3.75	169.27	+4.54	335.2°	-1°	476.61	+0.33
PBB	-125.87	-92.49	150.41	+1.58	196.2	+21.17	320.1°	-16.1°	437.87	-7.83

Note: ASF = Anterior Joint Shear Force; PSF = Posterior Joint Shear Force; SSF = Superior Joint Shear Force; ISF = Inferior Joint Shear Force; JCF = Joint Compression Force; SLAP = Superior Labrum Antero-to-Posterior Lesion; BKT = Bankart Lesion; RBKT = Reverse Bankart Lesion; ReSLAP = Repaired Superior Labrum Antero-to-Posterior Lesion; ReBKT = Repaired Bankart Lesion; ReRBKT = Repaired Reverse Bankart Lesion; LTJ = Latarjet; PBB = Posterior Bone Block.

Table B-7. Mean and direction of glenohumeral joint contact forces during isometric grooming under all simulated conditions.

Condition	ASF(+)/PSF(-) (N)		SSF(+)/ISF(-) (N)		Resultant Shear Force (N)				JCF (N)	
	Mean	%Change	Mean	%Change	Mean	%Change	Direction	Change	Mean	%Change
Intact	-75.16		10.76		85.88		259.3°		139.05	
No Labrum	-71.62	+4.71	8.3	-22.86	82.31	-4.16	255.8°	-3.5°	154.28	+10.95
Ages 41–60	-75.06	+0.13	10.65	-1.02	85.71	-0.2	259.3°	0°	138.97	-0.06
Ages 61–80	-74.65	+0.68	11.17	+3.81	85.11	-0.9	259.9°	+0.6°	143.06	+2.88
Ages >80	-74.2	+1.28	11.66	+8.36	84.53	-1.57	261.3°	+2°	147.89	+6.36
SLAP	-75.34	-0.24	12.15	+12.92	85.52	-0.42	262.1°	+2.8°	140.6	+1.11
BKT	-75.06	+0.13	10.84	+0.74	85.77	-0.13	259.3°	0°	138.94	-0.08
RBKT	-70.54	+6.15	6.67	-38.01	81.76	-4.8	254.1°	-5.2°	142.63	+2.57
ReSLAP	-75.09	+0.09	10.66	-0.93	85.77	-0.13	259.3°	0°	138.38	-0.48
ReBKT	-74.79	+0.49	10.5	-2.42	85.41	-0.55	259.2°	-0.1°	138.74	-0.22
ReRBKT	-74.87	+0.39	10.6	-1.49	85.59	-0.34	259.1°	-0.2°	139.39	+0.24
LTJ	-75.04	+0.16	10.75	-0.09	85.71	-0.2	259.3°	0°	139.01	-0.03
PBB	-79.56	-5.85	17.76	+65.06	87.77	+2.2	270.4°	+11.1°	137.53	-1.09

Note: ASF = Anterior Joint Shear Force; PSF = Posterior Joint Shear Force; SSF = Superior Joint Shear Force; ISF = Inferior Joint Shear Force; JCF = Joint Compression Force; SLAP = Superior Labrum Antero-to-Posterior Lesion; BKT = Bankart Lesion; RBKT = Reverse Bankart Lesion; ReSLAP = Repaired Superior Labrum Antero-to-Posterior Lesion; ReBKT = Repaired Bankart Lesion; ReRBKT = Repaired Reverse Bankart Lesion; LTJ = Latarjet; PBB = Posterior Bone Block.

Table B-8. Mean and direction of glenohumeral joint contact forces during one-arm row under all simulated conditions.

Condition	ASF(+)/PSF(-) (N)		SSF(+)/ISF(-) (N)		Resultant Shear Force (N)				JCF (N)	
	Mean	%Change	Mean	%Change	Mean	%Change	Direction	Change	Mean	%Change
Intact	-92.58		-14.66		97.07		263°		250.5	
No Labrum	-79.93	+13.66	-28.49	-94.34	87.33	-10.03	252.3°	-10.7°	261.06	+4.22
Ages 41–60	-92.7	-0.13	-14.6	+0.41	97.12	+0.05	263.1°	+0.1°	250.54	+0.02
Ages 61–80	-88.76	+4.13	-19.51	-33.08	93.34	-3.84	259.4°	-3.6°	249.63	-0.35
Ages >80	-86.11	+6.99	-21.09	-43.86	90.86	-6.4	258°	-5°	250.99	+0.2
SLAP	-92.93	-0.38	-14.34	+2.18	97.17	+0.1	263.3°	+0.3°	250.9	+0.16
BKT	-92.54	+0.04	-14.7	-0.27	97.02	-0.05	263°	0°	250.43	-0.03
RBKT	-76.57	+17.29	-40.69	-177.56	89.5	-7.8	243.7°	-19.3°	250.04	-0.18
ReSLAP	-92.46	+0.13	-15.07	-2.8	97.13	+0.06	262.8°	-0.2°	250.14	-0.14
ReBKT	-92.6	-0.02	-14.59	+0.48	97.06	-0.01	263.1°	+0.1°	250.45	-0.02
ReRBKT	-91.04	+1.66	-18.51	-26.26	95.71	-1.4	260.4°	-2.6°	249.74	-0.3
LTJ	-92.6	-0.02	-14.68	-0.14	97.07	0	263°	0°	250.4	-0.04
PBB	-99.2	-7.15	+11.16	+176.13	105.96	+9.16	278.4°	+15.4°	234.74	-6.29

Note: ASF = Anterior Joint Shear Force; PSF = Posterior Joint Shear Force; SSF = Superior Joint Shear Force; ISF = Inferior Joint Shear Force; JCF = Joint Compression Force; SLAP = Superior Labrum Antero-to-Posterior Lesion; BKT = Bankart Lesion; RBKT = Reverse Bankart Lesion; ReSLAP = Repaired Superior Labrum Antero-to-Posterior Lesion; ReBKT = Repaired Bankart Lesion; ReRBKT = Repaired Reverse Bankart Lesion; LTJ = Latarjet; PBB = Posterior Bone Block.

Table B-9. Mean and direction of glenohumeral joint contact forces during one-arm chest press under all simulated conditions.

Condition	ASF(+)/PSF(-) (N)		SSF(+)/ISF(-) (N)		Resultant Shear Force (N)				JCF (N)	
	Mean	%Change	Mean	%Change	Mean	%Change	Direction	Change	Mean	%Change
Intact	-38.38		19.92		55.2		292.4°		254.02	
No Labrum	-26.74	+30.33	5.2	-73.9	38.72	-29.86	277.8°	-14.6°	267.02	+5.12
Ages 41–60	-38.34	+0.1	19.85	-0.35	55.01	-0.34	292.6°	+0.2°	253.45	-0.22
Ages 61–80	-36.18	+5.73	16.42	-17.57	50.93	-7.74	291.2°	-1.2°	256.02	+0.79
Ages >80	-34.03	+11.33	13.12	-34.14	47.42	-14.09	289.6°	-2.8°	259.42	+2.13
SLAP	-38.52	-0.36	20.23	+1.56	55.02	-0.33	293°	+0.6°	253.66	-0.14
BKT	-38.23	+0.39	18.71	-6.07	54	-2.17	292.3°	-0.1°	255.1	+0.43
RBKT	-25.75	+32.91	-2.19	-110.99	40.66	-26.34	270.3°	-22.1°	263.07	+3.56
ReSLAP	-38.33	+0.13	19.58	-1.71	55.09	-0.2	292°	-0.4°	253.49	-0.21
ReBKT	-38.34	+0.1	19.77	-0.75	54.95	-0.45	292.4°	0°	253.84	-0.07
ReRBKT	-37.48	+2.34	18.54	-6.93	54.18	-1.85	291.2°	-1.2°	253.26	-0.3
LTJ	-38.43	-0.13	20.23	+1.56	55.3	+0.18	292.6°	+0.2°	253.27	-0.3
PBB	-45.24	-17.87	30.54	+53.31	65.58	+18.8	297.9°	+5.5°	243.99	-3.95

Note: ASF = Anterior Joint Shear Force; PSF = Posterior Joint Shear Force; SSF = Superior Joint Shear Force; ISF = Inferior Joint Shear Force; JCF = Joint Compression Force; SLAP = Superior Labrum Antero-to-Posterior Lesion; BKT = Bankart Lesion; RBKT = Reverse Bankart Lesion; ReSLAP = Repaired Superior Labrum Antero-to-Posterior Lesion; ReBKT = Repaired Bankart Lesion; ReRBKT = Repaired Reverse Bankart Lesion; LTJ = Latarjet; PBB = Posterior Bone Block.

Table B-10. Mean and direction of glenohumeral joint contact forces during one-arm face pull under all simulated conditions.

Condition	ASF(+)/PSF(-) (N)		SSF(+)/ISF(-) (N)		Resultant Shear Force (N)				JCF (N)	
	Mean	%Change	Mean	%Change	Mean	%Change	Direction	Change	Mean	%Change
Intact	-50.26		22.37		64.72		304°		214.56	
No Labrum	-38.44	+23.52	4.31	-80.73	53.88	-16.75	300.9°	-3.1°	219.9	+2.49
Ages 41–60	-50.26	0	22.36	-0.04	64.72	0	304°	0°	214.53	-0.01
Ages 61–80	-48.97	+2.57	21.37	-4.47	63.21	-2.33	304.6°	+0.6°	215.82	+0.59
Ages >80	-47.47	+5.55	20.1	-10.15	61.46	-5.04	305.1°	+1.1°	216.78	+1.03
SLAP	-50.25	+0.02	22.36	-0.04	64.71	-0.02	304°	0°	214.55	0
BKT	-49.9	+0.72	17.04	-23.83	60.4	-6.67	300.5°	-3.5°	216.16	+0.75
RBKT	-37.9	+24.59	4.18	-81.31	53.04	-18.05	300.7°	-3.3°	220.31	+2.68
ReSLAP	-50.26	0	22.37	0	64.72	0	304°	0°	214.56	0
ReBKT	-50.08	+0.36	21.93	-1.97	64.27	-0.7	303.9°	-0.1°	215.15	+0.27
ReRBKT	-50.95	-1.37	23.91	+6.88	66.4	+2.6	304.3°	+0.3°	213.89	-0.31
LTJ	-50.9	-1.27	23.42	+4.69	65.95	+1.9	304.1°	+0.1°	214.21	-0.16
PBB	-53.96	-7.36	24.32	+8.72	68.29	+5.52	301.6°	-2.4°	210.26	-2

Note: ASF = Anterior Joint Shear Force; PSF = Posterior Joint Shear Force; SSF = Superior Joint Shear Force; ISF = Inferior Joint Shear Force; JCF = Joint Compression Force; SLAP = Superior Labrum Antero-to-Posterior Lesion; BKT = Bankart Lesion; RBKT = Reverse Bankart Lesion; ReSLAP = Repaired Superior Labrum Antero-to-Posterior Lesion; ReBKT = Repaired Bankart Lesion; ReRBKT = Repaired Reverse Bankart Lesion; LTJ = Latarjet; PBB = Posterior Bone Block.

Table B-11. Mean and direction of glenohumeral joint contact forces during box lifting under all simulated conditions.

Condition	ASF(+)/PSF(-) (N)		SSF(+)/ISF(-) (N)		Resultant Shear Force (N)				JCF (N)	
	Mean	%Change	Mean	%Change	Mean	%Change	Direction	Change	Mean	%Change
Intact	-68.32		-36.21		88.09		235.6°		274.49	
No Labrum	-58.11	+14.94	-41.12	-13.56	83.91	-4.75	226.8°	-8.8°	290.58	+5.86
Ages 41–60	-68.38	-0.09	-36.39	-0.5	88.36	+0.31	235.5°	-0.1°	274.73	+0.09
Ages 61–80	-66.32	+2.93	-34.88	+3.67	86.64	-1.65	236°	+0.4°	281.73	+2.64
Ages >80	-64.11	+6.16	-34.22	+5.5	85.1	-3.39	235.7°	+0.1°	288.35	+5.05
SLAP	-69.07	-1.1	-32.35	+10.66	87.17	-1.04	239.1°	+3.5°	280.22	+2.09
BKT	-68.36	-0.06	-36.32	-0.3	88.24	+0.17	235.5°	-0.1°	274.85	+0.13
RBKT	-60.24	+11.83	-45.13	-24.63	86.59	-1.7	225.3°	-10.3°	260.87	-4.96
ReSLAP	-68.2	+0.18	-37.55	-3.7	88.62	+0.6	234.5°	-1.1°	272.39	-0.77
ReBKT	-68.24	+0.12	-36.48	-0.75	88.14	+0.06	235.4°	-0.2°	274.43	-0.02
ReRBKT	-67.16	+1.7	-38.06	-5.11	88.21	+0.14	233.7°	-1.9°	272.95	-0.56
LTJ	-68.29	+0.04	-36.45	-0.66	88.12	+0.03	235.5°	-0.1°	274.68	+0.07
PBB	-81.17	-18.81	-16.26	+55.1	90.73	+3	257.1°	+21.5°	290.3	+5.76

Note: ASF = Anterior Joint Shear Force; PSF = Posterior Joint Shear Force; SSF = Superior Joint Shear Force; ISF = Inferior Joint Shear Force; JCF = Joint Compression Force; SLAP = Superior Labrum Antero-to-Posterior Lesion; BKT = Bankart Lesion; RBKT = Reverse Bankart Lesion; ReSLAP = Repaired Superior Labrum Antero-to-Posterior Lesion; ReBKT = Repaired Bankart Lesion; ReRBKT = Repaired Reverse Bankart Lesion; LTJ = Latarjet; PBB = Posterior Bone Block.

Table B-12. Mean and direction of glenohumeral joint contact forces during weight relief under all simulated conditions.

Condition	ASF(+)/PSF(-) (N)		SSF(+)/ISF(-) (N)		Resultant Shear Force (N)				JCF (N)	
	Mean	%Change	Mean	%Change	Mean	%Change	Direction	Change	Mean	%Change
Intact	-819.99		-286.32		973.76		252.2°		1495.52	
No Labrum	-764.81	+6.73	-289.4	-1.08	921.58	-5.36	250.7°	-1.5°	1479.67	-1.06
Ages 41–60	-818.58	+0.17	-285.3	+0.36	971.73	-0.21	252.1°	-0.1°	1495.01	-0.03
Ages 61–80	-810.72	+1.13	-274.79	+4.03	964.74	-0.93	252.8°	+0.6°	1526.04	+2.04
Ages >80	-802.07	+2.19	-266.9	+6.78	956.78	-1.74	253.3°	+1.1°	1550.95	+3.71
SLAP	-821.35	-0.17	-272.91	+4.68	972.9	-0.09	252.8°	+0.6°	1529.92	+2.3
BKT	-817.86	+0.26	-285.68	+0.22	971.45	-0.24	252.1°	-0.1°	1492.65	-0.19
RBKT	-795.28	+3.01	-337.59	-17.91	959.31	-1.48	238.1°	-14.1°	1380.59	-7.68
ReSLAP	-817.48	+0.31	-290.53	-1.47	971.64	-0.22	251.8°	-0.4°	1482.06	-0.9
ReBKT	-818.72	+0.15	-285.96	+0.13	972.37	-0.14	252.1°	-0.1°	1493.93	-0.11
ReRBKT	-814.44	+0.68	-289.87	-1.24	968.88	-0.5	252°	-0.2°	1483.41	-0.81
LTJ	-817.33	+0.32	-285.92	+0.14	970.68	-0.32	252°	-0.2°	1491.84	-0.25
PBB	-841.43	-2.61	-249.37	+12.91	996.05	+2.29	254.7°	+2.5°	1533.46	+2.54

Note: ASF = Anterior Joint Shear Force; PSF = Posterior Joint Shear Force; SSF = Superior Joint Shear Force; ISF = Inferior Joint Shear Force; JCF = Joint Compression Force; SLAP = Superior Labrum Antero-to-Posterior Lesion; BKT = Bankart Lesion; RBKT = Reverse Bankart Lesion; ReSLAP = Repaired Superior Labrum Antero-to-Posterior Lesion; ReBKT = Repaired Bankart Lesion; ReRBKT = Repaired Reverse Bankart Lesion; LTJ = Latarjet; PBB = Posterior Bone Block.